

STRUCTURAL STUDIES OF
DIETHYLPHENYLPHOSPHONITE-
TRANSITION METAL COMPLEXES

Thesis by
Donald Dean Titus

In Partial Fulfillment of the Requirements

For the Degree of
Doctor of Philosophy

California Institute of Technology

Pasadena, California

1971

(Submitted February 24, 1971)

To Carlta

ACKNOWLEDGMENTS

The direction and encouragement of Drs. Harry B. Gray and Richard E. Marsh during the course of this work is gratefully acknowledged. Thanks are due to Dr. A. A. Orio, who carried out the initial stages of the investigation.

For assistance with the x-ray structural studies, I am indebted to Drs. Michael T. Flood, T. J. Kistenmacher, Sten Samson, and William P. Schaefer. The programming assistance of Mr. Benes Trus and Mrs. Jean Westphal is deeply appreciated.

I thank Messrs. Albert Schweizer and Daniel C. Harris, and Dr. D. K. Ottesen for their assistance and helpful discussions concerning the spectral studies.

This work would have been impossible without the encouragement and moral support provided by the members of my family, and the financial support provided by the National Science Foundation and the California Institute of Technology.

ABSTRACT

The syntheses and spectral properties of several tetrakis(diethylphenylphosphonite) transition metal complexes are reported.

The crystal structures of the hydrido complexes $\text{H}_2\text{Fe}((\text{C}_6\text{H}_5)\text{P}(\text{OC}_2\text{H}_5)_2)_4$ and $\text{HCo}((\text{C}_6\text{H}_5)\text{P}(\text{OC}_2\text{H}_5)_2)_4$ have been determined. The phosphorus ligands are disposed nearly tetrahedrally about the metal atoms, with the hydrogen ligands occupying faces of the tetrahedra.

Infrared and n.m.r. studies of the hydrido complexes in methylcyclohexane solution indicate that the molecules are stereochemically non-rigid. The classical coordination structures used in discussing rearrangements of five- and six-coordinate complexes (octahedron, square pyramid, and trigonal bipyramid) are found to be inadequate in the discussion of the present complexes. A structure based on a tetrahedral skeleton of phosphorus atoms is presented as an alternative.

TABLE OF CONTENTS

Acknowledgments	iii
Abstract	iv
GENERAL INTRODUCTION	
<u>Properties of Phosphorus Ligands</u>	1
SECTION I - <u>Experimental</u>	
Preparations	8
Spectra	24
Calculations	25
SECTION II - <u>Dihydridotetrakis(diethylphenyl-</u>	
<u>phosphonite)iron(II)</u>	26
Introduction	27
The X-Ray Crystal Structure of $H_2Fe((C_6H_5P(OC_2H_5)_2)_4$	36
Collection and Treatment of Data	36
Description of the Structure	49
Discussion of the Spectral Properties of $H_2Fe((C_6H_5)P(OC_2H_5)_2)_4$	65
SECTION III - <u>Hydridotetrakis(diethylphenyl-</u>	
<u>phosphonite)cobalt(I)</u>	82
Introduction	83

The X-Ray Crystal Structure of	
$\text{HCo}((\text{C}_6\text{H}_5)\text{P}(\text{OC}_2\text{H}_5)_2)_4$	88
Collection and Treatment of Data	88
Description of the Structure	94
Discussion of the Spectral Properties of	
$\text{HCo}((\text{C}_6\text{H}_5)\text{P}(\text{OC}_2\text{H}_5)_2)_4$	109
SECTION IV - <u>Tetrakis(diethylphenylphosphonite)</u>	
<u>Complexes of Ni(0), Cu(I), Pd(0),</u>	
<u>and Pt(0)</u>	118
SUMMARY	132
REFERENCES	137
APPENDIX I - Additional Structural Data for	
$\text{H}_2\text{Fe}((\text{C}_6\text{H}_5)\text{P}(\text{OC}_2\text{H}_5)_2)_4$	145
APPENDIX II - Additional Structural Data for	
$\text{HCo}((\text{C}_6\text{H}_5)\text{P}(\text{OC}_2\text{H}_5)_2)_4$	156
PROPOSITIONS	166

GENERAL INTRODUCTION

Properties of Phosphorus Ligands

Properties of Phosphorus Ligands

If a poll were taken among the transition metals to determine which ligand atom they considered to be most versatile, chances are good that a majority of the metals would cast their vote for phosphorus. As the huge amount of work published in the past twenty years shows, the trivalent phosphorus atom is a veritable Jack-of-all-trades. It forms ligands which can behave similarly to the amines, and yet, with an increase in the electronegativity of its substituents, a phosphorus ligand can resemble carbon monoxide in behavior.

The ability to form complexes resembling those of carbon monoxide was attributed by Chatt (1) to "dative π -bonding" in which the empty d orbitals of the phosphorus atoms accept electron density from the metal atom. Chatt based this argument on studies of PF_3 , in which the high electronegativity of the fluorine atoms contracts the phosphorus d orbitals to a point where significant interaction with the metal d orbitals is possible. Since a

Similar back donation can occur from the metal d to the carbon p orbitals of carbon monoxide ligands, and PF_3 and CO can be expected to show similar behavior as ligands.

As the knowledge of various ligands increased through subsequent work, it became clear that other phosphorus ligands, although certainly electron donors, had special properties not observed with amines and other σ -donors. The π -back donation theory eventually became generally accepted for all phosphorus ligands, not just those having electronegative substituents. Although blessed with a good deal of merit, the theory of back donation to phosphorus ligands, especially those such as triethyl- and triphenylphosphine, has been greatly overemphasized. Inevitably, doubt has arisen as to the extent of back bonding in some complexes, although the argument that all the observable behavior can be explained in terms of σ -bonding (2) seems less tenable than the overworked π -bonding theory.

A more moderate view is probably nearer to the truth in this case. Although π -back bonding is indeed possible for all phosphorus ligands, it is unlikely that it becomes of real significance unless the phosphorus substituents are highly electronegative. Thus, it is observed that PF_3 is very similar to CO (3) while PPh_3 acts more like a simple σ -donor ligand. The lower oxidation states

of metals are generally stabilized by PF_3 and various phosphite esters, while the higher oxidation states are favored by the alkyl and aryl phosphines. Infrared studies of carbonyl complexes substituted with a variety of phosphines indicate that the π -acceptor properties of phosphorus ligands decrease in the order $\text{PF}_3 > \text{PCl}_3 > \text{POR}_3 > \text{PR}_3$ (4,5).

The present work reports the properties of an intermediate ligand, $(\text{C}_6\text{H}_5)\text{P}(\text{OC}_2\text{H}_5)_2$. The initial investigations of complexes of this ligand indicated that it had significant π - as well as σ -bonding capabilities (6). The ultraviolet spectrum of the nickel complex showed a much lower energy for the $d \rightarrow \pi^*$ transition than was observed for its $\text{P}(\text{OC}_2\text{H}_5)_3$ analog (7). It was inferred from this observation that $(\text{C}_6\text{H}_5)\text{P}(\text{OC}_2\text{H}_5)_2$ is a better π -acceptor than $\text{P}(\text{OC}_2\text{H}_5)_3$.

The versatility of this ligand is itself quite interesting. Although a zero-valent tetracarbonyl complex is unknown for platinum, nickel tetracarbonyl has been known and studied for years. Platinum apparently tends to favor ligands which do not require a strong π -interaction and forms a zero-valent tetrakis(triphenylphosphine) complex. The corresponding nickel-triphenylphosphine complex is unknown. The σ - and π -bonding capabilities of $(\text{C}_6\text{H}_5)\text{P}(\text{OC}_2\text{H}_5)_2$ appear to be balanced in such a manner that stable zero-valent complexes of both nickel and

platinum can be prepared.

Stable hydrides of Fe(II) and Co(I) with $(C_6H_5)P(OC_2H_5)_2$, analogous to the carbonyl complexes first prepared by Hieber (8,9), have also been prepared. With triphenylphosphine, the Fe(III) and Co(III) hydrides are more stable, and have been extensively studied in the past few years (10-16).

In the following pages are reported syntheses and structural studies of several complexes of diethylphenylphosphonite, $(C_6H_5)P(OC_2H_5)_2$. In the initial stages of this work, various substituents were investigated in place of the ethyl group in an attempt to improve the bonding capabilities of the ligand. These were: isopropyl, isobutyl, tertiary butyl, trifluoroethyl, and phenyl. The ligands were all prepared from the corresponding alcohols by the prescribed method (see Experimental Section), but none provided any apparent advantages over the ethoxy-substituted ligand, and they were not investigated further. In contrast to expectation, fluorinating the phenyl ring does not appear to improve the complexing ability of the phosphonite. Since the synthesis of the fluorinated ligand is somewhat more complex, it is reported in the Experimental Section.

The hydride complexes reported below are non-rigid in solution, a feature which has been observed for several

complexes of this type (17). It is found that the classical coordination structures used in discussing five- and six-coordinate complexes (octahedron, square pyramid, trigonal bipyramid) are less than adequate in the discussion of these compounds. A general structure based on a tetrahedral skeleton of phosphorus atoms is presented as an alternative.

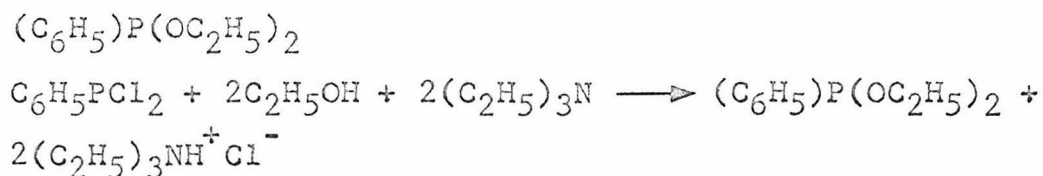
SECTION I

EXPERIMENTAL

PREPARATIONS

Because of the poisonous nature of phosphines, phosphonites, and their transition metal complexes, the experimental procedures outlined in this section all should be carried out in an efficient fume hood. Care must also be taken to avoid physical contact with these compounds; plastic gloves are desirable. While the volatile phosphines and phosphonites can usually be detected by smell before their concentration reaches the danger level, the non-volatile metal complexes can easily escape detection, and therefore, should be treated with a reasonable amount of respect.

All of the reactions reported here were carried out in an atmosphere of nitrogen or argon. The solvents used were saturated with argon by bubbling the gas through the solvent for at least an hour at room temperature.

Diethylphenylphosphonite

The large bulk of amine hydrochloride by-product produced in this reaction necessitates the use of a powerful mechanical stirring motor. This preparation is an adaptation of the method of Rabinowitz and Pellon (18).

In a 2 liter, 3-necked flask fitted with a 300 ml dropping funnel, mechanical stirrer, and nitrogen inlet and outlet, are combined 163 gm triethylamine (1.6 mole), 74 gm absolute ethanol (1.6 mole), and 700 ml benzene. The resultant solution is then cooled in an ice bath to 0 - 10°C. A large plastic ice bucket is useful for this and later operations requiring cooling for the large flask. Phenylphosphonous dichloride (143 gm, 0.8 mole) is weighed out in the hood (it is a fuming liquid with an extremely irritating odor) and transferred to the dropping funnel. The brief exposure of PhPCl_2 to air during the weighing does not lower the yield appreciably, although the yield is significantly reduced if the dichloride has spent several months on the shelf. While the solution is stirred, the dichloride is added dropwise from the funnel. Because of the volatility of the reactants, some

amine hydrochloride forms in the vapors above the solution and tends to form clouds which obscure the reaction mixture from view. This effect can be minimized by reducing the addition rate and making certain that the temperature in the flask does not exceed 10°C . The nitrogen flow should be kept at a minimum to reduce the chances of clogging the outlet and bubbler with amine hydrochloride.

The addition requires about 1 to 2 hours, depending on the temperature of the flask and how much of the amine hydrochloride one is willing to have floating around above the reaction mixture. By the time all of the dichloride has been added, the reaction mixture consists of a thick cream-colored slush. The stirring is continued for an hour, after which the ice bath is removed and the flask allowed to warm to room temperature. The mixture is stirred for an additional hour.

The nitrogen flow is increased (by this time the amine hydrochloride clouds have been absorbed by the slush) and the stirring rod and blade are removed. After wiping the stopcock grease away from the ground glass joint which held the stirring apparatus, a 10 mm tube with a medium porosity filter at one end is lowered into the mixture. The tube passes through a rubber stopper, which is used to seal the contents of the flask from the atmosphere while still allowing the height of the filter to be

adjusted. At the opposite end of the filter tube is a ball joint which is connected to another 10 mm tube leading into a 2 liter 2-necked flask. The other neck of this flask is connected through a stopcock to a vacuum pump. Since the receiving flask is never completely evacuated during the filtration, it is best to flush it with nitrogen before the filtration begins.

The receiving flask is immersed in an ice bath, and the filter tube in the reaction flask is adjusted until it almost touches the bottom. The stopcock to the vacuum pump is then opened for a few seconds to get the filtration started. Only a small pressure differential is needed; too great a pressure reduction in the receiving flask causes the filter to become clogged. The ice bath for the receiving flask reduces the vapor pressure of the benzene, and thus only occasional use of the vacuum pump is required. When most of the liquid has passed into the receiving flask, 200 ml of cold benzene are added to the amine hydrochloride in the reaction flask. This and two additional washes of 200 ml each are filtered into the receiving flask. Some amine hydrochloride usually is able to pass through the filter during washing, but this is removed later.

After adding nitrogen to the receiving flask to equalize the pressure inside with atmospheric pressure, the

tube from the filter is removed and replaced with a stopper. The filtrate can be stored for several days under nitrogen in the refrigerator.

A large magnetic stirbar is added to the filtrate flask, which is then attached to a distillation apparatus with a 2 liter receiving flask. The receiving flask is immersed in an ice water bath, with the ice water being circulated through the condenser by a centrifugal pump. The system is then evacuated and the filtrate warmed on an oil bath until the benzene begins to distill. Vigorous stirring with the magnetic stirbar reduces bumping and splashing. The system usually does not need to be open to the vacuum pump after the initial evacuation, as long as the receiving flask and condenser are kept in ice water. After the benzene has been distilled into the receiver, a light-yellow cloudy liquid remains in the flask. The cloudiness is the result of small amounts of amine hydrochloride which elude the first filtration or which precipitate out after removal of the benzene. It cannot be removed by distillation since it comes over with the phosphine in much the same manner as a steam distillation.

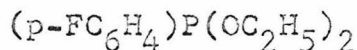
The flask containing the residue is then attached to a filter tube heading to a 300 ml flask. The smaller flask is partially evacuated and the liquid filtered into it. When the filtration is complete, a magnetic stirring bar

is added to the flask, and the flask is attached to a small vacuum distillation apparatus.

The system is evacuated and the crude phosphine heated on an oil bath. The distillation column should be wrapped in glass wool. After a small initial fraction containing some benzene, the water-white product is collected at 56 - 57°C, 0.05 mm Hg. Yield: 97.3 gm, 61%. Anal Calc for $C_{10}H_{15}PO_2$: C, 60.60; H, 7.63, P, 15.63. Found: C, 60.44; H, 7.64; P, 15.53.

The product is moderately air sensitive and should be stored under nitrogen. Its infrared spectrum has been reported (19).

Diethyl-p-fluorophenylphosphonite



This compound is prepared in the same manner as $(\text{C}_6\text{H}_5)\text{P}(\text{OC}_2\text{H}_5)_2$, substituting $p\text{-FC}_6\text{H}_4\text{PCl}_2$ for $\text{C}_6\text{H}_5\text{PCl}_2$. The $p\text{-FC}_6\text{H}_4\text{PCl}_2$ is prepared according to the method of Schindlbauer (20).

In a 2 liter 3-necked flask equipped with a mechanical stirrer, dropping funnel, reflux condenser, and nitrogen inlet and outlet are combined 188 gm AlCl_3 (1.4 mole) and 579 gm PCl_3 (4.2 mole). The mixture is heated to reflux on an oil bath. After stirring for 15 minutes (all of the AlCl_3 does not dissolve), dropwise addition

of 100 gm fluorobenzene (1.04 mole) is begun. As the fluorobenzene is added, the solution becomes brown and most of the remaining AlCl_3 eventually dissolves. When the addition is complete (about 1 hour addition time), the reaction mixture is cloudy, and light brown in color. The mixture is then stirred at refluxing temperature for about 4 hours.

After cooling the contents of the flask to about 60°C , 216 gm POCl_3 (1.4 mole) are added dropwise. The $\text{POCl}_3 \cdot \text{AlCl}_3$ adduct precipitates immediately from the solution. The mixture is stirred for $\frac{1}{2}$ hour after addition is complete, and is then filtered in the same manner as described above for $(\text{C}_6\text{H}_5)\text{P}(\text{OC}_2\text{H}_5)_2$. The solid is washed six times with 200 ml portions of petroleum ether, the washes being filtered into the receiver with the reaction filtrate.

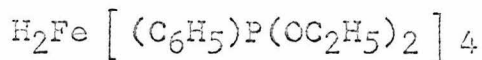
The petroleum ether and PCl_3 are removed by the same method used to remove solvent benzene from the $(\text{C}_6\text{H}_5)\text{P}(\text{OC}_2\text{H}_5)_2$ reaction mixture. The crude product (about 125 ml) was transferred to a smaller flask and vacuum distilled. Bp. $58 - 60^\circ\text{C}$, 0.05 mm Hg. Yield: 118 gm, 60%.

The preparation of the corresponding diethyl ester is carried out using the method reported above for the synthesis of $(\text{C}_6\text{H}_5)\text{P}(\text{OC}_2\text{H}_5)_2$. The quantities of reactants are 70 gm (1.52 mole) absolute ethanol, 130 gm (1.27 mole)

triethylamine, and 118 gm (0.6 mole) (p-FC₆H₄)PCl₂.
The solvent again is benzene (700 ml).

Upon vacuum distillation of the crude product about 70 gm p-FC₆H₄P(OC₂H₅) are obtained. This represents a 55% yield based on the dichloride. The p.m.r. spectrum indicates only two types of aromatic protons, as is expected for para disubstituted benzene. Anal Calc for C₁₀H₁₅FO₂P: C, 55.56; H, 6.53; F, 8.79; P, 14.33. Found: C, 55.36; H, 6.45; F, 8.98; P, 14.39.

Dihydridotetrakis(diethylphenylphosphonite)iron(II)

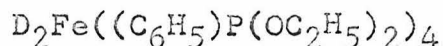


In a 100 ml 3-necked flask equipped with a reflux condenser, dropping funnel (10 ml), magnetic stirring bar, and nitrogen inlet and outlet are combined 1.27 gm (0.01 mole) anhydrous ferrous chloride, 10 gm (0.05 mole) diethylphenylphosphonite, and 50 ml absolute ethanol. This mixture is stirred at reflux temperature for three hours. The resultant solution is nearly colorless, although in some cases it has a light gray or green cast (If heating is continued for an additional hour or two, the solution becomes yellow, presumably due to the formation of small amounts of H₂FeL₄.) The contents of the flask are cooled to 40 - 50°C and a freshly prepared solution of sodium borohydride (0.2 gm in 10 ml absolute

ethanol) was added slowly from the dropping funnel. It is extremely important that the sodium borohydride used in this step be of high quality. Although this reaction has been successfully carried out using $\text{FeCl}_2 \cdot 4\text{H}_2\text{O}$ instead of anhydrous material, it invariably gives a low yield if the sodium borohydride used in the reaction is lumpy or crusty in appearance. Initially upon addition of the borohydride, the solution turns red with some evolution of gas, but after a few moments the reddish color fades and the final color at the completion of addition is dark yellow-brown. A small amount of gray powder precipitates from the solution during the addition. The mixture is then stirred for about an hour, and the dropping funnel is replaced by a medium porosity filter tube leading into a 100 ml round bottom flask fitted with a sidearm and stopcock. The sidearm is connected to a vacuum pump and the stopcock opened to evacuate the receiving flask. The nitrogen flow is increased into the reaction flask, thus flushing the filter tube and the receiving flask. The stopcock to the pump is then closed, and the nitrogen pressure allowed to equilibrate on both sides of the filter. The system is then tilted so that the reaction mixture can flow into the filter tube. The stopcock connected to the vacuum line is then opened for a second or two, to lower the pressure slightly in the receiving flask. A large pressure

differential can cause the filter to clog. After all of the solution has passed into the receiver, the vacuum line is replaced with a nitrogen line. The stopcock is opened, and with a rapid stream of nitrogen flowing through the receiving flask, the filter tube is removed and replaced with a glass stopper. The solution is allowed to stand at room temperature for several hours. If crystallization has not occurred by this time, the solution can be stored in a refrigerator. Large yellow holohedral prisms separate from the solution, which is drawn off with a syringe and concentrated for a second crop of crystals. The product is washed several times with cold (10°C) absolute ethanol and dried in vacuo. Yield: 3 - 4 gm, about 40%. The crystals are best stored under an inert atmosphere in a refrigerator, although they can be stored indefinitely at room temperature in a light-free, carefully evacuated vessel. Anal Calc for $C_{40}H_{62}FeO_8P_4$: C, 56.48; H, 7.35; Fe, 6.57; P, 14.56. Found: C, 56.46; H, 7.30; Fe, 6.72; P, 14.73.

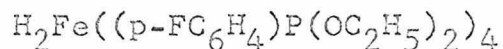
Dideuteridotetrakis(diethylphenylphosphonite)iron(II)



This complex is prepared in a manner analogous to the corresponding hydride complex except that C_2H_5OD is used as the solvent and $NaBD_4$ is used as the reducing agent.

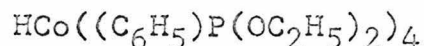
Attempts to prepare the deuteride from the hydride by treatment with D_2 and recrystallization from C_2H_5OD failed to yield anything but unsubstituted starting material.

Dihydridotetrakis(diethyl-p-fluorophenylphosphonite)iron(II)



The preparation of this complex is the same as that reported for $H_2Fe((C_6H_5)P(OC_2H_5)_2)_4$. In this case, however, the product was apparently impure. The removal of the final traces of solvent appears to be part of the difficulty. Otherwise, the color is light yellow, and the infrared spectrum indicates nothing unusual. The iron-hydrogen stretching frequency is observed at 1978 cm^{-1} .

Hydridotetrakis(diethylphenylphosphonite)cobalt(I)



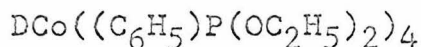
In the same apparatus used for preparing the iron complexes are combined 1.30 gm anhydrous cobaltous chloride and 50 ml absolute ethanol. After warming to $50 - 60^\circ C$ and stirring for a few minutes, all but a few particles of the chloride dissolve, yielding a dark blue solution. With a stream of nitrogen passing through the flask, diethylphenylphosphonite (10 gm, 0.05 mole) is then added from a syringe, giving rise immediately to a dark green

suspension. After stirring this mixture for 15 minutes, a freshly prepared, saturated solution of sodium borohydride in ethanol is added dropwise until the color of the reaction mixture becomes bright yellow. The addition is accompanied by a vigorous evolution of gas; about 4 - 5 ml of borohydride solution are usually required. The mixture is stirred for 15 minutes and then filtered. Occasionally, some of the product precipitates from the solution before the filtration. This is crystalline rather than granular, distinguishing it from the usual grey bi-product of the reaction. The crystals can be redissolved by heating, or the addition of more ethanol. After filtering as for the iron complexes, the yellow-orange solution is allowed to stand under nitrogen at room temperature for several hours. The product separates from solution as orange holohedral prisms. The mother liquor is drawn off and reduced in volume to obtain more product. The crystals are washed with cold ethanol several times, and dried in vacuo.

Yield: 6 - 7 gm, 70 - 80%. The compound can also be prepared in the absence of sodium borohydride by merely refluxing together for several hours the CoCl_2 , phosphonite, and ethanol. Presumably this reaction involves the transfer of a hydride ion from the alpha carbon of the alcohol (21). The yield by this process is only about 10%. Anal Calc for $\text{C}_{40}\text{H}_{61}\text{CoO}_8\text{P}_4$: C, 56.34; H, 7.21; Co, 6.91; P, 14.53.

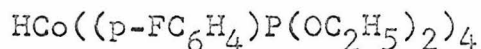
Found: C, 56.25; H, 7.22; Co, 7.00; P, 14.28. The crystals are stable to air for a few days, and can be stored indefinitely at room temperature under nitrogen.

Deuteridotetrakis(diethylphenylphosphonite)cobalt(I)



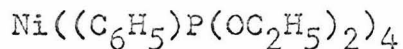
This complex is prepared by the method above except for the substitution of $\text{C}_2\text{H}_5\text{OD}$ and NaBD_4 for $\text{C}_2\text{H}_5\text{OH}$ and NaBH_4 . As in the case with iron complexes, attempts to deuterate the hydride complex by exchange with D_2 and $\text{C}_2\text{H}_5\text{OD}$ failed.

Hydridotetrakis(diethyl-p-fluorophenylphosphonite)cobalt(I)

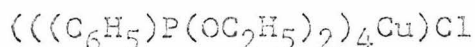


The above method was used to prepare this complex. The product resembled the diethylphenylphosphonite complex in appearance although the weak cobalt-hydrogen stretching absorption was not observed in the infrared spectrum.

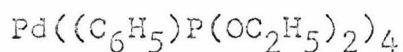
Tetrakis(diethylphenylphosphonite)nickel(0)



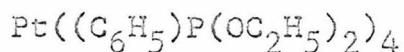
This compound was prepared by the reported method (7). The product crystallizes as light-yellow, square plates.

Tetrakis(diethylphenylphosphonite)copper(I)chloride

The literature method (7) for the preparation of this complex is unreliable. For the present study, 0.495 gm CuCl (0.005 mole) is combined in the usual reaction apparatus (see preparations above) with 4.5 gm $(\text{C}_6\text{H}_5)\text{P}(\text{OC}_2\text{H}_5)_2$ (0.0225 mole). The mixture is heated to 110°C on an oil bath. The solid slowly dissolves yielding a clear, colorless liquid. After stirring at $100 - 110^\circ\text{C}$ for about 6 hours, the heating bath is removed and the flask immersed in a liquid nitrogen bath. The flask is then stored at -20°C for several hours. The contents of the flask are then allowed to warm to room temperature. The residual white crystals are broken up and washed several times with 10 ml portions of cold (10°C) petroleum ether, and dried in vacuo (at 5°C). Yield: 3.5 gm, 80%. The complex tends to dissociate in a vacuum at room temperature, yielding free phosphine and $((\text{C}_6\text{H}_5)\text{P}(\text{OC}_2\text{H}_5)_2)_3\text{CuCl}$. Anal Calc for $\text{C}_{40}\text{H}_{60}\text{ClCuO}_8\text{P}_4$: C, 53.75; H, 6.76; Cl, 3.98; P, 13.88. Found: C, 52.49; H, 6.88; Cl, 4.67; P, 13.95. The compound is best stored under nitrogen in a refrigerator.

Tetrakis(diethylphenylphosphonite)palladium(O)

This compound was prepared by the literature method (7), although in much lower yield than reported (10%). Crystals could only be obtained by storing the reaction mixture at -20°C . After washing the product with cold ethanol, it is dried in vacuo (-10°C), and can be stored indefinitely in a vacuum at -20°C .

Tetrakis(diethylphenylphosphonite)platinum(O)

In a 100 ml 3-necked flask containing a magnetic stirring bar and fitted with a reflux condenser, dropping funnel, and nitrogen inlet and outlet are combined 1 gm PtCl_2 (3.75 mole) and 25 ml absolute ethanol. To this dark brown mixture is added 4 gm $(\text{C}_6\text{H}_5)\text{P}(\text{OC}_2\text{H}_5)_2$ (0.02 mole), and the flask is warmed on an oil bath. The color of the mixture begins to lighten immediately (even before it is warm), and the solid gradually dissolves. After ten minutes a clear, nearly colorless solution remains. The solution is stirred at reflux temperature for one hour. A freshly prepared, saturated solution of sodium borohydride in absolute ethanol is transferred to the dropping funnel. With the oil bath temperature at 60°C , the borohydride

solution is added dropwise to the reaction mixture. Addition is continued until further drops of the borohydride solution fail to produce a vigorous evolution of gas. The resultant mixture (very light yellow) is stirred at a bath temperature of 50°C for one hour. It is filtered while hot, using the method described above for the iron complex. The filtrate is allowed to stand under nitrogen at room temperature for several hours. The mother liquor is drawn off with a syringe and the nearly colorless platelets washed six times with 5 ml portions of absolute ethanol (10°C). The crystals are dried in vacuo. Yield: 3.18 gm, 86%. A second crop of crystals can be obtained by placing the mother liquor in a refrigerator for a few days, raising the yield to 98%. The product is stable to air for several hours; it can be stored indefinitely under argon or nitrogen. Anal Calc for $C_{40}H_{60}O_8Y_4Pt$: C, 48.63; H, 6.12; P, 12.54; Pt, 19.74. Found: C, 49.30; H, 6.25; P, 12.12; Pt, 19.88.

SPECTRA

Infrared spectra were obtained on a Perkin-Elmer 225 spectrophotometer. Samples were run either as Nujol or fluorocarbon mulls or as thin films between CsI and KBr plates. Low temperature solution work was carried out using an AgCl 0.01 mm cell encased in a vacuum chamber having KBr windows. A thermocouple attached to the cell monitored the temperature. Raman spectra were obtained on a Cary model 80 spectrophotometer utilizing helium-neon laser exciting radiation. N.m.r. spectra were obtained using a Varian Associates 220 megacycle instrument.

CALCULATIONS

The crystal structure calculations were carried out using programs of the CRYM system on an IBM 360/75 computer. The weighting function used was $w = 1/\sigma$ where σ is the standard deviation of the intensity. The residual index, R, was calculated from the relationship:

$$R = \frac{\sum ||F_{\text{obs}}| - |F_{\text{calc}}||}{\sum |F_{\text{obs}}|}$$

In the least-squares refinements the function minimized was:

$$\sum w(k^2 |F_{\text{obs}}|^2 - |F_{\text{calc}}|^2)^2$$

Standard deviations of the parameters derived from the least-squares refinements were calculated using:

$$\sigma_i = \left\{ (A^{-1})_{ii} \left[\frac{\sum w(k^2 F_{\text{obs}}^2 - F_{\text{calc}}^2)^2}{m - s} \right] \right\}^{\frac{1}{2}}$$

where σ_i is the standard deviation of parameter i , $(A^{-1})_{ii}$ is the diagonal element of the inverse matrix corresponding to parameter i , m is the number of observations, s is the number of parameters being refined, and k is the scale factor for F_{obs} .

SECTION II

DIHYDRIDOTETRAKIS (DIETHYLPHENYLPHOSPHONITE) IRON(II)

INTRODUCTION

The first complex transition metal hydride, $\text{H}_2\text{Fe}(\text{CO})_4$, was reported by Hieber in 1931 (8). It is an air sensitive, thermally unstable liquid which decomposes at -10°C (22). In spite of a great deal of research into the properties of the complex, its structure is still in question (23). Probably the most significant structural work to date has been reported by Ewens and Lister (24) (electron diffraction) and G. Wilkinson, et al (25) (broad line proton magnetic resonance spectra).

The electron diffraction experiment yielded data which were best explained by a tetrahedral disposition of the carbonyl groups about the iron atom. Unfortunately, only planar and regular tetrahedral geometries for the four carbonyl groups were considered as possible models. No attempt was made to compare the data with those calculated for tetrahedra which had been distorted by the positioning of hydrogen atoms in face and edge positions. The assignment of a regular tetrahedral configuration to the carbonyl

skeleton led to the belief, popular for several years, that the hydrogens were bonded to the carbonyl groups (23).

In the broad-line p.m.r. work, it was assumed that the width of the band was due entirely to intramolecular proton-proton interactions. The H-H distance was then calculated to be $1.88 \pm 0.05 \text{ \AA}$. In order to calculate the metal-hydrogen distance, it was necessary to assume a specific geometry for the hydride ligands. At the time of the p.m.r. work, the belief that the hydrogen was buried in the electron cloud of the metal was enjoying some popularity. Using an undistorted tetrahedron of carbonyls as a base, the authors decided upon a rather unfortunate range for the H-Fe-H angle (109° - 125°). The Fe-H distance was then calculated to be a fashionable, but as we know now, unrealistic 1.1 \AA . Neutron diffraction and x-ray diffraction studies of other complex metal hydride complexes (including the present work) have since shown that transition metal-hydrogen distances lie in the range 1.45 - 1.65 \AA . A very accurate M-H distance, $1.601(16) \text{ \AA}$, has been obtained from a neutron diffraction investigation of $\text{HMn}(\text{CO})_5$ (26). If a 90° H-Fe-H angle had been assumed, the Fe-H distance calculated would have been a more reasonable 1.33 \AA . With corrections for the probable intermolecular H-H interactions, this value would approach the 1.45 - 1.65 \AA now generally accepted for M-H bond distances. It is likely that the configuration of $\text{H}_2\text{Fe}(\text{CO})_4$ approximates a tetrahedron of carbonyl ligands, with

the hydrogen atoms lying on two of the 3-fold axes. A recent report of the infrared and Mössbauer spectra of $\text{H}_2\text{Fe}(\text{CO})_4$ is consistent with such a structure (27). A weak band at 1887 cm^{-1} in the infrared spectrum has been assigned to the metal-hydrogen stretching frequency.

In 1960, Chatt (28) reported the preparation of a new complex iron dihydride, $\text{H}_2\text{Fe}(\text{o-C}_6\text{H}_4(\text{PEt}_2)_2)_2$. In contrast to the carbonyl dihydride, this compound is crystalline and thermally stable (dec. 250°C). On the basis of the n.m.r. spectrum (3 lines of the expected quintet were observed, $\tau 23.1$) and the low dipole moment, 1.80 D, the complex was assigned a trans configuration. The results of the present work indicate that such an assignment cannot be made on the basis of n.m.r. or dipole moment data alone. The n.m.r. spectrum, for example, could also be explained by a cis configuration, if the triplet of doublets (as found for the cis form of the analogous dihydride complex (29), $\text{H}_2\text{Fe}(\text{C}_6\text{H}_5\text{P}(\text{OC}_2\text{H}_5)_2)_4$) were not well resolved.

Fortunately, other evidence is available which tends to confirm the trans assignment. The iron-hydrogen stretching frequency shows up as a strong band at 1726 cm^{-1} . The corresponding dideuteride band appears at 1259 cm^{-1} . These data are valuable in three respects. First, there is only one band; this is expected from the symmetry of a trans isomer. Second, the band is very intense by comparison with bands of known cis-dihydrides. This is expected

for the asymmetric mode of a trans isomer. Third, and most important, the band is observed at a relatively low energy. Alkyl, aryl, and hydride ligands are thought to have a very large σ trans influence, the effect of which is to weaken σ bonds trans to them. In the case of phosphine or carbonyl ligands trans to a hydride, the weakening of the trans σ bond apparently can be compensated for at least partially by an increase in the $d\pi - d\pi$ or $d\pi - p\pi$ interactions. This compensation is impossible for the hydride ligands in a trans dihydride complex, and thus the Fe-H bonds are weakened, resulting in a lower energy for the Fe-H stretching vibration. In dihydride complexes the shift in bands going from cis to trans is quite significant. Cis isomers display metal-hydrogen stretching absorptions in the range $1800 - 2050 \text{ cm}^{-1}$, and may be as high as 2200 cm^{-1} in cases where the hydride is trans to a ligand such as Cl^- ; trans isomers absorb in the $1600 - 1750 \text{ cm}^{-1}$ range.

As is generally observed for transition metal hydride complexes of tertiary organo-phosphines, the hydrogens in $\text{H}_2\text{Fe}(\text{o-C}_6\text{H}_4(\text{PEt}_2)_2)_2$ show no acidic character (31). This is markedly different from the behavior of transition metal carbonyl hydrides, which are generally quite acidic (k_1 for $\text{H}_2\text{Fe}(\text{CO})_4$ is 4×10^{-5}) (32). The phosphine complexes are usually unaffected by treatment with strong bases, and are usually prepared in the presence of such bases as NaOH

and NaBH_4 . In contrast, the carbonyl complexes often react with bases to form salts in which the carbonyl hydride complex, having lost a proton, serves as an anion.

Trifluorophosphine has been shown to be the phosphorus ligand best equipped electronically and sterically to form compounds analogous to the carbonyl complexes (1,3-5,33-37). PF_3 has been shown, by infrared evidence (33) and more recently by photoelectron spectroscopy (37), to exceed CO in its electron acceptor capabilities. The complex $\text{H}_2\text{Fe}(\text{PF}_3)_4$ has been discussed only briefly (3). It is a colorless liquid, melting at about -80°C ; the metal-hydrogen stretching absorption is observed at 1935 cm^{-1} . Much more stable thermally than the carbonyl complex, it decomposes at 205°C . Unlike similar complexes with organo-phosphines and phosphites, this compound is acidic, and, in general, its properties resemble those of $\text{H}_2\text{Fe}(\text{CO})_4$.

More recently, the triethylphosphite member of this series, $\text{H}_2\text{Fe}(\text{P}(\text{OEt})_3)_4$, was reported (38). The metal-hydrogen stretching frequency was observed at 1912 cm^{-1} (CS_2 solution); an absorption at this relatively high energy is usually indicative of a cis configuration. The n.m.r. spectrum shows a quintet at τ 26.0, from which the authors concluded that the configuration of the hydride ligands must be trans. The five lines observed in the room temperature n.m.r. spectrum might well have been

attributed to nonrigidity of the molecule, especially since both the low temperature proton n.m.r. and the ^{31}P n.m.r. spectra indicated a structure of lower symmetry.

In comparison with the complexes mentioned above, the subject of the present work, $\text{H}_2\text{Fe}((\text{C}_6\text{H}_5)\text{P}(\text{OC}_2\text{H}_5)_2)_4$, is relatively easy to prepare (see Experimental Section). The compound is obtained as well-formed light yellow crystals, which decompose after a few hours' exposure to air. If stored in a carefully sealed vessel under nitrogen or argon, the compound is stable indefinitely. Because of its relatively high thermal stability (decomposition occurs at $130 - 150^\circ\text{C}$), the complex is well suited for spectral study.

Initial n.m.r. data (39) indicated that in methylcyclohexane solution the complex perhaps was undergoing a rapid rearrangement. At room temperature a symmetric quintet (τ 24.3) was observed, having peak area ratios of 1:4:6:4:1. At -60°C , however, two resonances were observed. The first, at τ 21.0, was another quintet, but not as well resolved as the first. The second, at τ 23.4, was a poorly resolved triplet of doublets. Figure 1 shows the high-field p.m.r. spectrum of the complex. (More recent n.m.r. experiments have given much better resolution of the bands (40). The compound is unstable in solution, and the long periods of time between sample preparation and the

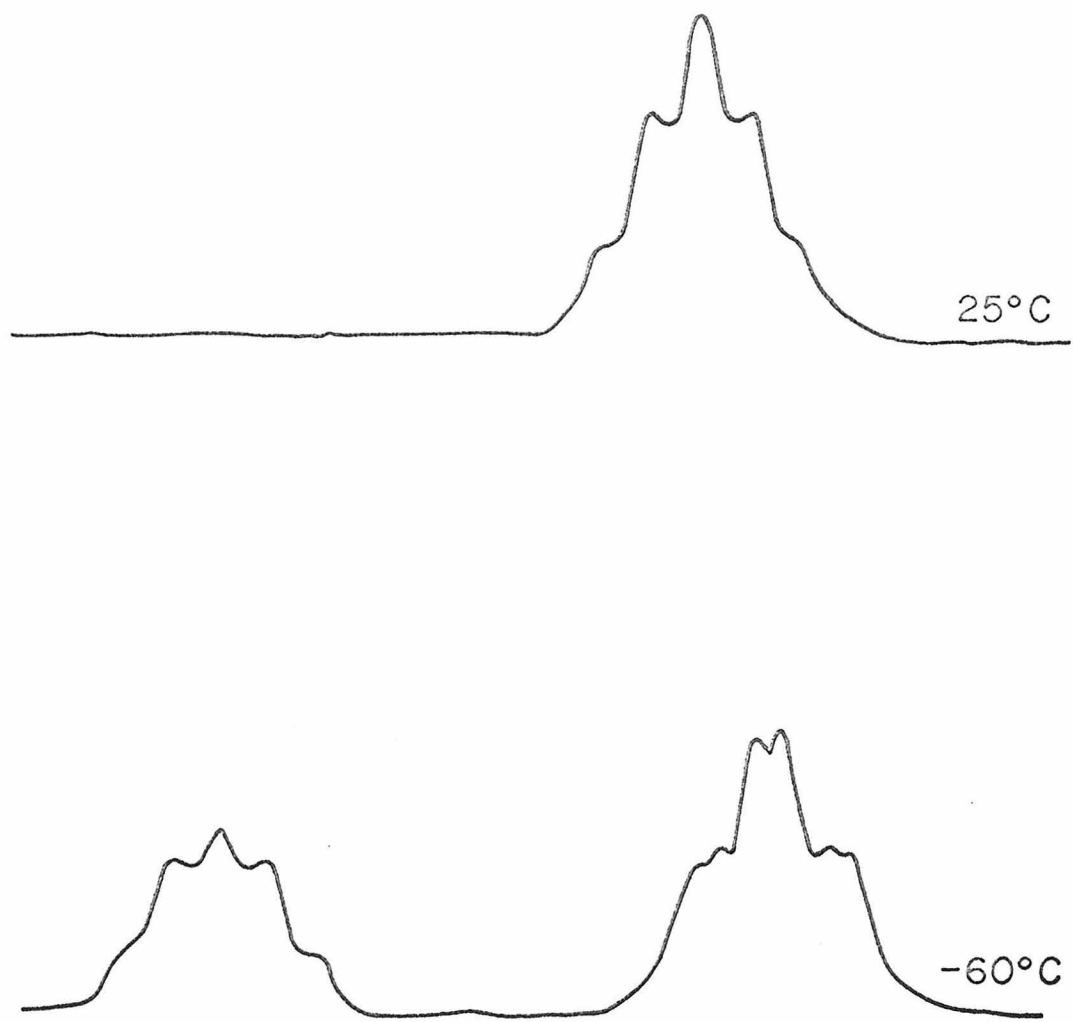


Figure 1. High-Field N.m.r. Spectrum of
 $\text{H}_2\text{Fe}((\text{C}_6\text{H}_5)\text{P}(\text{OC}_2\text{H}_5)_2)_4$

actual determinations apparently caused enough decomposition in the initial samples to lower the resolution.)

The infrared spectra of $\text{H}_2\text{Fe}((\text{C}_6\text{H}_5)\text{P}(\text{OC}_2\text{H}_5)_2)_4$ also indicated changes were taking place in solution. Spectra of Nujol mulls and KBr pellets of the compound in the solid state showed a broad, medium band at 1973 cm^{-1} which was tentatively assigned to the metal-hydrogen stretching frequency. In solution, however, this band disappeared, and the only band in the $1700 - 2200 \text{ cm}^{-1}$ region not observed in spectrum of the phosphine ligand was a weak, broad absorption including several peaks, the most prominent of these being observed at 1918 and 1946 cm^{-1} . By comparison with the intensities of several other peaks in the spectrum, the intensity of the Fe-H absorption in solution was found to be about half the intensity observed for $\nu(\text{Fe-H})$ in the spectrum of the solid.

Although it seemed apparent that a rearrangement was taking place, the evidence at this stage was insufficient to give a reasonable explanation of the observations. There were two apparent directions for further study. The crystals could be studied by x-ray diffraction, or solutions of the complex could be investigated by n.m.r. and ir. spectroscopy. An x-ray crystal structure of the complex would give the configuration of the molecule in the solid state, and might supply some hints for the elucidation of

the species in solution. An infrared and n.m.r. study might produce enough evidence to assign approximate configurations to the species in solution, but the configuration in the solid state still would be uncertain. It was decided to proceed along the former path for three reasons: A) the crystal structure of a complex transition metal dihydride had never been determined (23,41); such an investigation would serve as a test of the theory that cis dihydrides generally absorb infrared radiation in the 1800 - 2050 cm^{-1} region; B) crystals of $\text{H}_2\text{Fe}((\text{C}_6\text{H}_5)\text{P}(\text{OC}_2\text{H}_5)_2)_4$ are large, transparent, well-defined, and from all outward appearances generally well suited for x-ray investigation; and C) the necessary equipment for a thorough n.m.r. study was not readily available.

THE X-RAY CRYSTAL STRUCTURE OF $\text{H}_2\text{Fe}((\text{C}_6\text{H}_5)\text{P}(\text{OC}_2\text{H}_5)_2)_4$ Collection and Treatment of the Data

Since all of the observed iron-hydrogen stretching absorptions of this compound were located well within the 1800 - 2050 cm^{-1} range, this determination began and was carried out with the expectation that the two hydride ligands would be shown to have a cis configuration.

As noted, the crystals of $\text{H}_2\text{Fe}((\text{C}_6\text{H}_5)\text{P}(\text{OC}_2\text{H}_5)_2)_4$ are large, and in many cases, too large for accurate x-ray work. X-ray absorption by a large irregularly-shaped crystal alters the values of the recorded intensities, makes solution of the structure difficult, and in extreme cases, can yield an incorrect solution for the structure. For this reason, it is desirable to collect intensity data from small crystals which are at least approximately spherical in shape. Most of the crystals on hand at the beginning of this determination had at least one dimension equal to or

exceeding 1 mm. The optimum crystal thickness, defined as $2/\mu$ where μ equals the linear absorption coefficient, is found to be 0.69 mm for this compound. Several recrystallizations from absolute ethanol were required to obtain well-defined crystals that were small enough for investigation.

Since the crystals are moderately air sensitive, a means of protecting them from the atmosphere was necessary. The usual method of encapsulation in a glass capillary tube was found to be unsatisfactory. The very soft crystals could not be positioned firmly in a capillary tube because of their tendency to crumble as they were pushed into the tube. As an alternative, the crystals were mounted on thin glass fibers with a clear epoxy cement, and after the mounting cement had hardened, they were carefully coated with more cement. The mounting operation was carried out with an 8-inch aluminum foil wall built up around the microscope and mounting apparatus. A rapid flow of argon was admitted at the bottom of the chamber. Argon is denser than air, and thus kept the concentration of oxygen inside the walls much lower than that outside. Once a crystal was mounted, it was placed in an evacuated dessicator until the cement hardened. The coating procedure was carried out under the same conditions as mounting, and the crystals were stored under argon until the cement was fully cured.

Initial Weissenberg photographs indicated that the unit

cell was triclinic. In order to get accurate cell constants for data collection, it was necessary to obtain photographs along an additional two axes, requiring the mounting of several crystals at different angles. (Although in theory a precession camera could have been used to obtain the additional cell dimensions, in practice this was found to be a very difficult and time consuming procedure.) When, after some time, three suitable axes were located from the preliminary Weissenberg photographs, precision Weissenberg photographs were obtained of crystals mounted perpendicular to these axes. From a least-squares refinement of 20 values from the photographs, initial cell constants were obtained.

For the collection of intensity data, a crystal measuring 0.10 x 0.26 x 0.25 mm was mounted with its b axis parallel to the ϕ axis of the diffractometer. The b axis corresponds to the long axis of the crystal. Initially there was some difficulty in alignment because of confusion in the sign of the b axis, resulting eventually in the use of a left-handed cell. The cell dimensions used for the remainder of the determination were obtained from a least-squares refinement based on 20 values of 47 reflections measured on the diffractometer. The cell parameters are given in Table 1.

The experimental density was measured by the flotation

Table 1. Cell Parameters for $\text{H}_2\text{Fe}((\text{C}_6\text{H}_5)\text{P}(\text{OC}_2\text{H}_5)_2)_4$

$$\begin{array}{ll} a = 17.4945(30) \text{ \AA} & \alpha = 122.998(43)^\circ \\ b = 12.7325(74) & \beta = 90.207(36) \\ c = 11.9404(59) & \gamma = 94.441(39) \end{array}$$

Reduced Cell*:

$$\begin{array}{ll} a = 11.7938(34) \text{ \AA} & \alpha = 89.724(31)^\circ \\ b = 11.9397(63) & \beta = 94.966(27) \\ c = 17.4908(28) & \gamma = 115.135(32) \end{array}$$

* Derived from 25 2θ values

Index Relationships:

$$h_r = k + 1$$

$$k_r = -1$$

$$l_r = h$$

(The numbers in parentheses indicate the standard deviations of the final significant figures of each value.)

method using aqueous KI solutions. The experimental value was $1.24(5) \text{ gm/cm}^3$; using the cell constants from Table 1, a calculated density of 1.27 gm/cm^3 is obtained.

Intensity data were collected on a Datex-automated General Electric diffractometer using iron oxide-filtered cobalt radiation. Although molybdenum radiation is preferable in cases such as this where absorption may become important, the large unit cell precluded its use. The $\theta - 2\theta$ scanning mechanism was programmed with a scan range of 2 degrees at $2\theta = 4$ degrees to 4.5 degrees at $2\theta = 150$ degrees. The scanning speed was 2° per minute. Stationary background counts of 30 seconds each were obtained at the extremes of each scan.

Check reflections were monitored every twenty reflections, and indicated a 15% drop in intensity by the end of data collection. Subsequent examination of the crystal under a microscope indicated that the crystal had not been sealed off completely from the atmosphere, and that the intensity loss was probably due to decomposition by atmospheric oxygen rather than the x-rays. The linear absorption coefficient was calculated to be $\mu = 29 \text{ cm}^{-1}$, yielding transmission factors which varied from 0.45 to 0.74. A total of 5240 reflections were collected in 13 sets. The intensities of the reflections were scaled to the intensity of one of the check reflections which had been assigned a

fixed $|F|$ value (100.0) for all of the data sets. Lorentz and polarization corrections were applied to all the data, but no absorption corrections were made. The data were put on an approximately absolute scale with a Wilson plot; the over-all thermal parameter was $B = 1.93 \text{ \AA}^2$.

Application of the zero moment test (42) for a center of symmetry yielded a result which indicated that the cell was non-centrosymmetric. A visual test can also be made for a center of symmetry, since centrosymmetric cells usually give photographs which display reflections which have intensities varying over a wide range. Non-centrosymmetric cells, on the other hand, tend to have reflections which do not vary greatly in intensity. From this aspect, the cell appeared to be almost certainly centrosymmetric (43). The error in the statistical test was later found to be the result of a large number of positive high-angle reflections which were introduced by a high noise level in the data collection system. Near the end of the refinement, about eighty reflections were noted for which F_{calc} was at or near zero. As the 2θ value of these reflections increased, the F_{obs} values tended to increase also, indicating that the errors were in some way related to the length of the 2θ scan. Unfortunately, the errors were not consistent enough to allow suitable corrections to be made. Several attempts were made to find a satisfactory correction

function, but all tended to cause excessive corrections. The error introduced, however, did not become significant for most reflections until 2θ exceeded 100° ; therefore, in the final refinements of the structure the data were limited to those reflections with $2\theta < 103^\circ$ ($\sin \theta / \lambda < 0.436$, 3088 reflections).

The atomic scattering factors were taken from the International Tables for X-ray Crystallography (44); those of iron and phosphorus were corrected for the real part of anomalous dispersion. Although no corrections have been calculated for cobalt radiation, Cromer (45) has tabulated those for several other radiations including iron and copper. By extrapolation of these values, anomalous dispersion corrections were obtained for Fe and P using cobalt radiation. The values used were: for Fe, $\Delta f' = -3.55e^-$; for P, $\Delta f' = 0.30e^-$.

Using the entire data set (5240 reflections) a sharpened three-dimensional Patterson map was calculated. Eight major peaks were observed at distances from the origin of about $2 \overset{\circ}{\text{A}}$, the approximate Fe-P bond distance. By examination of the various possible vectors between these images of the phosphorus atoms it was possible to separate the eight vectors into two groups of four vectors each. One group corresponded to the Fe_1 to P_1 vectors, the other to the P_1 - Fe_1 vectors. Thus, at this stage, the configuration

of the phosphorus atoms about the iron atom was determined. It was found to be approximately tetrahedral, with one angle of the tetrahedron opened to about 135° . This configuration had been predicted for the structure of the analogous complexes $\text{H}_2\text{Fe}(\text{CO})_4$ (23) and $\text{H}_2\text{Fe}(\text{PF}_3)_4$ (3).

Although the location of the Fe-P vectors presented no difficulty, the location of the important $\text{Fe}_1\text{-Fe}_2$ vector was more complex. The large number of possible Fe-Fe vectors in the map made selection of symmetry related pairs very difficult. Several attempts at phasing using different $\text{Fe}_1\text{-Fe}_2$ vectors as the bases for determining the iron position failed to produce models which could be refined to realistic structures.

The difficulties encountered in the assignment of the Patterson vectors led to an attempt to phase the data using the symbolic addition method (96). Only 418 reflections were used in the determination and thus the positions of any atoms revealed would at best be approximate. The cell was assumed to be centrosymmetric since this greatly simplified the operation. When the addition procedure was complete, two possible phasing assignments were found to have low conflict ratios. Both of these were used to phase the reflections and a Fourier map was calculated for each case. In retrospect, it can be seen that one map approximated the actual atomic positions rather well,

but due to the distortion and the high noise level, this was not obvious at the time.

A second attempt was made to determine the position of the $\text{Fe}_1\text{-Fe}_2$ vector from the sharpened Patterson map. Instead of searching specifically for the $\text{Fe}_1\text{-Fe}_2$ vector, all the possible vectors corresponding to a reasonable distance between iron atoms ($7 - 11 \text{ \AA}$) were tentatively assumed to be Fe_1 to P_2 vectors, that is, vectors from the iron atom of molecule 1 (at the origin) to the phosphorus atoms of molecule 2. For a centrosymmetric cell, the endpoints of four of these " Fe_1 to P_2 " vectors should have the same spatial configuration as the images of the four P_1 atoms located about the origin. In order to identify these four endpoints, all possible vectors were calculated between the endpoints of the 14 most intense " $\text{Fe}_1\text{-P}_2$ " vectors. The resulting vectors were then compared to the analogous vectors calculated between the images about the origin of the four P_1 atoms. Eventually, four endpoints of " $\text{Fe}_1\text{-P}_2$ " vectors were found which had the same localized spatial arrangement as the endpoints of the four Fe_1 to P_1 vectors and which were related to them by a center of symmetry. The Fe_1 to Fe_2 vector was then found by extrapolation. The image of the Fe_1 to Fe_2 vector appeared as a shoulder on a larger peak resulting from the superposition of Fe-P and P-P vectors.

The positional parameters of the iron atom and the four phosphorus atoms derived from the Patterson map, along with the average isotropic temperature factor from the Wilson plot were used in a calculation of structure factors. The R at this stage was 0.52. Three successive calculations of structure factors interspersed with Fourier syntheses provided the positions of the remaining non-hydrogen atoms. With all of these atoms included in the input of the structure factor calculation, the R stood at 0.30. Adjustment of the scale factor and refinement of the positional parameters using a difference Fourier map reduced the R to 0.24. A full-matrix least-squares refinement of the positional parameters and their isotropic temperature factors yielded an R of 0.19.

At this point in the refinement, the poor quality of the higher-angle data was realized. The full data set was not used during the final stages of refinement except for one instance in which it was used to investigate the nature of the errors at high values of 2θ (see above). The remaining procedures were carried out using the reduced data set of 3088 reflections ($2\theta < 103^\circ$).

Anisotropic thermal parameters were then introduced for all of the non-hydrogen atoms. This greatly increased the number of parameters to be refined, from 213 to 531. As a result, it was necessary to refine the parameters in

three successive operations. First, the positional parameters of the 53 non-hydrogen atoms were refined while the scale factor and anisotropic thermal parameters were held constant. Second, the thermal parameters of 30 of the atoms plus the scale factor were refined with the previously refined positional parameters and the remaining thermal parameters being held constant. Third, the thermal parameters of the remaining atoms plus the scale factor (and any of the thermal parameters from the previous step which underwent large shifts) were refined with the previously refined positional parameters and thermal parameters being held constant. After one complete refinement operation, the R stood at 0.15.

The ethyl and phenyl hydrogen atoms were then added to the least-squares input as fixed contributions. They were positioned according to their known geometries with the carbon-hydrogen distance in the phenyl rings assumed to be 0.9 \AA and the carbon-hydrogen distance in the ethyl group assumed to be 1.09 \AA . The methyl group hydrogen atoms were staggered with respect to the oxygen atom. Each hydrogen atom was assigned an isotropic temperature factor 1 \AA^2 greater than the final isotropic value calculated for the carbon to which it was bonded. Following the inclusion of the phenyl and ethyl hydrogen atoms and the completion of 3 complete cycles of least-squares

refinement, the R was reduced to 0.092.

A difference Fourier map was then calculated in an attempt to determine the positions of the hydrogen atoms coordinated to the iron atom. The most prominent features of the map were two peaks, of height 0.67 and 0.49 $e^{-}/\text{\AA}^3$, in the regions expected for the hydrogen atoms. Four other peaks on the map exceeded 0.40 $e^{-}/\text{\AA}^3$; these were associated with remote ethoxy and phenyl carbon atoms which displayed particularly high anisotropic thermal parameters. A second difference Fourier map was calculated (47), limiting the data to those reflections having $\sin \theta / \lambda$ less than 0.346 ($2\theta < 77^\circ$). The two peaks near the iron atom were again the most prominent of the map, at 0.41 and 0.29 $e^{-}/\text{\AA}^3$, but the next highest peaks of this map did not correspond to those of the previous map. The two peaks were the largest in volume as well as intensity in both of the maps, leading to the conclusion that they indeed represented the ligand hydrogen atom peaks.

The coordinates of the two hydrogens were included in the last two cycles of the least-squares refinement; each atom was assigned an isotropic thermal parameter of 4\AA^2 . The R value from the final structure factor calculated was 0.091; the goodness of fit for the final refinement was 3.26. The highest peak on the final difference Fourier map was 0.47 $e^{-}/\text{\AA}^3$. The rather high R value at

the end of the refinement can be traced to two possible sources of error. The slow decomposition of the crystal might be considered as one source, although the scaling procedure used should minimize this problem. The more important problem was that of the noise in the 2θ scanning mechanism, which undoubtedly caused some very large errors in the intensities of high-angle and weak reflections. After the refinement was complete, a structure factor calculation was made using only those reflections for which $F_{\text{obs}} > 20$ (2320 reflections). The R value derived from this calculation was 0.059. Absorption of x-rays due to the irregular shape of the crystal might also have introduced some error, but an examination of the derived anisotropic thermal ellipsoids (see below) indicates that the error introduced by absorption was small.

A second collection of data in order to get better agreement between the observed and calculated structure factors was considered, but the structure has now been investigated by other workers (48). The agreement of parameters derived from the two separate determinations is quite good (49); a joint publication is presently in preparation.

Description of the Structure

The structure of the crystal consists of discrete monomeric units, the closest Fe-Fe distance being $9.606(2)\text{\AA}$. The interatomic distances and angles are presented in Tables 2 and 3. The standard deviations are derived from the standard deviations of the x, y, and z parameters of the final least-squares refinement. The root-mean-square amplitudes of vibration of the thermal ellipsoids are given in Table 4. Tables of structure factors, positional and anisotropic thermal parameters, and the derived parameters for the phenyl and ethyl hydrogen atoms are given in Appendix I. The inner coordination of the iron atom is shown in Figure 2. The configuration is that of a distorted tetrahedron of phosphorus atoms with the hydrogen atoms occupying two of the tetrahedral faces. The two phosphorus atoms common to both of these faces form a P-Fe-P angle of $136.6(1)^\circ$, a distortion of 27° from the normal tetrahedral angle.

The average Fe-P bond distance of $2.138(3)\text{\AA}$ compares

Table 2. Interatomic Distances in $\text{H}_2\text{Fe}((\text{C}_6\text{H}_5)\text{P}(\text{OC}_2\text{H}_5)_2)_4$
(in Angstroms)

FE - FE	9.606 (2)	C4 - C5	1.361 (17)
FE - P1	2.132 (3)	C5 - C6	1.385 (18)
FE - P2	2.127 (2)	C6 - C1	1.365 (14)
FE - P3	2.146 (3)	P2 - O3	1.618 (5)
FE - P4	2.147 (3)	O3 - C17	1.404 (11)
FE - H1	1.435 (59)	C17 - C18	1.495 (13)
FE - H1	1.457 (--)*	P2 - O4	1.618 (7)
FE - H2	1.562 (73)	O4 - C19	1.441 (11)
FE - H2	1.542 (--)*	C19 - C20	1.403 (18)
P1 - P2	3.957 (3)	P2 - C11	1.830 (9)
P1 - P3	3.221 (3)	C11 - C12	1.360 (12)
P1 - P4	3.472 (4)	C12 - C13	1.374 (14)
P1 - H1	2.248 (65)	C13 - C14	1.353 (16)
P1 - H1	2.093 (--)*	C14 - C15	1.348 (17)
P1 - H2	2.259 (58)	C15 - C16	1.366 (17)
P1 - H2	2.328 (--)*	C16 - C11	1.392 (12)
P2 - P3	3.462 (3)	P3 - O5	1.621 (6)
P2 - P4	3.260 (3)	O5 - C27	1.439 (11)
P2 - H1	2.111 (58)	C27 - C28	1.451 (14)
P2 - H1	2.202 (--)*	P3 - O6	1.619 (7)
P2 - H2	2.296 (70)	O6 - C29	1.427 (10)
P2 - H2	2.175 (--)*	C29 - C30	1.458 (16)
P3 - P4	3.343 (4)	P3 - C21	1.841 (8)
P3 - H1	3.542 (62)	C21 - C22	1.378 (14)
P3 - H1	3.509 (--)*	C22 - C23	1.376 (14)
P3 - H2	2.518 (57)	C23 - C24	1.329 (19)
P3 - H2	2.578 (--)*	C24 - C25	1.347 (17)
P4 - H1	2.682 (66)	C25 - C26	1.365 (13)
P4 - H1	2.865 (--)*	C26 - C21	1.353 (15)
P4 - H2	3.703 (74)	P4 - O7	1.634 (5)
P4 - H2	3.761 (--)*	O7 - C37	1.433 (12)
H1 - H2	1.909 (104)	C37 - C38	1.468 (13)
H1 - H2	1.680 (--)*	P4 - O8	1.614 (6)
P1 - O1	1.614 (5)	O8 - C39	1.367 (10)
O1 - C7	1.418 (12)	C39 - C40	1.401 (18)
C7 - C8	1.438 (15)	P4 - C31	1.817 (9)
P1 - O2	1.631 (6)	C31 - C32	1.393 (12)
O2 - C9	1.404 (15)	C32 - C33	1.379 (14)
C9 - C10	1.423 (15)	C33 - C34	1.356 (16)
P1 - C1	1.807 (11)	C34 - C35	1.351 (17)
C1 - C2	1.373 (13)	C35 - C36	1.372 (15)
C2 - C3	1.382 (20)	C36 - C31	1.388 (14)
C3 - C4	1.359 (18)		

* Derived from difference Fourier parameters.

Table 3. Interatomic Angles of $\text{H}_2\text{Fe}((\text{C}_6\text{H}_5)\text{P}(\text{OC}_2\text{H}_5)_2)_4$

P1	-	FE	-	P2	136.6 (1)
P1	-	FE	-	P3	97.7 (1)
P1	-	FE	-	P4	108.4 (1)
P1	-	FE	-	H1	75.3 (26)
P1	-	FE	-	H1	68.4 (--)*
P1	-	FE	-	H2	73.6 (21)
P1	-	FE	-	H2	76.8 (--)*
P2	-	FE	-	P3	108.3 (1)
P2	-	FE	-	P4	99.4 (1)
P2	-	FE	-	H1	69.6 (23)
P2	-	FE	-	H1	73.2 (--)*
P2	-	FE	-	H2	75.3 (23)
P2	-	FE	-	H2	70.7 (--)*
P3	-	FE	-	P4	102.3 (1)
P3	-	FE	-	H1	162.8 (31)
P3	-	FE	-	H1	153.4 (--)*
P3	-	FE	-	H2	83.9 (22)
P3	-	FE	-	H2	87.1 (--)*
P4	-	FE	-	H1	94.9 (30)
P4	-	FE	-	H1	103.6 (--)*
P4	-	FE	-	H2	172.9 (23)
P4	-	FE	-	H2	168.3 (--)*
H1	-	FE	-	H2	79.0 (37)
H1	-	FE	-	H2	68.1 (--)*
O1	-	P1	-	O2	101.3 (3)
C1	-	P1	-	O2	94.2 (4)
O1	-	P1	-	C1	100.7 (4)
P1	-	O1	-	C7	123.6 (6)
O1	-	C7	-	C8	109.9 (9)
P1	-	O2	-	C9	123.2 (6)
O2	-	C9	-	C10	112.8 (11)
P1	-	C1	-	C4	177.1 (5)
P1	-	C1	-	C2	124.4 (8)
P1	-	C1	-	C6	119.3 (8)
C6	-	C1	-	C2	116.3 (10)
C1	-	C2	-	C3	121.6 (10)
C2	-	C3	-	C4	120.5 (11)
C3	-	C4	-	C5	119.4 (14)
C4	-	C5	-	C6	119.1 (11)
C5	-	C6	-	C1	123.0 (10)
O3	-	P2	-	O4	102.6 (3)

* Derived from difference Fourier parameters.

Table 3. Continued

03	-	P2	-	C11	94.9 (3)
04	-	P2	-	C11	100.8 (4)
P2	-	03	-	C17	121.4 (5)
03	-	C17	-	C18	110.3 (8)
P2	-	04	-	C19	122.4 (6)
04	-	C19	-	C20	112.7 (8)
P2	-	C11	-	C14	176.3 (6)
P2	-	C11	-	C12	120.0 (7)
P2	-	C11	-	C16	123.5 (7)
C12	-	C11	-	C16	116.5 (8)
C11	-	C12	-	C13	122.7 (9)
C12	-	C13	-	C14	118.8 (9)
C13	-	C14	-	C15	120.9 (11)
C14	-	C15	-	C16	119.9 (10)
C15	-	C16	-	C11	121.2 (9)
05	-	P3	-	06	101.2 (3)
05	-	P3	-	C21	99.7 (3)
06	-	P3	-	C21	94.1 (4)
P3	-	05	-	C27	123.0 (6)
05	-	C27	-	C28	111.9 (9)
P3	-	06	-	C29	123.4 (6)
06	-	C29	-	C30	109.9 (8)
P3	-	C21	-	C22	118.8 (8)
P3	-	C21	-	C26	124.4 (7)
C22	-	C21	-	C26	116.8 (8)
C22	-	C23	-	C24	121.2 (10)
C23	-	C24	-	C25	118.1 (10)
C24	-	C25	-	C26	122.0 (12)
C25	-	C26	-	C21	120.9 (10)
07	-	P4	-	08	99.7 (3)
07	-	P4	-	C31	98.8 (3)
08	-	P4	-	C31	95.7 (4)
P4	-	07	-	C37	122.6 (5)
07	-	C37	-	C38	109.8 (9)
P4	-	08	-	C39	129.1 (7)
08	-	C39	-	C40	115.9 (10)
P4	-	C31	-	C32	120.8 (7)
P4	-	C31	-	C36	123.4 (6)
C32	-	C31	-	C36	115.8 (8)
P4	-	C31	-	C34	178.4 (5)
C31	-	C32	-	C33	122.2 (9)
C32	-	C33	-	C34	119.3 (9)
C33	-	C34	-	C35	120.6 (11)
C34	-	C35	-	C36	120.2 (11)
C35	-	C36	-	C31	121.8 (9)

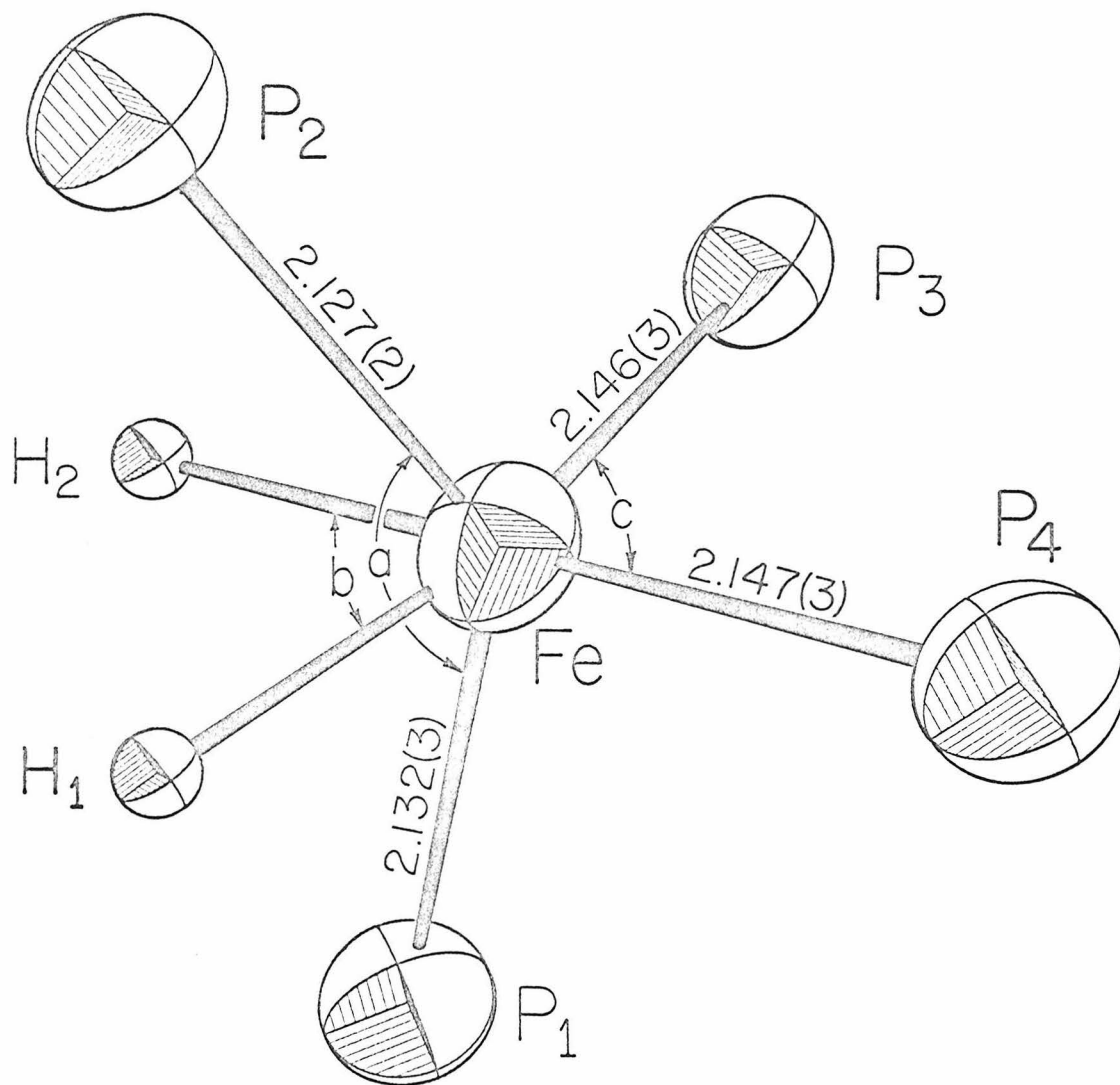


Figure 2. Inner Coordination Sphere of the Iron Atom in $\text{H}_2\text{Fe}((\text{C}_6\text{H}_5)\text{P}(\text{OC}_2\text{H}_5)_2)_4$

$$a = 136.6(1)^\circ$$

$$b = 79(4)$$

$$c = 102.3(1)$$

Table 4. Root-Mean-Square Amplitudes of Vibration of the
Thermal Ellipsoids of $\text{H}_2\text{Fe}((\text{C}_6\text{H}_5)\text{P}(\text{OC}_2\text{H}_5)_2)_4$
(in Angstroms)

FE	0.16765	0.18817	0.21571
P1	0.19190	0.21779	0.22488
P2	0.17951	0.20767	0.22315
P3	0.18247	0.19685	0.21942
P4	0.19532	0.20379	0.21317
O1	0.17285	0.23074	0.29493
O2	0.18502	0.25206	0.33072
O3	0.17188	0.24485	0.25967
O4	0.15745	0.20900	0.28224
O5	0.20110	0.20352	0.23504
O6	0.15409	0.20957	0.27831
O7	0.16379	0.20887	0.26935
O8	0.16116	0.22746	0.31908
C1	0.17934	0.23412	0.26076
C2	0.22234	0.25905	0.33649
C3	0.21828	0.32496	0.37258
C4	0.17836	0.29745	0.38664
C5	0.25628	0.28902	0.32387
C6	0.16858	0.28785	0.32844
C7	0.23509	0.29244	0.32961
C8	0.22386	0.36670	0.39598
C9	0.23077	0.30085	0.40880
C10	0.23469	0.35353	0.50130
C11	0.19483	0.20539	0.26228
C12	0.18036	0.24918	0.29758
C13	0.22579	0.30912	0.32894
C14	0.17798	0.34154	0.39964
C15	0.20410	0.35529	0.41377
C16	0.18453	0.27884	0.36411
C17	0.18163	0.25149	0.28666
C18	0.22053	0.27905	0.29327
C19	0.15965	0.26229	0.41389
C20	0.17908	0.32226	0.40677
C21	0.17842	0.18209	0.24660
C22	0.20685	0.22398	0.38262
C23	0.18177	0.27566	0.42362
C24	0.20751	0.28607	0.38641
C25	0.16742	0.29878	0.39309
C26	0.17988	0.23482	0.34878

Table 4. Continued

C27	0.19645	0.27169	0.32011
C28	0.22758	0.25469	0.30278
C29	0.20684	0.24573	0.33374
C30	0.18537	0.28039	0.35661
C31	0.15165	0.20176	0.24593
C32	0.21039	0.22417	0.27697
C33	0.21301	0.25302	0.34712
C34	0.20064	0.22640	0.41586
C35	0.20879	0.25074	0.38119
C36	0.20653	0.25302	0.29337
C37	0.18880	0.27107	0.30180
C38	0.18890	0.32353	0.39512
C39	0.17203	0.27908	0.34373
C40	0.22194	0.33876	0.39232

with 2.23 Å for $C_5H_5Fe(C_6H_5)CO(P(C_6H_5)_3)_5$ (50,51), 2.15 Å for $C_5H_5Fe(P(OC_6H_5)_3)_2I$ (52), and 2.25 Å for $Fe_3(CO)_{11}P(C_6H_5)_3$ (53). Although the estimated accuracy of these literature values was not reported, it appears that the iron-phosphorus bond is somewhat shorter for phosphite ligands than it is for phosphines. This is consistent with the expectation that the inductive effects of the electronegative oxygens increase the metal to phosphorus back donation, and thus shorten the Fe-P bond. The Fe-P bond distances trans to the hydride ligands are slightly, though significantly, longer than those which are cis; the trans Fe-P distances are 2.132(3) and 2.127(2) Å, while the cis bond distances are 2.146(3) and 2.147(3) Å. Presumably, the longer bond distances for the trans ligands result from the strong trans influence of the hydride ligand (2).

The average Fe-H bond length of 1.499(66) Å is not significantly different from the metal-hydrogen distances reported for $HRh(CO)(P(C_6H_5)_3)_3$ 1.6(1) Å (x-ray) (47), $HCo(N_2)(P(C_6H_5)_3)_3$ 1.6(1) Å (x-ray) (54), and $HMn(CO)_5$ 1.601(16) Å (neutron diffraction) (26). It should be noted that x-ray diffraction depends upon scattering by electrons and that the positions of maximum electron density are generally assumed to be the positions of the corresponding nuclei. In the case of the electron-poor

hydrogen atom, especially when it is bonded to a much heavier atom, the indicated electron density maximum does not necessarily coincide with the proton position. For this reason, it is doubtful that an x-ray determined iron-hydrogen bond distance can be accurate to more than 0.1 \AA . A more reasonable value of the Fe-H bond distance would then be $1.5(1) \text{ \AA}$, in agreement with the corrected Fe-H distance derived from the broad-line p.m.r. spectrum of $\text{H}_2\text{Fe}(\text{CO})_4$ (see above).

The structures of the ligand has been determined previously in an x-ray study of $\text{Ni}(\text{CN})_2(\text{P}(\text{C}_6\text{H}_5)(\text{OC}_2\text{H}_5)_2)_3$ (55). Table 5 compares average bond distances for the ligand derived from the crystal structures of the nickel complex just mentioned, the present iron complex, and a cobalt complex reported below.

Clearly, the carbon-carbon distances are unrealistic, especially in the case of the ethoxy groups. The shortened distances are probably the result of partial disordering in the ethoxy and phenyl groups (55). As might be expected, the average of the relatively rigid phenyl carbon-carbon distances is only 0.02 \AA shorter than the usual 1.39 \AA , while the average of the less restricted ethoxy carbon-carbon distances is 0.10 \AA shorter than the usually quoted 1.54 \AA value.

If all P-O distances are assumed to be equivalent,

Table 5. Average Bond Distances in Coordinated
 $C_6H_5P(OC_2H_5)_2$

<u>Bond</u>	<u>Ni(CN)₂L₃*</u>	<u>H₂FeL₄</u>	<u>HCoL₄</u>
P-O	1.58 Å ^o	1.62 Å ^o	1.63 Å ^o
P-C	1.79	1.82	1.83
O-C	1.45	1.42	1.42
ethyl C-C	1.43	1.44	1.41
phenyl C-C	-----	1.37	1.37

* from Ref. 55

the standard deviation from the mean is found to be 0.020 \AA . This is 3 to 4 times the standard deviations derived from the least-squares refinement. Similarly, if all P-C distances are assumed equal, the standard deviation from the mean is 0.026 \AA , about 3 times the values derived from the least-squares. Thus, the standard deviations reported for these bonds in Table 2 are underestimated by a factor of approximately 4, probably as a result of some disorder in the carbon and oxygen atom positions. Similar behavior is displayed by the carbon atoms of $\text{ReNCI}_2(\text{P}(\text{C}_2\text{H}_5)_2\text{C}_6\text{H}_5)_3$ (56).

A stereoscopic view of the H_2FeL_4 molecule is given in Figure 3. Atoms P3, P4, Fe, H1, and H2 are roughly planar, the maximum deviation from the least-squares plane being 0.05 \AA . The atomic deviations from this least-squares plane, as well as those of the four phenyl rings, are given in Table 6. As can be seen from the Figure, the configuration of the four phosphorus atoms about the iron atom is nearly tetrahedral. The deviations from the normal tetrahedral angle vary from 1 to 27° . (In the iso-electronic cobalt complex, $\text{HCo}((\text{C}_6\text{H}_5)\text{P}(\text{OC}_2\text{H}_5)_2)_4$ (see below) the range of deviations is reduced to 1 to 15° . The corresponding nickel complex, $\text{Ni}((\text{C}_6\text{H}_5)\text{P}(\text{OC}_2\text{H}_5)_2)_4$, is very probably tetrahedral, although twinning problems have prevented any direct confirmation by x-ray diffraction.)

Table 6. Deviations from Least-Squares Planes in
 $\text{H}_2\text{Fe}((\text{C}_6\text{H}_5)\text{P}(\text{OC}_2\text{H}_5)_2)_4$
 (in Angstroms)

EQUATORIAL PLANE

ATOM	DEVIATION
FE	0.0114
P3	0.0251
P4	-.0288
H1	0.0429
H2	-.0506

RING 1		RING 2	
ATOM	DEVIATION	ATOM	DEVIATION
C1	-.0009	C11	-.0119
C2	-.0017	C12	0.0097
C3	0.0025	C13	-.0029
C4	-.0008	C14	-.0015
C5	-.0018	C15	-.0012
C6	0.0026	C16	0.0077

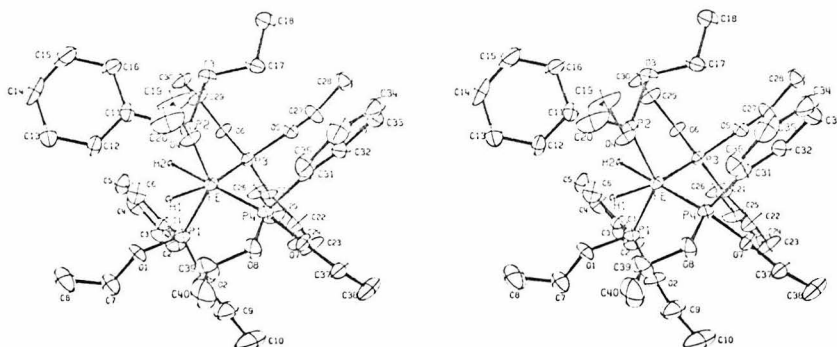
RING 3		RING 4	
ATOM	DEVIATION	ATOM	DEVIATION
C21	0.0026	C31	-.0067
C22	-.0031	C32	-.0042
C23	0.0049	C33	0.0047
C24	-.0062	C34	0.0058
C25	0.0058	C35	-.0170
C26	-.0040	C36	0.0174

The hydrogen atoms occupy two faces of the tetrahedral skeleton, distorting the common P1-Fe-P2 angle to $136.6(1)^\circ$.

Alternatively, the configuration of the complex could be considered as a highly distorted octahedron. In view of the general tendency toward tetrahedral coordination of the non-hydrogen ligands in complexes of this type, the tetrahedral skeleton provides the more realistic model.

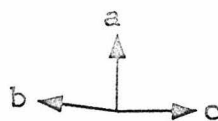
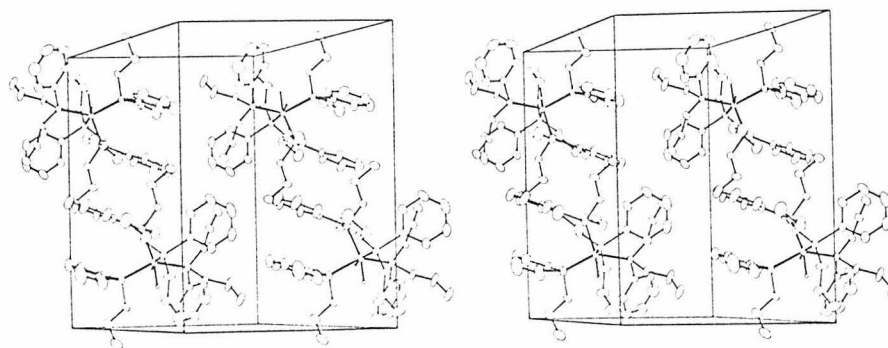
From the root-mean-square amplitudes of vibration of the thermal ellipsoids (Table 4) and the stereoscopic drawing of the molecule (Figure 3), it can be seen that the thermal ellipsoids are greatest for carbon atoms far removed from the iron atom. Again it appears likely that many of these atoms suffer at least partially from disorder. The absence of any correction for absorption casts some doubt on the values derived for the thermal parameters. However, comparison of the vibrations of this molecule with those of the very similar $\text{HCo}((\text{C}_6\text{H}_5)\text{P}(\text{OC}_2\text{H}_5)_2)_4$ molecule (see below), shows that the directions of the vibrations, if not the magnitudes, are nearly identical. The crystal sizes and shapes for the two determinations were quite different and would be expected to yield different directions for the thermal vibrations if absorption was a major problem. The similarity of the thermal vibrations in the two structures can then be taken as an indication that absorption was only of minor importance.

Figure 3. Stereoscopic Drawing of $\text{H}_2\text{Fe}((\text{C}_6\text{H}_5)\text{P}(\text{OC}_2\text{H}_5)_2)_4$

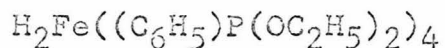


A stereoscopic drawing of the unit cell is given in Figure 4. Because of the large distance between molecules and the bulk of the phosphonite ligands, there is no apparent intermolecular interaction between hydride ligands. Such an interaction has been suggested for $\text{HMn}(\text{CO})_5$ (26).

Figure 4. Stereoscopic Drawing of the Unit Cell of
 $\text{H}_2\text{Fe}((\text{C}_6\text{H}_5)\text{P}(\text{OC}_2\text{H}_5)_2)_4$



DISCUSSION OF THE SPECTRAL PROPERTIES OF



As the x-ray structure determination was drawing to a close, a paper reporting the n.m.r. spectrum of $\text{H}_2\text{Fe}((\text{C}_6\text{H}_5)\text{P}(\text{OC}_2\text{H}_5)_2)_4$ was published (29). The authors of the paper observed the same basic features in the spectrum that we had observed earlier, although the chemical shifts reported differ from our values by about 0.5 ppm. (More recent determinations in our laboratory are in much better agreement with the reported values.) In the spectrum at -50°C , the triplet of doublets ($\tau = 22.93$) was assigned to a cis configuration, and the symmetric quintet ($\tau = 20.55$) to a trans isomer. The ^{31}P spectrum was consistent with the cis assignment, but a definitive resonance for the "trans" isomer could not be detected, presumably because of line broadening effects. A broad, featureless rise in the baseline was assigned to the "trans" isomer.

In view of the n.m.r. evidence presented, and the

known cis configuration of the molecule in the solid state, the assignment of the triplet of doublets to a cis isomer is probably correct (57). The assignment of the symmetric quintet to a trans isomer is more difficult to evaluate. Clearly the five line spectrum observed implies that the phosphorus atoms are equivalent, and an octahedral trans isomer obviously should lead to such a situation. In the present case, however, some assumptions have to be made in view of the steric difficulties in having four phosphonite ligands in the same plane. The authors concluded that the four phosphorus ligands in the "trans" isomer were undergoing rapid intramolecular exchange.

As mentioned in the introduction, there appears to be an additional means of differentiating cis and trans dihydride isomers, namely the infrared spectrum in the metal-hydrogen stretching region. Table 7 gives the reported values of ν (M-H) for dihydride complexes containing phosphorus ligands. The absorptions listed for compounds I through VIII are generally very intense and sharp. As an example, the peak at 1642 cm^{-1} in compound III is one of the strongest bands in the spectrum, almost equal in intensity to the very strong P-O-C absorption at 1030 cm^{-1} . The Raman spectrum displays a strong band at 1886 cm^{-1} (40). It is unusual for the symmetric stretch to be observed at a higher energy than the asymmetric

Table 7. Metal-Hydrogen Stretching Frequencies for Complex Metal Dihydrides

	<u>Compound</u>	<u>ν (M-H) cm^{-1}</u>	<u>Ref.</u>
<u>I</u>	$\text{H}_2\text{Ru}(\text{C}_2\text{H}_4(\text{PEt}_2)_2)_2$	1615	59
<u>II</u>	$\text{H}_2\text{Ru}(\text{o-C}_6\text{H}_4(\text{PEt}_2)_2)_2$	1617*	59
<u>III</u>	$\text{H}_2\text{Ru}(\text{C}_6\text{H}_5\text{P}(\text{OEt})_2)_4$	1643	40
<u>IV</u>	$\text{H}_2\text{Pt}(\text{PEt}_3)_2$	1670	60,61
<u>V</u>	$\text{H}_2\text{Os}(\text{Ph}_2\text{PCH}_2\text{PPh}_2)_2$	1712	62
<u>VI</u>	$\text{H}_2\text{Os}(\text{o-C}_6\text{H}_4(\text{PEt}_2)_2)_2$	1720*	59
<u>VII</u>	$\text{H}_2\text{Os}(\text{C}_2\text{H}_4(\text{PEt}_2)_2)_2$	1721	59
<u>VIII</u>	$\text{H}_2\text{Fe}(\text{o-C}_6\text{H}_4(\text{PEt}_2)_2)_2$	1726	28,30,31
<u>IX</u>	$\text{H}_2\text{Ru}((\text{C}_6\text{H}_5)_2\text{PCH}_3)_4$	1940,1885	57
<u>X</u>	$\text{H}_2\text{Fe}(\text{PF}_3)_4$	1935	3
<u>XI</u>	$\text{H}_2\text{Fe}(\text{C}_6\text{H}_5\text{P}(\text{OEt})_2)_4$	1973	--
<u>XII</u>	$\text{H}_2\text{IrCl}(\text{C}_6\text{H}_5\text{PEt}_2)_3$	2162,2026	21
<u>XIII</u>	$\text{H}_2\text{IrCl}(\text{PPh}_3)_3$	2215,2110	63,64
<u>XIV</u>	$\text{H}_2\text{PtCl}_2(\text{PEt}_3)_2$	2254,2265 _{sh}	65

* in benzene solution

stretch, but similar relationships have been observed in cases involving carbonyls. Such a relationship implies that as the bond strength of one M-H bond increases, the strength of the other decreases, in agreement with the behavior expected from consideration of the trans influence of the hydride ligand (58). The bands reported for compounds IX through XIV are only weak to medium in intensity. In some cases, two bands are observed; for others, only one broad band is detected. These observations are consistent with the belief that in compounds I through VIII the hydride ligands have a trans configuration, and in compounds IX through XIV a cis configuration. The x-ray crystal structure described above for compound XI is in agreement with the cis structure predicted from the metal-hydrogen stretching frequency.

It should be noted that at present structural data are available for only one of the trans dihydride complexes, compound III. Preliminary results indicate that the complex is indeed trans. The P-Ru-P angle is approximately 160° , indicating only a 20° distortion from the regular octahedral geometry (49).

An interesting aspect of the infrared study of compound III is that in the spectrum of a solution of III (in methylcyclohexane) the intense band at 1643 cm^{-1} is absent, and a very broad, weak band is observed at 1895 cm^{-1}

(40). This implies that the trans isomer has rearranged in solution to form a species in which there is no longer a strong trans interaction between the hydride ligands. Such a rearrangement is apparently not universal for this type of complex, since strong, low energy metal hydride absorptions have been observed for both II and VI in benzene solution. The n.m.r. spectrum of $\text{H}_2\text{Ru}((\text{C}_6\text{H}_5)\text{P}(\text{OC}_2\text{H}_5)_2)_4$ reportedly shows the presence of cis and trans isomers in solution (48); no details were given.

The subject of the present work, $\text{H}_2\text{Fe}((\text{C}_6\text{H}_5)\text{P}(\text{OC}_2\text{H}_5)_2)_4$ X in Table 7, displays an infrared spectrum which is markedly different from that of its ruthenium analog (see Figure 5). By comparison with the spectrum of the dideuteride complex, it is possible to assign the rather broad band at 1973 cm^{-1} to the iron-hydrogen stretching mode. In the Raman spectrum a band of similar shape and intensity is observed at 1978 cm^{-1} . The $\nu(\text{M-D})$ absorption could only be detected as a broadening of a ligand C-C band at 1434 cm^{-1} . Although the intensities and shapes of several bands were altered on conversion of the hydride to the deuteride, it was not possible to isolate the P-Fe-H bending mode. Because of the low symmetry of the molecule, extensive mixing of the bending modes is expected.

The spectra of the complex in solution are quite different (compare Figures 6 and 7). At $290^\circ\text{K}(17^\circ\text{C})$ only

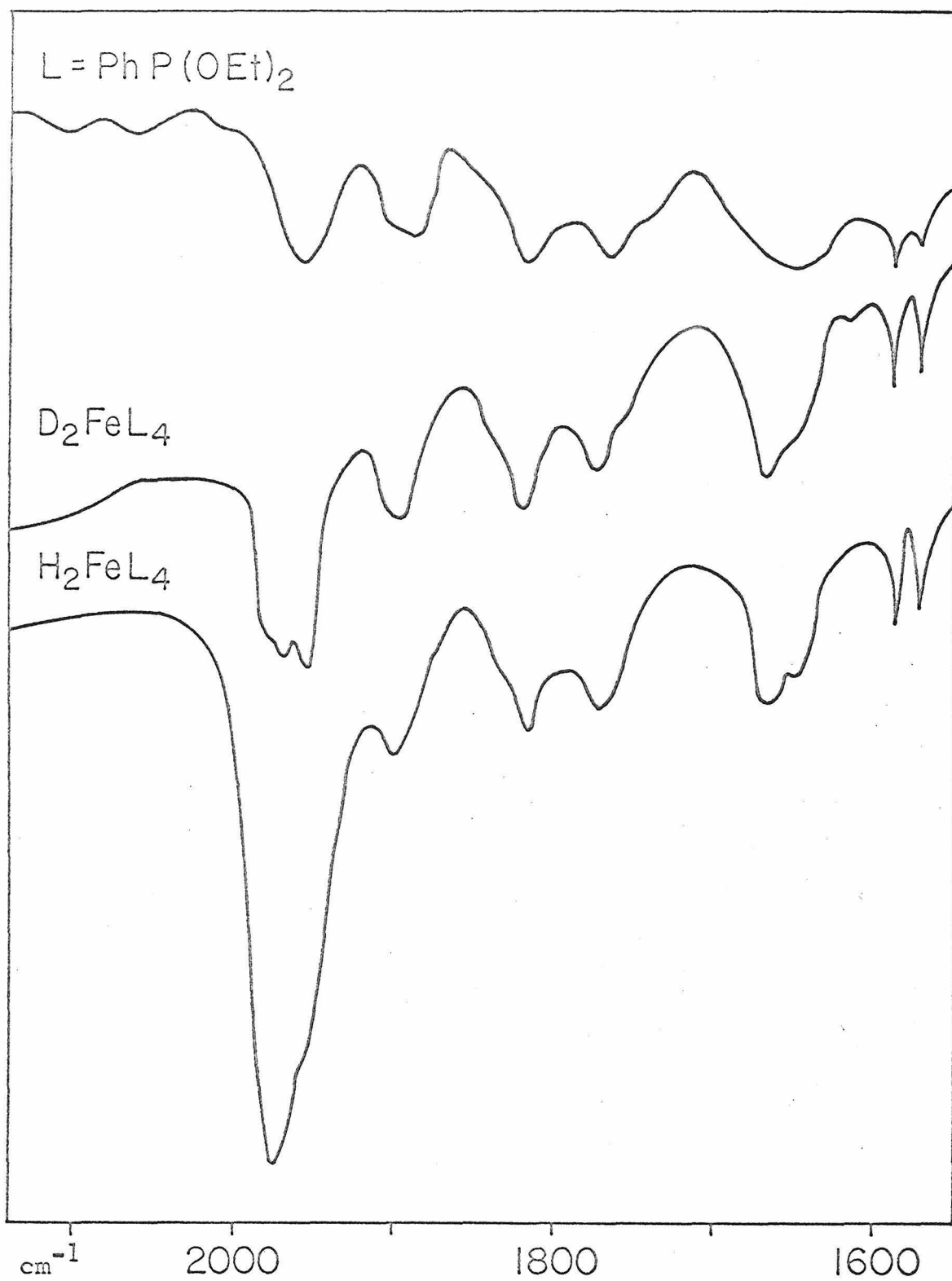


Figure 5. Infrared Spectrum of Solid $\text{H}_2\text{Fe}((\text{C}_6\text{H}_5)\text{P}(\text{OC}_2\text{H}_5)_2)_4$

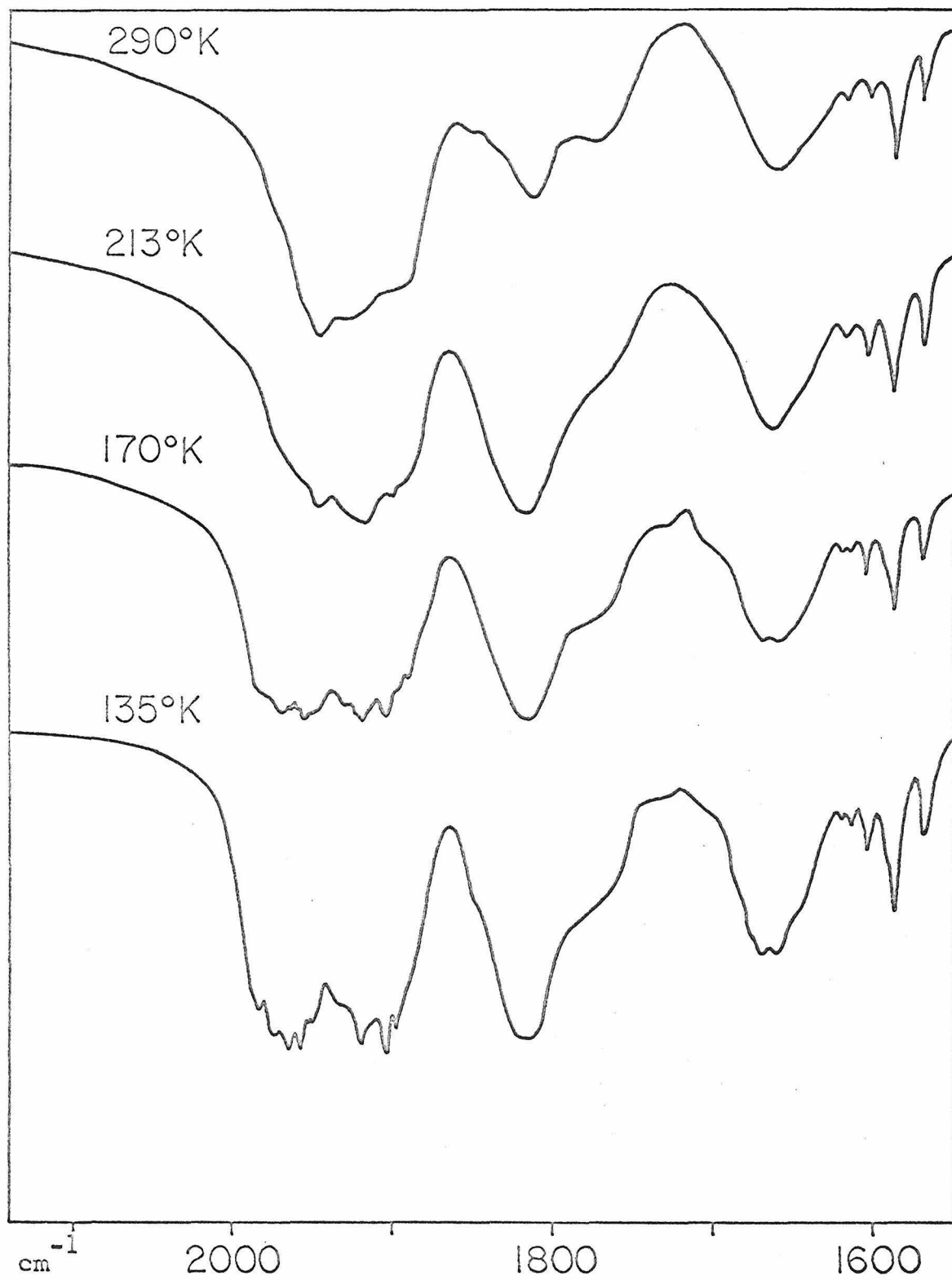


Figure 6. Low-Temperature Infrared Spectrum of $\text{H}_2\text{Fe}((\text{C}_6\text{H}_5)\text{P}(\text{OC}_2\text{H}_5)_2)_4$

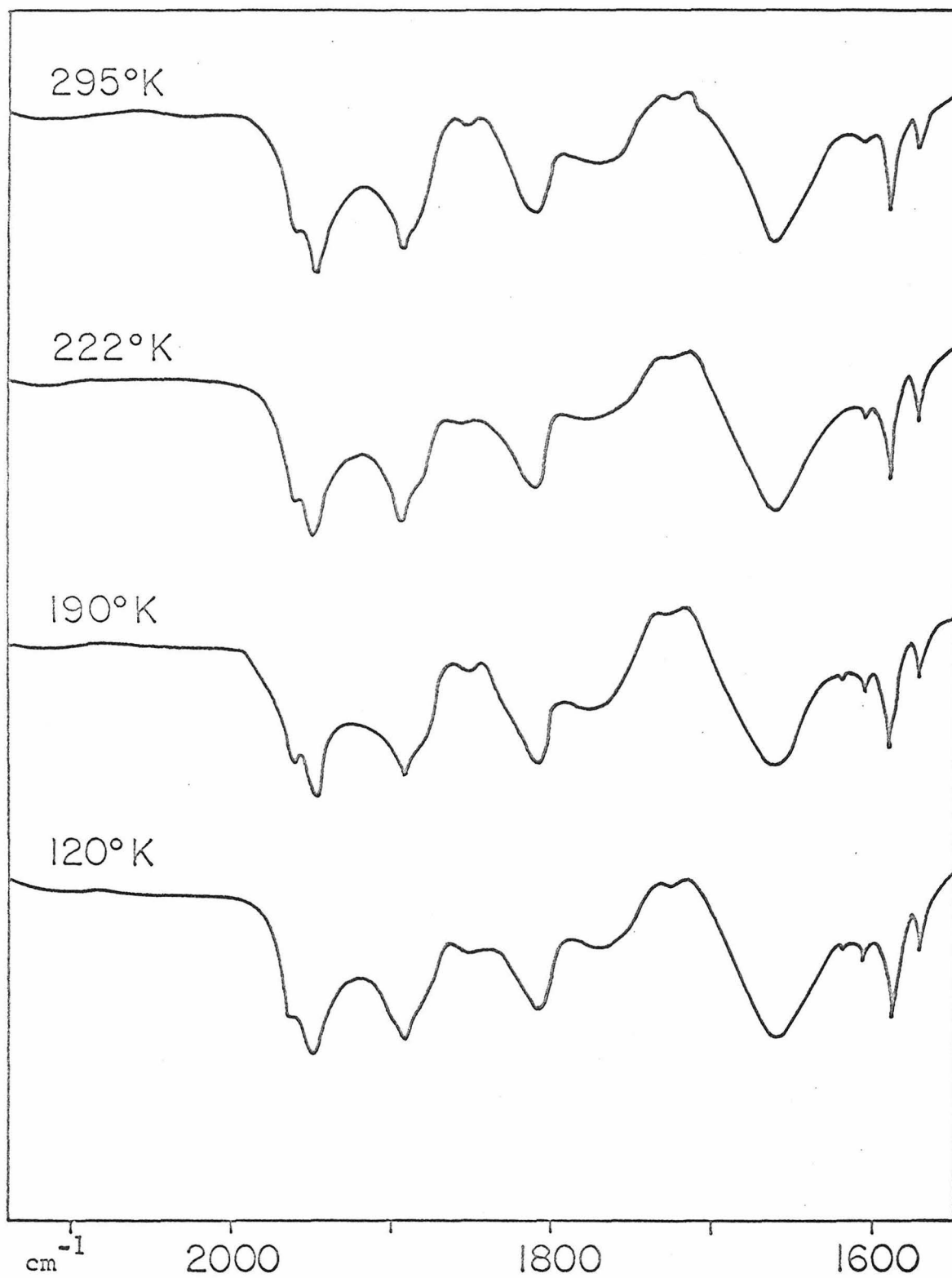


Figure 7. Low-Temperature Infrared Spectrum of $D_2Fe((C_6H_5)P(OC_2H_5)_2)_4$

a small peak (1929 cm^{-1}) can be assigned to metal-hydrogen stretching. As the temperature is reduced to $213^{\circ}\text{K}(-50^{\circ}\text{C})$ this band shifts to 1919 cm^{-1} and an additional band appears at 1818 cm^{-1} . This temperature corresponds approximately to the low temperature limit of the n.m.r. data. As the temperature is reduced even further, a third peak appears at about 1965 cm^{-1} . In the two higher energy peaks, some fine structure is seen, most of which is probably due to enhancement of underlying ligand modes which are mixed with the hydride modes (compare with low temperature spectrum of the deuterated species, Figure 7).

Assuming that the assignment of the low temperature n.m.r. signals are correct, the three bands observed should correspond to cis and trans isomers. Since two bands are expected for the cis isomer, and since the cis isomer is expected to absorb at higher energies than the trans isomer, the bands at 1919 and 1965 cm^{-1} can be assigned to the cis species. This leaves the lower energy band (1818 cm^{-1}) available for a "trans" assignment, in agreement with the expected lower energy absorption for a trans species. If this is the case, however, the trans influence of the hydrides upon one another must be reduced considerably, since 1818 cm^{-1} is still higher in energy than the usual $1600 - 1750\text{ cm}^{-1}$ observed for trans species.

Although the assignment of bands in this case is not

unambiguous, two important observations can be made concerning the nature of the species in solution. First, no changes are observed in the spectrum below 1750 cm^{-1} . If a true trans isomer were present, a narrow low-energy band would be expected in this region. Although some minor changes occur in the broad band at 1664 cm^{-1} , these are not observed until about 170°K , far below the temperature at which the "trans" quintet is observed in the n.m.r.. Second, none of the bands observed at any of the temperatures has the intensity expected for a trans isomer. The n.m.r. spectrum indicates nearly equal population of the cis and "trans" states at -50°C , and yet in the infrared spectrum at 213°K (-60°C) no band clearly dominates the spectrum. In fact, if one uses as standards the relative intensities of the phenyl C-C bands at 1589 and 1572 cm^{-1} in both the solid (Figure 3) and solution (Figure 4) spectra, it is seen that the $\nu(\text{M-H})$ bands in solution are even weaker than the weak to medium metal-hydrogen stretch observed for the solid.

The infrared data indicate, then, that there is no trans isomer in solution at low temperature. To be more specific, there is no trans isomer having the two hydride ligands positioned at or near 180° from one another. It is possible, however, to describe two isomeric species which could produce the observed spectra.

The crystal structures of $\text{H}_2\text{Fe}((\text{C}_6\text{H}_5)\text{P}(\text{OC}_2\text{H}_5)_2)_4$ and $\text{HCo}((\text{C}_6\text{H}_5)\text{P}(\text{OC}_2\text{H}_5)_2)_4$ and much of the data available for similar complexes favor a tetrahedral arrangement for the phosphorus atoms about the metal atoms. Although it is traditional to discuss the rearrangement of six-coordinate species on the basis of octahedral symmetry, such a configuration, even if considered in a distorted form, is of little value in the present case. A tetrahedral phosphorus skeleton gives a fairly accurate representation of the true structure of the molecule. In the following discussion this configuration is used as a basis for the examination of possible hydride positions.

In order to place two hydrogens in the framework of the tetrahedron, there are five possible pairs of positions to consider (see Figure 8): A) two adjacent faces, B) two adjacent edges, C) two non-adjacent edges, D) a face and an adjacent edge, and E) a face and a non-adjacent edge. A and B both are cis type isomers, and since the crystal structure shows the complex is a distorted form of A, it is probably the A species which produces the triplet of doublets in the low temperature n.m.r. C represents the trans type isomer which has been proposed (29) to explain the n.m.r. spectra, but which is not consistent with the infrared data. D is not expected to be a realistic alternative because of the large nonbonded repulsion.

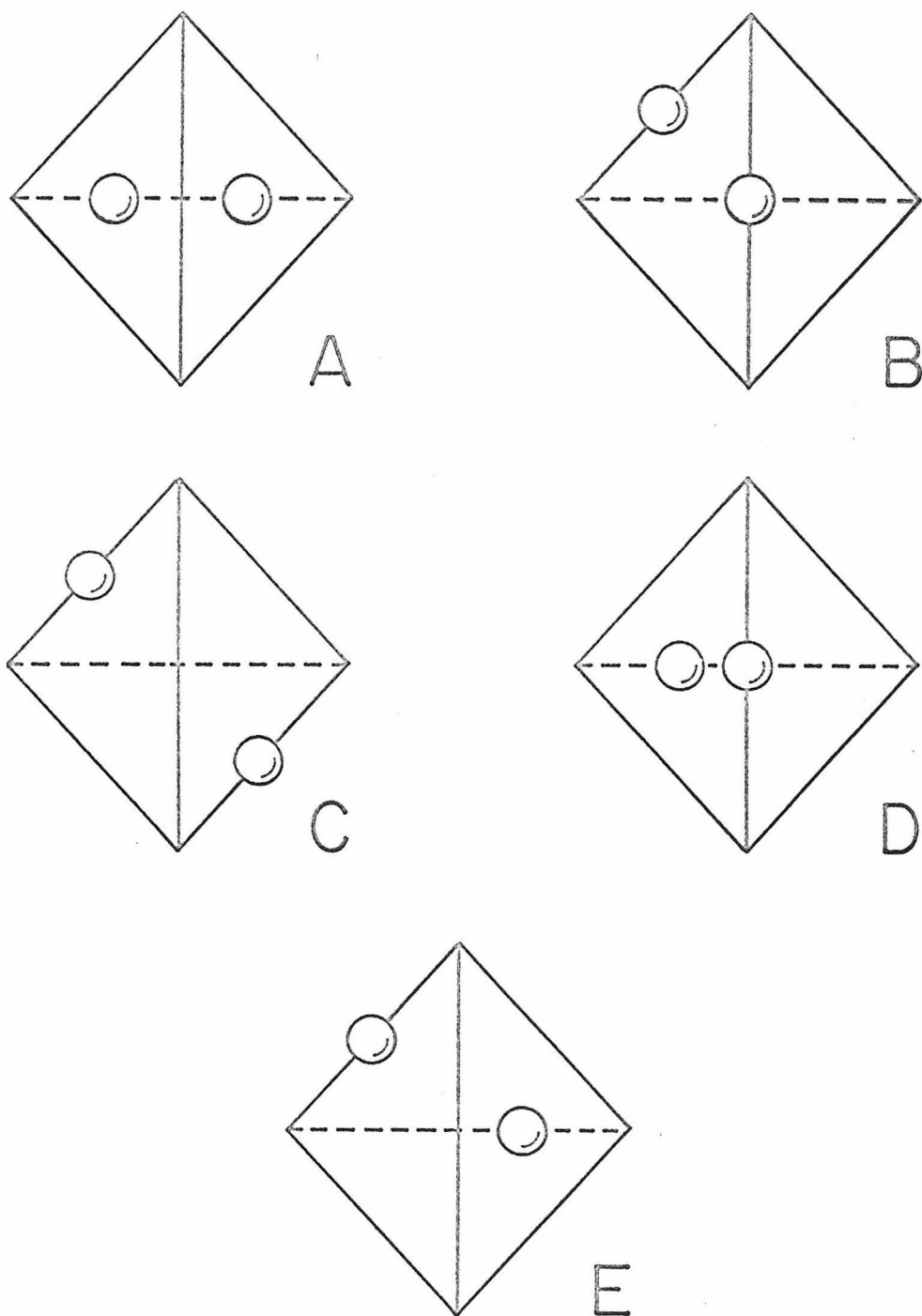


Figure 8. Possible Locations for Two Hydrogen Ligands in a Tetrahedral Phosphorus Skeleton

between hydride ligands. The E species remains as a possible trans-type isomer in solution.

A structure of the E type is in better agreement with the spectral data than the C type. The H-Fe-H angle in such a molecule would be approximately 125° . Even allowing for an expected $10 - 20^\circ$ distortion from the regular symmetry, this angle is significantly less than 180° , and the Fe-H stretching absorption thus is not expected to be significantly more intense than that of a cis isomer. The trans influence of the hydride ligands with respect to one another should decrease with the H-Fe-H angle, and the Fe-H stretching frequency is not expected to be found in the low energy ($1600 - 1750 \text{ cm}^{-1}$) region. Rapid rearrangement of the hydrides from face to edge and edge to face about the tetrahedron of phosphorus atoms would produce an apparent equivalence of the phosphorus atoms and lead to a quintet in the high field p.m.r. spectrum. The rearrangements of the phosphorus atoms during this process are much smaller than those required to produce the same effect in the C species. (In fact, the rearrangements necessary for the hydrogen to "see" four apparently equivalent phosphorus atoms in the C species are even greater than the rearrangement required to convert the C species to the A species.)

It should be emphasized that although the two species

in solution resemble types A and E in form, the distortion of the iron-phosphorus skeleton from regular tetrahedral symmetry is undoubtedly significant. The form of the A species in solution is probably similar to the structure found for the solid, with an H-Fe-H angle of $80 - 100^\circ$ (as opposed to 109° for the undistorted case). The structure of the E species is difficult to predict, although in the n.m.r. spectrum its resonance is observed at a lower field, indicating that the metal-hydrogen distance is longer than in the A form (66). This may be the result of trans influence effects, which are expected to increase with the H-Fe-H angle. It might also be due to the higher degree of crowding in the edge position, which could be decreased by a longer Fe-H bond. In view of this, it seems likely that the H-Fe-H angle lies somewhere between 125° and 145° . The maximum deviation of the P-Fe-P angle from 109° is likely to be about $25 - 28^\circ$ for both species. The relatively high energy required to rearrange the phosphorus atoms from the distorted A form to the distorted E form and vice versa leads to an increase in the lifetime of each state until at -50°C both states can be observed in the n.m.r. spectrum. Distortions of the phosphorus atom skeleton which accompany the hydrogen atom rearrangement within the E form are apparently less difficult and an averaged spectrum is observed for this species, even at low temperature.

It is interesting to speculate on the nature of species if extensive ($20 - 30^\circ$) distortions of the phosphorus atom skeleton were not possible. In such instances, the edge positions become energetically unfavorable, since positioning of a ligand in an edge position implies a rather large distortion ($20 - 25^\circ$ in this case) of the P-Fe-P angle. A ligand in a facial position requires distortions of only $5 - 15^\circ$. We would expect that species of an A type would predominate, since all other possibilities require the participation of at least one edge position. In recent work, low temperature n.m.r. spectra were investigated for fourteen H_2ML_4 complexes (where M = Fe or Ru, and L = various phosphines and phosphites) (48). Only the complexes of $(C_6H_5)P(OC_2H_5)$ indicated the presence of any "trans" (E) species at low temperatures; the other complexes displayed the cis (A) spectrum exclusively.

An examination of Table 6 shows that of the eight complexes which appear to have a trans (C) configuration, only III and IV do not contain bidentate phosphorus ligands. Since IV cannot have a tetrahedral skeleton of phosphorus atoms, III remains as the only compound of this type not containing bidentate ligands. Any tetrahedral skeleton formed by two chelating phosphorus ligands will have two edges which cannot be distorted to allow hydride occupation. However, because of the reduced bulk of a

bidentate ligand compared to 2 similar monodentate ligands, the remaining four edge positions are relatively easy to "open up" for a hydride ligand. Also, molecular models of bidentate ligand structures indicate that both square-planar and tetrahedral arrangements of the phosphorus atoms are sterically unfavorable. An intermediate structure, which in effect results in the opening of two edge positions, seems more favorable. This may account for the predominance of bidentate ligands in the complexes which appear to have trans (C) configurations. The presence of chelating ligands will also be expected to reduce the number of possible rearrangements in this type of complex; unfortunately, no low temperature n.m.r. or ir. work has been reported for the complexes containing chelating ligands. The ability of $((C_6H_5)P(OC_2H_5)_2)_2$ to produce a trans (C) complex (III) is again probably due to its ability to distort from a regular tetrahedral configuration about the metal atom.

Thus, it appears that $H_2Fe((C_6H_5)P(OC_2H_5)_2)_4$, having a cis-like structure in the solid state, forms two isomers in solution, one similar to the solid state structure, and the other resembling a distorted "trans" species in which the hydrides occupy a face and non-adjacent edge of a distorted tetrahedron of phosphorus atoms. Although the infrared spectra indicate that several dihydride complexes

have the trans (C) structure in the solid state, no n.m.r. spectra have been observed for a C species in solution.

SECTION III

HYDRIDOTETRAKIS (DIETHYLPHENYLPHOSPHONITE) COBALT (I)

INTRODUCTION

The first complex cobalt metal hydride, $\text{HCo}(\text{CO})_4$, was reported a few years after the preparation of its iron analog (9,67). Its properties are generally quite similar to those of the iron complex. It is a thermally unstable liquid which decomposes at -20°C (68). The dissociation constant for $\text{HCo}(\text{CO})_4$ has been found to be about 1, indicating that the complex acts as a very strong acid (69). As in the case of the iron compound, the structure is uncertain, but the results of the electron diffraction experiments (24) imply that the carbonyls are disposed tetrahedrally about the cobalt atom, suggesting that the hydrogen probably occupies one of the faces of the tetrahedron.

It was not until 1963 that the first complex cobalt hydride containing phosphorus ligands, $\text{HCo}(\text{Ph}_2\text{PC}_2\text{H}_4\text{PPh}_2)_2$, was reported (70). The red crystals are thermally stable (dec. 280°C), but darken after a few hours exposure to air. On the basis of the dipole moment (3.50 D) and isomorphism

with the isoelectronic nickel complex, the compound is believed to have the same tetrahedral structure proposed for the carbonyl complex (71). No high-field p.m.r. spectrum could be observed, presumably because of the low solubility of the complex.

The trifluorophosphine analog of this series, $\text{HCo}(\text{PF}_3)_4$, was reported in 1965 (72). The properties of the PF_3 complex closely resemble those of the carbonyl hydride. The complex is a yellowish liquid with strong acidic character. Unlike the carbonyl complex, however, the PF_3 derivative is thermally stable (dec. 250°C) (3). The n.m.r. spectrum displays a single broad signal at high field which is unchanged even at -80°C . A recent low temperature x-ray investigation of this complex shows the phosphorus atom configuration is very nearly tetrahedral (deviations of the P-Fe-P angles from 109.5° vary from 0.2 to 8.5°). The hydrogen atom was not located (73).

Kruse and Atalla (38) have reported the synthesis and spectral properties of a phosphite analog, $\text{HCo}(\text{P}(\text{OEt})_3)_4$. The complex is moderately stable toward oxygen in the solid state, and is oxidized rapidly in solution. A quintet (τ 25.8) is observed in the high-field p.m.r. spectrum; it remains unchanged even when spectra are obtained at -58°C . Because of this apparent lack of temperature dependence, the authors concluded that the structure of the

complex must be square-pyramidal.

Triarylphosphite complexes, $\text{HCo}(\text{P}(\text{OAr}))_4$, have also been reported (74), with $\text{Ar} = \text{Ph}$, $m\text{-MeC}_6\text{H}_4$, $p\text{-MeC}_6\text{H}_4$, and $p\text{-ClC}_6\text{H}_4$. The complexes form pale yellow, hexagonal platelets which are stable to air for several weeks. The n.m.r. spectra of these complexes display the same features observed for the triethylphosphite compound. No change in the quintet resonance was observed over a temperature range of $+30$ to -40°C . Isomorphism (x-ray powder photographs) with the corresponding tetrakis-triarylphosphite nickel complexes led the authors to suggest that there was not yet enough evidence to eliminate the possibility of a non-rigid structure in solution. It was concluded that the complexes in the solid state probably have a trigonal bipyramidal skeleton, with the phosphorus atoms distorted toward a tetrahedral arrangement.

The subject of the present study, $\text{HCo}((\text{C}_6\text{H}_5)\text{P}(\text{OC}_2\text{H}_5)_2)_4$, is similar in many respects to the trialkyl- and triarylphosphite complexes. The compound crystallizes as well-formed yellow-orange crystals which are stable to the atmosphere for several days. The crystals are similar in habit to those of the corresponding iron complex, although an increased elongation along the b axis gives them a more needle-like appearance. The n.m.r. spectrum (Figure 9) shows a quintet (τ 24.3, $J = 21.5$ cps), which eventually

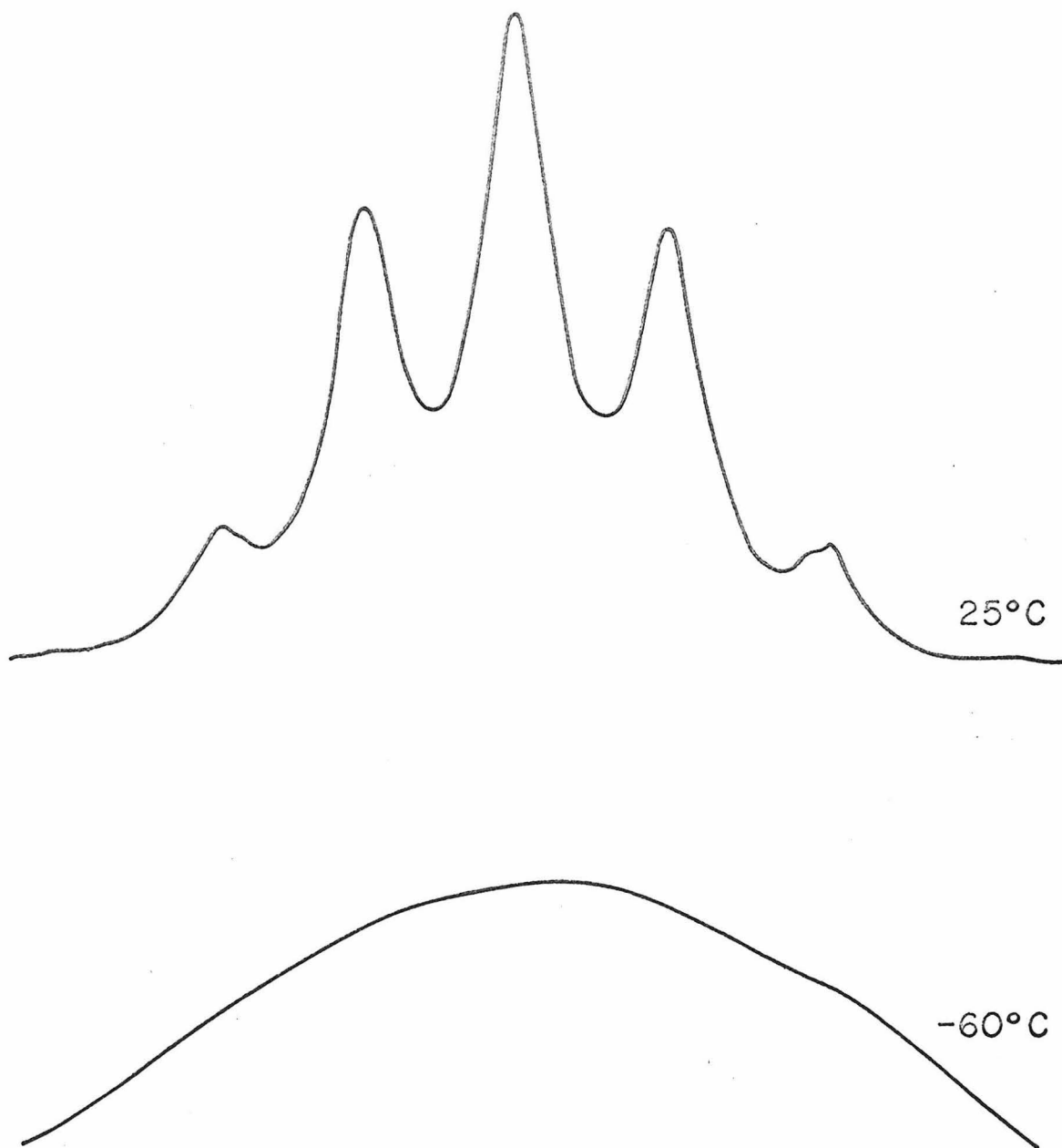


Figure 9. High-Field P.m.r. Spectrum of
 $\text{HCo}(\text{C}_6\text{H}_5)\text{P}(\text{OC}_2\text{H}_5)_2)_4$

coalesces to a broad singlet (band width 250 cps, τ 22.5) at low temperature (-50°C). Because of the structural questions which had arisen concerning this series of compounds, an x-ray structure determination was undertaken.

THE X-RAY CRYSTAL STRUCTURE OF $\text{HCo}((\text{C}_6\text{H}_5)\text{P}(\text{OC}_2\text{H}_5)_2)_4$ Collection and Treatment of Data

As in the case of the corresponding iron complex, several recrystallizations were necessary to obtain crystals small enough for x-ray investigation. Mounting of the crystals was carried out in the manner described above.

Initial Weissenberg photographs were remarkably similar to those of the iron complex. Photographs of both complexes could be superimposed upon one another with very little detectable difference, indicating that the structures of the two complexes were nearly identical. Instead of determining cell constants by the photographic method, the cell constants of the iron complex were used for orienting the crystal on the diffractometer. The a and c axes were interchanged in order to have a more conventional cell. (The iron cell had $a > b > c$; the normal convention is to have $c > b > a$.)

A crystal with dimensions 0.08 x 0.08 x 0.15 mm was chosen for data collection. The crystal was mounted with the b axis (0.15 mm) approximately parallel to the ϕ axis of the diffractometer. With the detector centered on an intense reflection, the window of the pulse-height analyzer was adjusted for an optimum signal to noise ratio. The 2θ values of fifteen high-angle reflections were determined by careful centering of each reflection. The values were then used in a least-squares calculation of the cell parameters. The resultant parameters, which were used in all of the subsequent operations, are given in Table 8. The corresponding ϕ and χ values for the fifteen reflections were used as input for the orientation program of the diffractometer.

A Datex-automated General Electric diffractometer with iron-oxide filtered cobalt radiation was used for the collection of intensity data. The scan range and speed were identical with those of the previous determination.

Four check reflections were monitored, one every twenty reflections. At the completion of the data collection, the intensities of the check reflections had decreased 3 - 5%. The intensities of 4294 reflections ($2\theta < 120^\circ$, $\sin \theta / \lambda < 0.483$) were determined in 15 sets. The data from each set were scaled to one of the check reflections which was given a fixed $|F|$ value for all of the sets.

Table 8. Cell Parameters for $\text{HCo}((\text{C}_6\text{H}_5)\text{P}(\text{OC}_2\text{H}_5)_2)_4$

$a = 11.9317(18) \text{ \AA}$	$\alpha = 95.503(14)^\circ$
$b = 12.8406(24)$	$\beta = 89.752(12)$
$c = 17.6800(15)$	$\gamma = 123.090(10)$
$V = 2255.23(98) \text{ \AA}^3$	Space Group $\text{P}\bar{1}$

Reduced Cell:

$a = 11.8302(17) \text{ \AA}$	$\alpha = 90.248(14)^\circ$
$b = 11.9317(20)$	$\beta = 95.724(11)$
$c = 17.6800(15)$	$\gamma = 114.582(14)$

Index Relationships:

$$h_r = h + k$$

$$k_r = -h$$

$$l_r = l$$

The value of $|F|$ used was that observed for the corresponding reflection in $\text{H}_2\text{Fe}((\text{C}_6\text{H}_5)\text{P}(\text{OC}_2\text{H}_5)_2)_4$. For extremely intense reflections, the x-ray tube current was reduced by 50% and extra filtration (iron foil, 0.0008 inch) was employed.

The linear absorption coefficient was calculated to be $\mu = 34 \text{ cm}^{-1}$, and the transmission factors thus varied from 0.60 to 0.76. No absorption corrections were applied to the data; Lorenz and polarization corrections were made. All reflections having intensities less than or equal to zero were assigned $F = 0$ with a zero weight. The intensities of the 4102 remaining non-zero reflections were used in all subsequent calculations. No unusual trends were noted in the intensities of the high-angle reflections.

The atomic scattering factors of the non-hydrogen atoms were taken from the tables of Hanson, Herman, Lea, and Skillman (75); those of the hydrogen atoms were taken from the calculations of Stewart, Davidson, and Simpson (76). The factors of cobalt and phosphorus were corrected for the real part of anomalous dispersion. Extrapolation from Cromer's values (45) for iron and copper radiation yielded $\Delta f'$ for cobalt = $-2.18 e^-$ and $\Delta f'$ for phosphorus = $0.30 e^-$.

A sharpened Patterson map was calculated in order to

locate the heavy atoms. By comparing with the map of the iron complex, and the known $\text{Fe}_1\text{-Fe}_2$ and $\text{Fe}_1\text{-P}_1$ vectors, it was relatively simple to locate the cobalt-cobalt and cobalt-phosphorus vectors. The $\text{Co}_1\text{-Co}_2$ vector was well resolved in this case; no coincident vectors masked its position. A calculation of structure factors using the Patterson-derived coordinates of cobalt and phosphorus atoms yielded an R value of 0.48. Two successive structure factor calculations interspersed with Fourier syntheses provided the positions of the remaining non-hydrogen atoms. A structure factor calculation with the positional and thermal (estimated isotropic) parameters for all of the non-hydrogen atoms yielded an R value of 0.324.

An initial cycle of least-squares refinement was carried out including the positional parameters of all of the non-hydrogen atoms with isotropic thermal parameters. The R was reduced to 0.187. An additional two cycles yielded an R value of 0.156. The atoms were then allowed to vibrate anisotropically (refinement carried out in three successive runs, as above), and following one complete cycle of refinement, the R stood at 0.081. The positional parameters of the phosphonite hydrogens were then calculated according to the known geometries of the atoms. The phenyl C-H distance was taken to be 0.09 \AA

and the ethyl C-H distance was 1.09 Å. These parameters were then included in the least-squares calculation as fixed contributions. The hydrogen atoms were assigned thermal parameters equal to 1 Å² greater than the final isotropic thermal parameters of the carbons to which they were bonded. Three complete cycles of least-squares refinement reduced the R to 0.055.

A difference Fourier map was then calculated in an attempt to locate the ligand hydrogen atom. The most prominent feature of the map had a peak height of 0.36 e⁻/Å³, at a logical position for the hydride ligand. The second highest peak on the map was 0.34 e⁻/Å³, which apparently represented an alternate position for carbon 4. The other relatively large peaks of the map also seemed to be related to possible alternate positions for carbon atoms. After reducing the data set to those reflections having $\sin \theta / \lambda < 0.387$ ($2\theta < 88^\circ$) a second difference Fourier map was calculated (47). The hydride peak was still the highest at 0.30 e⁻/Å³, while the alternate C4 position showed a peak of 0.28 e⁻/Å³. The isotropic thermal and positional parameters were included in two additional cycles of least-squares refinement. The final thermal parameter for the ligand hydrogen atom was $B = 8.79(116) \text{ \AA}^2$. The R at the end of the refinement was 0.050; the goodness of fit for the final refinement was 2.26.

Description of the Structure

The unit cell of $\text{HCo}((\text{C}_6\text{H}_5)\text{P}(\text{OC}_2\text{H}_5)_2)_4$ is very similar to that of $\text{H}_2\text{Fe}((\text{C}_6\text{H}_5)\text{P}(\text{OC}_2\text{H}_5)_2)_4$, as can be seen from Figure 10. Because of different numbering schemes applied to the molecules, a list of corresponding atoms along with the cell parameters of the two cells is given in Table 9. The closest Co-Co distance is $9.768(1) \text{ \AA}$.

The inner coordination sphere of the cobalt atom is shown in Figure 11. The phosphorus atoms are even closer to a tetrahedral configuration than in the case of the iron complex. The hydrogen occupies the face of the tetrahedron opposite phosphorus atom 4. The greatest distortion from the regular tetrahedral angle is 15° , between atoms P1 and P2 ($124.1(1)^\circ$). The interatomic distances and angles are presented in Tables 10 and 11. Tables of structure factors, positional and anisotropic thermal parameters, and the derived parameters for the phenyl and ethyl hydrogen atoms are given in Appendix II.

Figure 10. Stereoscopic Drawings of the Unit Cells

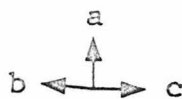
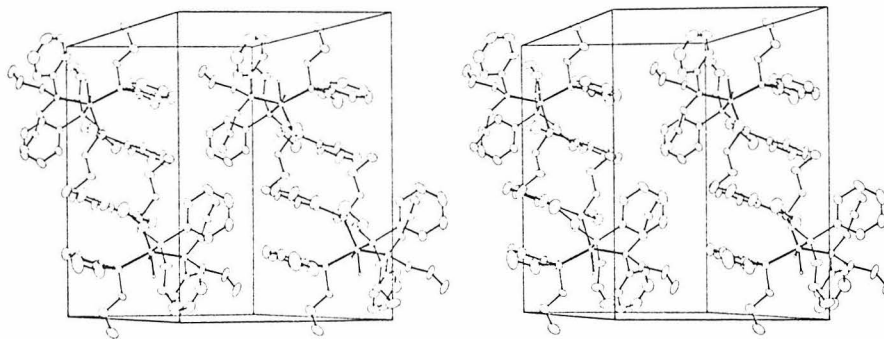
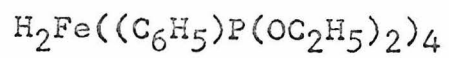
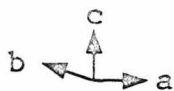
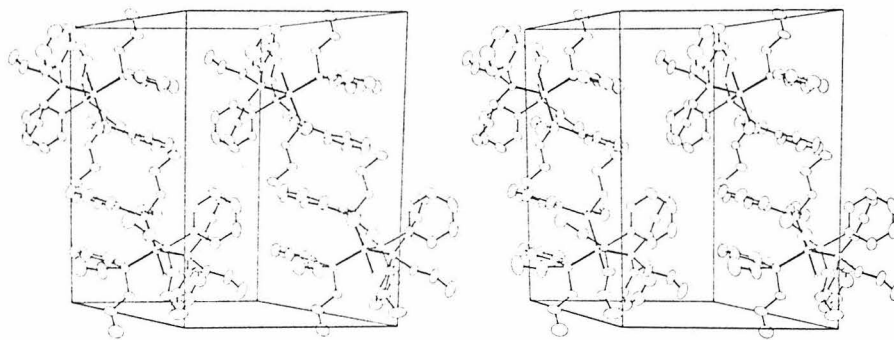
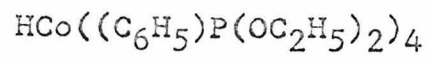


Table 9. Correspondence of the Unit Cells and Atoms of the Iron and Cobalt Complexes

<u>Iron Complex</u> <u>Unit Cell</u>		<u>Cobalt Complex</u> <u>Unit Cell</u>	
A = 17.4945 (30)		C = 17.6800 (15)	
B = 12.7325 (74)		B = 12.8406 (24)	
C = 11.9404 (59)		A = 11.9317 (18)	
α = 122.998 (43)		γ = 123.090 (10)	
β = 90.207 (36)		β = 89.752 (12)	
γ = 94.441 (39)		α = 95.503 (14)	
FE COMPLEX	CO COMPLEX	FE COMPLEX	CO COMPLEX
FE	CO	C15	C19
P1	P1	C16	C20
P2	P2	C17	C13
P3	P4	C18	C14
P4	P3	C19	C11
O1	O2	C20	C12
O2	O1	C21	C35
O3	O4	C22	C36
O4	O3	C23	C37
O5	O7	C24	C38
O6	O8	C25	C39
O7	O5	C26	C40
O8	O6	C27	C31
C1	C5	C28	C32
C2	C6	C29	C33
C3	C7	C30	C34
C4	C8	C31	C25
C5	C9	C32	C26
C6	C10	C33	C27
C7	C3	C34	C28
C8	C4	C35	C29
C9	C1	C36	C30
C10	C2	C37	C21
C11	C15	C38	C22
C12	C16	C39	C23
C13	C17	C40	C24
C14	C18	H1	H

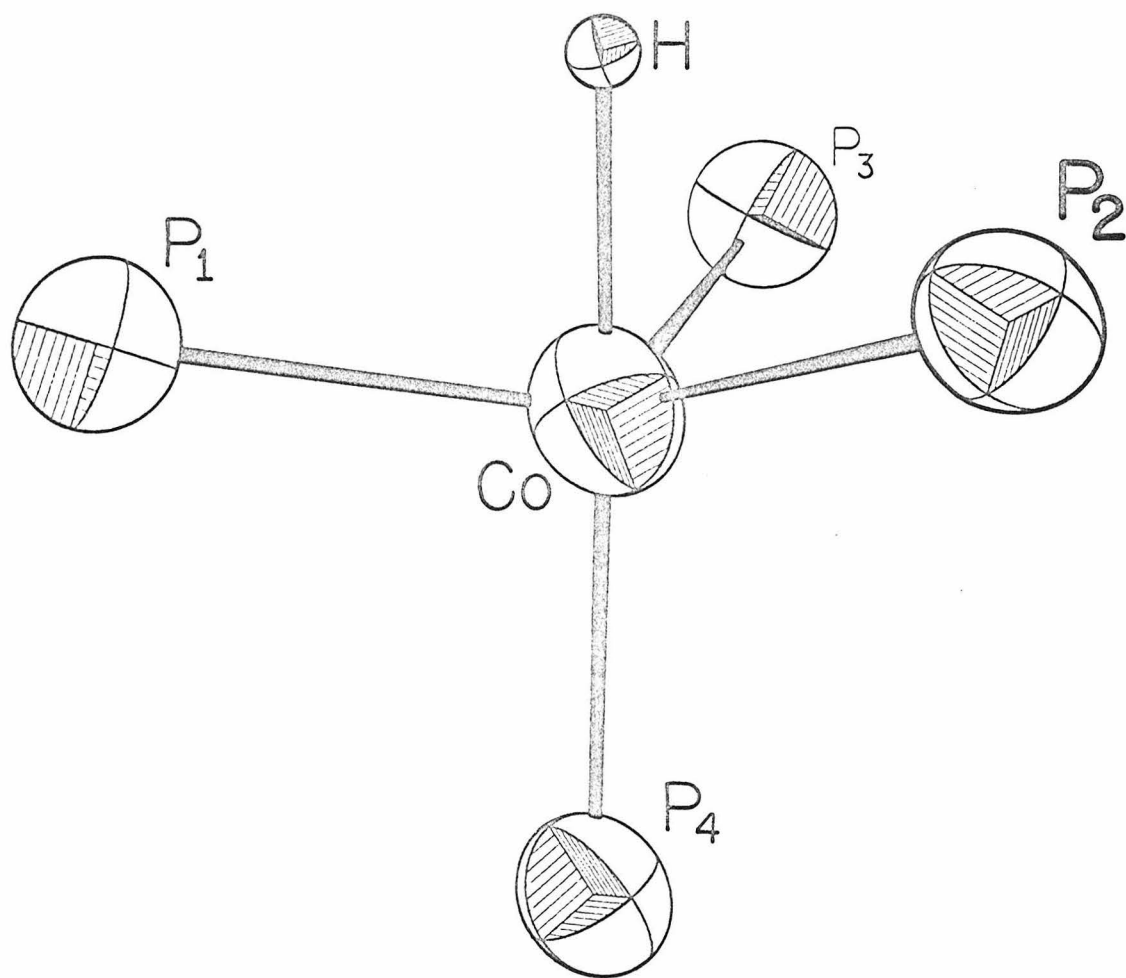


Figure 11. Inner Coordination Sphere of
 $\text{HCo}((\text{C}_6\text{H}_5)\text{P}(\text{OC}_2\text{H}_5)_2)_4$

Table 10. Interatomic Distances of $\text{HCo}((\text{C}_6\text{H}_5)\text{P}(\text{OC}_2\text{H}_5)_2)_4$
(in Angstroms)

CO - CO	9.768 (1)	P2 - O4	1.629 (3)
CO - P1	2.115 (2)	O4 - C13	1.431 (6)
CO - P2	2.103 (2)	C13 - C14	1.481 (8)
CO - P3	2.126 (1)	P2 - C15	1.832 (5)
CO - P4	2.128 (1)	C15 - C16	1.372 (7)
CO - H	1.376 (54)	C17 - C18	1.338 (11)
CO - H	1.540 (--)*	C16 - C17	1.383 (8)
P1 - P2	3.726 (2)	C18 - C19	1.359 (11)
P1 - P3	3.584 (2)	C19 - C20	1.376 (9)
P1 - P4	3.197 (2)	C15 - C20	1.372 (8)
P1 - H	2.297 (65)	P3 - O5	1.632 (3)
P1 - H	2.372 (--)*	O5 - C21	1.445 (6)
P2 - P3	3.344 (2)	C21 - C22	1.462 (9)
P2 - P4	3.431 (2)	P3 - O6	1.620 (3)
P2 - H	2.123 (--)*	O6 - C23	1.385 (6)
P2 - H	2.018 (58)	C23 - C24	1.395 (10)
P3 - P4	3.372 (2)	P3 - C25	1.830 (5)
P3 - H	2.436 (--)*	C25 - C26	1.377 (6)
P3 - H	2.412 (54)	C26 - C27	1.384 (8)
P4 - H	3.662 (--)*	C27 - C28	1.351 (9)
P4 - H	3.493 (52)	C28 - C29	1.342 (10)
P1 - O1	1.631 (4)	C29 - C30	1.392 (9)
O1 - C1	1.383 (8)	C25 - C30	1.377 (7)
C1 - C2	1.402 (11)	P4 - O7	1.623 (3)
P1 - O2	1.616 (3)	O7 - C31	1.437 (6)
O2 - C3	1.431 (9)	C31 - C32	1.457 (9)
C3 - C4	1.236 (10)	P4 - O8	1.621 (3)
P1 - C5	1.830 (6)	O8 - C33	1.424 (6)
C5 - C6	1.373 (9)	C33 - C34	1.479 (7)
C6 - C7	1.404 (10)	P4 - C35	1.825 (5)
C7 - C8	1.344 (11)	C35 - C36	1.364 (7)
C8 - C9	1.347 (12)	C36 - C37	1.375 (9)
C9 - C10	1.386 (9)	C37 - C38	1.351 (9)
C5 - C10	1.375 (8)	C38 - C39	1.350 (9)
P2 - O3	1.635 (3)	C39 - C40	1.386 (9)
O3 - C11	1.437 (8)	C35 - C40	1.378 (7)
C11 - C12	1.401 (10)		

* Derived from difference Fourier parameters

Table 11. Interatomic Angles of $\text{HCo}((\text{C}_6\text{H}_5)\text{P}(\text{OC}_2\text{H}_5)_2)_4$

P1	-	CO	-	P2	124.1	(1)
P1	-	CO	-	P3	115.4	(1)
P1	-	CO	-	P4	97.8	(1)
P1	-	CO	-	H	79.2	(27)
P1	-	CO	-	H	79.2	(--)*
P2	-	CO	-	P3	104.5	(1)
P2	-	CO	-	P4	108.4	(1)
P2	-	CO	-	H	67.2	(25)
P2	-	CO	-	H	69.3	(--)*
P3	-	CO	-	P4	104.9	(1)
P3	-	CO	-	H	84.2	(22)
P3	-	CO	-	H	81.6	(--)*
P4	-	CO	-	H	170.8	(22)
P4	-	CO	-	H	173.5	(--)*
CO	-	P1	-	O1	123.1	(1)
CO	-	P1	-	O2	112.1	(2)
CO	-	P1	-	C5	121.3	(2)
P1	-	O1	-	C1	124.0	(4)
O1	-	C1	-	C2	116.3	(6)
P1	-	O2	-	C3	121.8	(4)
O2	-	C3	-	C4	116.8	(10)
P1	-	C5	-	C6	124.0	(4)
P1	-	C5	-	C10	119.1	(5)
C6	-	C5	-	C10	116.9	(5)
C5	-	C6	-	C7	121.0	(6)
C6	-	C7	-	C8	120.0	(8)
C7	-	C8	-	C9	120.2	(7)
C8	-	C9	-	C10	120.1	(6)
C9	-	C10	-	C5	121.7	(6)
CO	-	P2	-	O3	111.1	(1)
CO	-	P2	-	O4	123.9	(1)
CO	-	P2	-	C15	121.1	(2)
P2	-	O3	-	C11	121.6	(3)
O3	-	C11	-	C12	111.9	(6)
P2	-	O4	-	C13	119.5	(3)
O4	-	C13	-	C14	109.3	(4)

* Derived from difference Fourier parameters

Table 11. Continued

P2	-	C15	-	C16	118.3	(4)
P2	-	C15	-	C20	124.3	(4)
C16	-	C15	-	C20	117.4	(5)
C15	-	C16	-	C17	121.3	(5)
C16	-	C17	-	C18	119.9	(6)
C17	-	C18	-	C19	120.4	(7)
C18	-	C19	-	C20	119.9	(7)
C19	-	C20	-	C15	121.2	(6)
C0	-	P3	-	O5	116.7	(1)
C0	-	P3	-	O6	120.3	(1)
C0	-	P3	-	C25	121.0	(1)
P3	-	O5	-	C21	123.1	(3)
O5	-	C21	-	C22	109.5	(5)
P3	-	O6	-	C23	126.9	(4)
O6	-	C23	-	C24	114.2	(6)
P3	-	C25	-	C26	119.8	(4)
P3	-	C25	-	C30	123.0	(3)
C26	-	C25	-	C30	117.2	(5)
C25	-	C26	-	C27	121.6	(5)
C26	-	C27	-	C28	119.8	(5)
C27	-	C28	-	C29	120.2	(6)
C28	-	C29	-	C30	120.7	(6)
C29	-	C30	-	C25	120.5	(5)
C0	-	P4	-	O7	115.8	(1)
C0	-	P4	-	O8	120.0	(1)
C0	-	P4	-	C35	119.6	(1)
P4	-	O7	-	C31	121.3	(3)
O7	-	C31	-	C32	110.6	(5)
P4	-	O8	-	C33	122.5	(3)
O8	-	C33	-	C34	108.6	(5)
P4	-	C35	-	C36	123.6	(4)
P4	-	C35	-	C40	119.2	(4)
C36	-	C35	-	C40	117.1	(5)
C35	-	C36	-	C37	120.9	(5)
C36	-	C37	-	C38	121.6	(6)
C37	-	C38	-	C39	118.8	(6)
C38	-	C39	-	C40	120.2	(6)
C39	-	C40	-	C35	121.3	(5)

The average Co-P distance of 2.118(2) Å is slightly longer than the 2.052(5) Å observed for Co-P bond in $\text{HCo}(\text{PF}_3)_4$ (73), and somewhat shorter than the 2.192(6) Å observed for the Co-P bond in $\text{HCo}(\text{N}_2)(\text{P}(\text{C}_6\text{H}_5)_3)_3$ (54). In view of the π -bonding capabilities of the three phosphorus ligands, such an order is expected. Averaging of the Co-P distances is probably not valid because of the significant variations observed. Similar variations have been observed in the Co-P bond distances of $\text{HCo}(\text{N}_2)(\text{P}(\text{C}_6\text{H}_5)_3)_3$ (54). An examination of Figure 9 and Table 10 shows that the trans P4 atom is farthest from the cobalt atom. This is expected for the ligand trans to the hydride, but the Co-P₃ bond is nearly as long, and this is more difficult to explain. By comparing this structure with that of the iron complex, it can be seen that atom P3 corresponds to one of the phosphorus atoms trans to a hydride. Thus in both complexes, atoms P3 and P4 are farther from the metal atoms than atoms P1 and P2. It is possible that the hydride ligand is disordered in the cobalt complex, taking a position corresponding to that of either H1 or H2 of the iron complex. Since a peak was not observed in the difference Fourier at the H2 position, it is assumed that the predominant species has the hydrogen in the H1 position. Although the hydrogen was not located in a recent crystal structure determination of $\text{HCo}(\text{PF}_3)_4$ (73),

it was concluded on the basis of the slight distortion of the phosphorus atoms from a tetrahedral configuration, that the hydrogen position is disordered, occupying either of two tetrahedral faces. It is possible that this situation obtains also in the present case. Since the phosphorus ligand configuration would very likely be different for the two species, we should expect large anisotropic thermal parameters for the atoms of the molecule. A comparison of the root-mean-square amplitudes of vibrations of the principal ellipsoid axes for the two complexes (Tables 4 and 12), shows that the vibrations are indeed larger for the cobalt complex. However, such a difference might also be expected from the relative increase in vibrational freedom in going from a six- to five-coordinate species. Thus, although the Co-P distances indicate that the structure is disordered with respect to the two possible hydride positions, the failure to detect a peak in the H2 position leaves such disorder open to question.

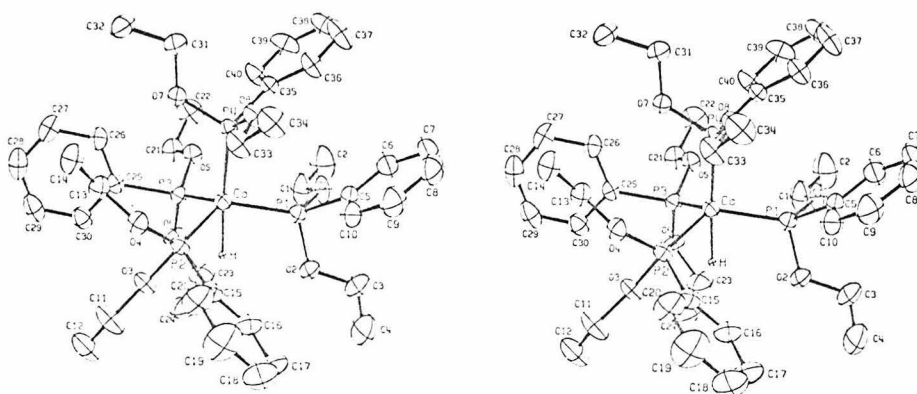
A stereoscopic drawing of the molecule is given in Figure 12. Although the phosphorus atoms are disposed nearly tetrahedrally about the cobalt atoms, the general configuration appears to be that of a trigonal bipyramid. The cobalt atom is 0.493 \AA out of the plane of the equatorial phosphorus atoms, P1, P2, P3. In the similar structure, $\text{HCo}(\text{N}_2)(\text{P}(\text{C}_6\text{H}_5)_3)_3$ (54), the cobalt atom was found

Table 12. Root-Mean-Square Amplitudes of Vibration of the
 Thermal Ellipsoids of $\text{HCo}((\text{C}_6\text{H}_5)\text{P}(\text{OC}_2\text{H}_5)_2)_4$
 (in Angstroms)

C0	0.21128	0.21460	0.25109
P1	0.22399	0.24157	0.26906
P2	0.21507	0.22693	0.25284
P3	0.22523	0.22972	0.23152
P4	0.20972	0.21770	0.24404
O1	0.23256	0.27718	0.35696
O2	0.21459	0.27275	0.36203
O3	0.19957	0.26240	0.31955
O4	0.22373	0.25916	0.28512
O5	0.22037	0.24437	0.28824
O6	0.21688	0.27089	0.34024
O7	0.22517	0.23354	0.27845
O8	0.21379	0.23456	0.30493
C1	0.25038	0.31553	0.44463
C2	0.29327	0.37491	0.49799
C3	0.22096	0.35073	0.48414
C4	0.27129	0.38789	0.72590
C5	0.20874	0.25421	0.30056
C6	0.25561	0.32018	0.34766
C7	0.22432	0.36912	0.42368
C8	0.23569	0.32777	0.44548
C9	0.25520	0.34778	0.37880
C10	0.24612	0.29743	0.33793
C11	0.22259	0.32442	0.42279
C12	0.23644	0.37497	0.45328
C13	0.24186	0.25854	0.29497
C14	0.25313	0.30552	0.35219
C15	0.22835	0.25838	0.27587
C16	0.24341	0.28978	0.32788
C17	0.23428	0.37063	0.38765
C18	0.21315	0.39921	0.45489
C19	0.23858	0.39568	0.48316
C20	0.23049	0.31329	0.40781
C21	0.23387	0.29190	0.33099
C22	0.23732	0.36390	0.39924
C23	0.23436	0.33644	0.39465
C24	0.26625	0.38354	0.51067
C25	0.20770	0.22684	0.26150

Table 12. Continued

C26	0.23407	0.26177	0.29718
C27	0.24575	0.27490	0.36982
C28	0.23629	0.26822	0.43141
C29	0.23015	0.28841	0.41233
C30	0.24435	0.26538	0.32287
C31	0.23638	0.28162	0.37426
C32	0.24362	0.30191	0.34541
C33	0.23213	0.26361	0.35582
C34	0.23368	0.30024	0.37671
C35	0.22510	0.23806	0.23969
C36	0.22827	0.26430	0.34579
C37	0.21938	0.31822	0.43804
C38	0.22024	0.31247	0.42196
C39	0.21740	0.30641	0.40181
C40	0.23731	0.25927	0.37045

Figure 12. Stereoscopic Drawing of $\text{HCo}((\text{C}_6\text{H}_5)\text{P}(\text{OC}_2\text{H}_5)_2)_4$ 

to be 0.321 and 0.283 Å from the plane (two independent molecules in the asymmetric unit). In $\text{HCo}(\text{PF}_3)_4$, the Co atom is 0.59 Å from the plane (78). The behavior of $\text{HCo}((\text{C}_6\text{H}_5)\text{P}(\text{OC}_2\text{H}_5)_2)_4$ strongly suggests that a description of the molecule which recognizes the tetrahedral tendency of the phosphorus ligands is preferred. For this reason, it is probably more correct to speak of the molecule as a distorted tetrahedral skeleton of phosphorus ligands with the hydrogen occupying a tetrahedral face.

The similarity of the unit cells of the iron and cobalt complexes has been noted above. Figure 10 presents stereoscopic drawings of both cells for comparison. The alternative hydrogen position in the cobalt complex can easily be seen by examination of the corresponding positions of the iron complex. As noted previously, the thermal ellipsoids generally show the same directions for their principal axes, although the absolute values are larger for the cobalt complex.

The parameters of the ligand atoms were found to be quite similar to those of the iron complex. In this case also there appears to be some disorder in the carbon atom framework (see for instance carbon 4), and the reported standard deviations of the bonds and angles are undoubtedly underestimated. As an example, assuming all of the O-C bond distances are equivalent, the standard deviation of

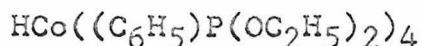
the values given is 0.023. This is over three times the average standard deviation (0.007) calculated from the least-squares refinement. The extremely short carbon-carbon distances are again indicative of disorder. A comparison of the average bond lengths was given in Table 5. The ligand bond angles are within the range usually found for phosphites and phosphines (55). The deviations of the carbon atoms from the least-squares planes of the four phenyl rings are given in Table 13.

Table 13. Deviations from Least-Squares Planes in
 $\text{HCo}((\text{C}_6\text{H}_5)\text{P}(\text{OC}_2\text{H}_5)_2)_4$

RING 1		RING 2	
ATOM	DEVIATION	ATOM	DEVIATION
C5	-.0038	C15	-.0115
C6	0.0059	C16	0.0086
C7	-.0019	C17	0.0024
C8	-.0041	C18	-.0103
C9	0.0062	C19	0.0070
C10	-.0022	C20	0.0039

RING 3		RING 4	
ATOM	DEVIATION	ATOM	DEVIATION
C25	0.0069	C35	0.0006
C26	-.0044	C36	-.0028
C27	-.0052	C37	0.0016
C28	0.0124	C38	0.0018
C29	-.0096	C39	-.0040
C30	-.0001	C40	0.0028

DISCUSSION OF THE SPECTRAL PROPERTIES OF



The presence of only one ligand hydrogen atom in this complex simplifies considerably the discussion of the nature of the metal-hydrogen bond. Several analogous complexes have been reported in the literature. In some cases a cobalt-hydrogen stretching frequency was not reported, perhaps due to the fact that the absorption is generally very weak. Table 14 lists $\nu(\text{Co-H})$ absorptions for several 5-coordinate cobalt hydride complexes. The cobalt-hydrogen stretching frequency for $\text{HCo}((\text{C}_6\text{H}_5)\text{P}(\text{OC}_2\text{H}_5)_2)_4$ is among the higher energy values reported in Table 14, indicating a relatively strong Co-H bond. The infrared spectrum of a Nujol mull of the complex is presented in Figure 13. The band is quite weak; if it had occurred at a lower energy it may well have been mistaken for one of the ligand bands. The corresponding $\nu(\text{Co-D})$ could not be detected, probably because of coincidence with one of the several strong C-C bands in the $1300 - 1500 \text{ cm}^{-1}$

Table 14. Cobalt-Hydrogen Stretching Frequencies

<u>Compound</u>	<u>ν(Co-H)</u>	<u>Ref.</u>
HCo(N ₂)(PPh ₃) ₃	2085 cm ⁻¹	54
HCo(PhP(OEt) ₂) ₄	2017	--
HCo(PF ₃) ₄	1973(R)	3
HCo(PF ₃) ₄	1964	77
HCo(PF ₃) ₄	1974(R)	77
HCo(P(OEt) ₃) ₄	1964	38
HCo(PMePh ₂) ₄	1958	11
HCo(CO) ₄	1934	78
HCo(C ₂ H ₄ (PPh ₂) ₂) ₂	1884	70
HCo(C ₂ H ₄ (PMe ₂) ₂) ₂	1855	79
HCo(P(OPh) ₃) ₄	not observed	74

(R = Raman)

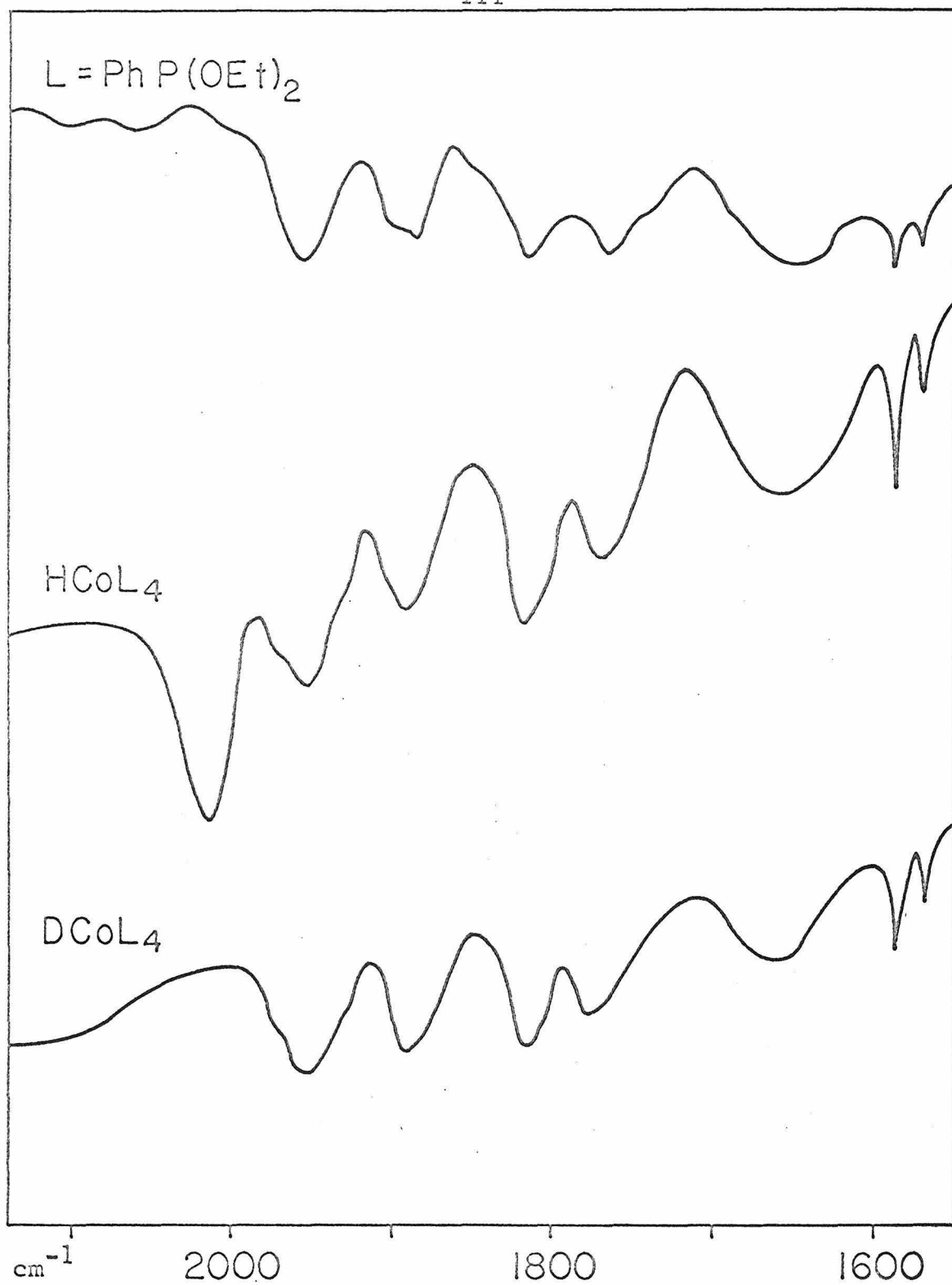
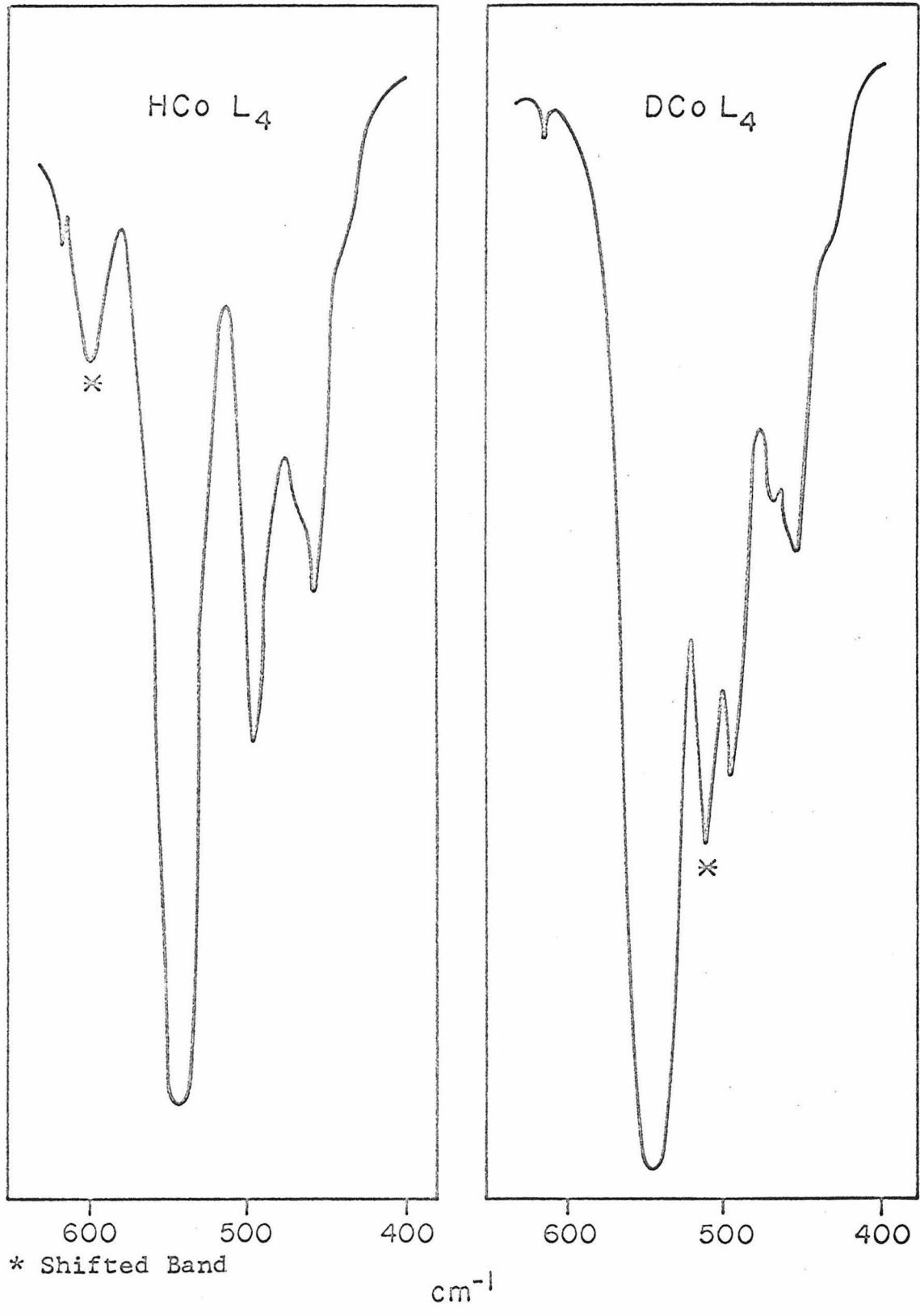


Figure 13. Infrared Spectrum of $\text{HCo}((\text{C}_6\text{H}_5)\text{P}(\text{OC}_2\text{H}_5)_2)_4$

Figure 14.

Infrared Spectra of $\text{HCo}((\text{C}_6\text{H}_5)\text{P}(\text{OC}_2\text{H}_5)_2)_4$
and $\text{DCo}((\text{C}_6\text{H}_5)\text{P}(\text{OC}_2\text{H}_5)_2)_4$ in the
400 - 600 cm^{-1} Region

Figure 14.



region. Consideration of the energies of the bands in Table 15 shows that the metal-hydrogen bands are comparable in energy to the bands in the cis dihydride complexes. It is interesting to note that for a series of H_3CoL_3 complexes (11), two ν (Co-H) bands are noted; a strong absorption at 1720 - 1750 cm^{-1} and a medium absorption at 1920 - 1940 cm^{-1} . The positions and intensities of these bands are strongly indicative of mer- H_3CoL_4 structures.

There are three bands present in the infrared spectrum of $DCo((C_6H_5)P(OC_2H_5)_2)_4$ which are not observed in that of $HCo((C_6H_5)P(OC_2H_5)_2)_4$. Two are of relatively high energy, 1259 and 1130 cm^{-1} , and probably represent modes which are mixed with δ (P-Co-D). The third band appears at 514 cm^{-1} ; this is probably related to the hydride band at 600 cm^{-1} which is not present in the spectrum of the deuteride (see Figure 14). The nearness of the two bands suggests that the δ (P-Co-H) modes undergo mixing with other bending modes of the molecule. A recent study of $HCo(PF_3)_4$ revealed a δ (P-Co-H) mode of 625 cm^{-1} which was shifted to about 550 cm^{-1} upon deuteration (77).

The infrared spectrum in solution shows no band which may be assigned to ν (Co-H). Several attempts to obtain the low temperature infrared spectrum of the complex failed because of a reaction of the AgCl cell windows with the compound. Although the nature of this reaction is

unknown, it is clear that the cobalt hydride complex acts as a reducing agent, leaving a silver mirror on the surface of the AgCl plate. Such reactivity is surprising since the iron dihydride has no detectable effect on the AgCl.

As noted above, the n.m.r. spectrum of $\text{HCo}(\text{C}_6\text{H}_5)\text{P}(\text{OC}_2\text{H}_5)_2)_4$ shows a quintet at room temperature which eventually coalesces to a single broad band at -50°C . The quadrupole moment of the ^{59}Co nucleus (spin = $7/2$) has an increasing influence on the proton resonance as the molecular rearrangement decreases (and the anisotropy of the molecule increases). The n.m.r. spectrum can thus be used as a rough gauge of the nonrigidity of a complex in solution. One example of a relatively rigid structure is $\text{HCo}(\text{PF}_3)_4$. For this complex only the single broad band is observed. From the crystal structure of this compound (73), it can be seen that the phosphorus ligands are distorted only slightly from a tetrahedral configuration. With such a small amount of distortion (9°) even in the solid state, it is not likely that major distortions will occur in solution. Movement of the hydrogen across the edge positions will be relatively difficult in such a situation (see Section II) and the intramolecular rearrangements are thus reduced. In the case of $\text{HCo}((\text{C}_6\text{H}_5)\text{P}(\text{OC}_2\text{H}_5)_2)_4$, the phosphorus ligands can be dislocated more

easily, and the single band of the more rigid model is not observed except at low temperature. Because of the quadrupole moment of the ^{59}Co nucleus, and the uncertainty of its effects upon the n.m.r. spectrum, arguments of this type are at best crude.

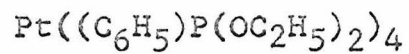
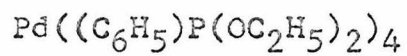
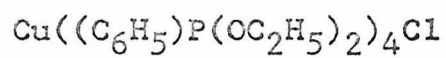
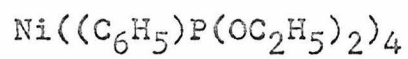
In solution at room temperature, $\text{HCo}((\text{C}_6\text{H}_5)\text{P}(\text{OC}_2\text{H}_5)_2)_4$, probably exists in an essentially tetrahedral form, with the hydride ligand moving rapidly from face to face. This should not be surprising, since the phosphine ligands of an analogous rhodium complex, $\text{HRh}(\text{P}(\text{C}_6\text{H}_5)_3)_4$, are tetrahedrally disposed even in the solid state (80). As the motion of the hydride ligand slows down at reduced temperatures, one face becomes preferentially distorted and eventually a pseudo-trigonal bipyramid arrangement results. If the coupling constants found for the iron complex were valid in this case, a quartet of doublets would be expected in the low temperature n.m.r. spectrum of the trigonal bipyramidal species. The cobalt quadrupole moment, which increasingly influences the spectrum as the molecule grows more rigid, very likely will prevent the resolution of such a spectrum.

On the basis of the ^{31}P chemical shift, it has been proposed that the ligand hydrogen atom of $\text{HCo}(\text{P}(\text{OPh}_3))_4$ is acidic, and that the cobalt atom has a -1 formal charge (74). The chemical evidence which accompanied the proposal was

in conflict with such an assignment. The authors therefore concluded that the hydrogen atom was shielded from reaction by one or more of the phenyl groups. The method of preparation of this complex is very similar to that used for $\text{HCo}((\text{C}_6\text{H}_5)\text{P}(\text{OC}_2\text{H}_5)_2)_4$, requiring reduction by sodium borohydride. It is difficult to understand how a complex which obtains its hydrogen ligand from a strong base such as NaBH_4 will act as an acid in the presence of triethylamine (the test for acidity used). The PF_3 analog, $\text{HCo}(\text{PF}_3)_4$, readily forms the anion $\text{Co}(\text{PF}_3)_4^-$ in the presence of triethylamine; this complex, however, is not prepared in the presence of NaBH_4 . All of the evidence presently available indicates that of the phosphorus ligands, only PF_3 has electron withdrawing capabilities great enough to produce acidic hydrido complexes.

SECTION IV

TETRAKIS(DIETHYLPHENYLPHOSPHONITE) COMPLEXES OF
NI(0), CU(I), PD(0), AND PT(0)



Tetrakis-phosphine and-phosphite complexes of d^{10} transition metals have been studied extensively in the past twenty years (30,35,74,81-98). The present work deals with the syntheses and vibrational spectra of complexes of $C_6H_5P(OC_2H_5)_2$ with Ni(0), Cu(I), Pd(0), and Pt(0). The ultraviolet spectra of the Ni(0), Cu(I), and Pd(0) complexes have been reported (7); because of reproducibility problems with the reported Cu(I) synthesis, an alternative method is suggested (see Experimental Section).

The Pt(0) complex, $Pt((C_6H_5)P(OC_2H_5)_2)_4$, is a nearly colorless (very light yellow) solid at room temperature. It can be easily recrystallized from absolute ethanol, yielding square platelets which are often twinned. The compound is relatively stable to air, being comparable in this respect to the cobalt complex. Unlike its tri-phenylphosphine analog (85,99), the present compound does not undergo dissociation in solution. Beer's law is followed in the concentration range of 5×10^{-6} to 1.3×10^{-4} m/l; addition of free ligand to solutions of the complex does not change the position or the intensity of the band at 3080 \AA (39).

It has been generally assumed (86) that the phosphorus skeletons of complexes of this type are tetrahedral. The observation that the x-ray powder photographs of

$(\text{CH}_3\text{C}(\text{CH}_2\text{O})_3\text{P})_4\text{Ni}(\text{O})$ and $-\text{Pt}(\text{O})$ are not identical is, however, disturbing (81). Since few structural data are available for these complexes, it is not known if this difference is general throughout the series, or merely confined to the complexes of $\text{CH}_3\text{C}(\text{CH}_2\text{O})_3\text{P}$. Because of the lack of structural work in this field, an attempt was made to determine the structure of $\text{Pt}((\text{C}_6\text{H}_5)\text{P}(\text{OC}_2\text{H}_5)_2)_4$.

About fifty crystals were mounted and coated in the manner described above. Unfortunately, those small enough for intensity data collection were all found to be twinned. A few larger crystals which were suitable for photographic cell determination suffered from only a small degree of twinning. These were used for obtaining precision Weissenberg photographs. A least-squares refinement of 2θ values taken from these photographs yielded the cell dimensions given in Table 15. From the Weissenberg photographs, it appears that the cell has pseudo-hexagonal symmetry. Possibly the reduced true symmetry is the result of the asymmetric phosphonite ligands, although a phosphorus skeleton of symmetry lower than tetrahedral certainly cannot be ruled out. It is notable, however, that the crystal habits of the Ni, Pd, and Pt complexes are the same, and oscillation photographs of the Ni complex (also twinned) indicate that the cell is similar to that of the Pt complex.

Table 15. Cell Parameters for $\text{Pt}((\text{C}_6\text{H}_5)\text{P}(\text{OC}_2\text{H}_5)_2)_4$

$a = 10.621(5) \text{ \AA}$	$\alpha = 82.96(4)^\circ$
$b = 11.611(4)$	$\beta = 117.32(3)$
$c = 20.011(9)$	$\gamma = 110.35(6)$
Volume: $2053(2) \text{ \AA}^3$	Space Group: $\text{P}\bar{1}$
Calc. Density: 1.597 gm/cm^3	
Exp. Density: $1.51(8) \text{ gm/cm}^3$	

Clearly, collection of intensity data for $\text{Pt}((\text{C}_6\text{H}_5)\text{P}(\text{OC}_2\text{H}_5)_2)_4$ presents some problems, the most important of which is twinning. Assuming an untwinned crystal were found, however, the problem of absorption remains. Because of the large cell, resolution of the reflections with molybdenum radiation would be marginal. On the other hand, the absorption coefficient for copper radiation is quite large, 86 cm^{-1} . If an untwinned crystal of the Pt complex eventually is found, it will undoubtedly be necessary to apply absorption corrections to the data.

As noted above and in the Experimental Section, the reported synthesis (7) of $\text{Cu}((\text{C}_6\text{H}_5)\text{P}(\text{OC}_2\text{H}_5)_2)_4\text{Cl}$ is not reproducible. The high solubility of these complexes presents an extraordinarily difficult problem in crystallizing the copper complex. It also appears that the loss of a phosphonite ligand can occur, $\text{CuL}_4\text{Cl} \rightarrow \text{CuL}_3\text{Cl} + \text{L}$, yielding a mixture of the two complexes. Examination of the elemental analysis indicates that the sample analyzed contained both the tetrakis- and the tris-phosphonite compounds. A silver complex can be prepared similarly to the copper complex by reacting silver nitrate with the phosphonite. Its properties have not been investigated because of the obvious low purity of the samples obtained, but the colorless crystals closely resemble those of the

copper complex. Similar complexes have been prepared by replacing the chloride and nitrate with perchlorate (81,83); no attempt was made to prepare this type of complex with diethylphenylphosphonite.

The infrared spectra of these compounds are essentially the same as those of the free ligand. The only characteristic bands which might be observed in the infrared region are those of the metal-phosphorus stretching absorptions. Because these bands appear at very low energy ($100 - 400 \text{ cm}^{-1}$), mixing of states with the numerous bending modes complicates the analysis significantly. It is not surprising, then, that there has been general disagreement as to the location of these bands, and a wide range of frequencies has been reported. Table 16 presents some of the reported metal-phosphorus stretching frequencies for tetrahedral complexes.

It has been suggested that zero-valent complexes display a $\nu(\text{M-P})$ below 265 cm^{-1} , while di-valent species absorb in the $320 - 460 \text{ cm}^{-1}$ region (100). This trend is not followed by the nickel complexes noted in Table 16, and an examination of other reported frequencies for di-valent nickel species indicates that the lack of agreement is general. If, however, the distinction between tetrahedral and square planar complexes is made, the rule becomes more acceptable. It seems generally true that tetrahedral

Table 16. Metal-Phosphorus Stretching Frequencies
of some Tetrahedral Complexes

<u>Compound</u>	<u>ν (M-P)</u>	<u>Ref.</u>
Ni(PPh ₃) ₂ Br ₂	196.8, 189.5 cm ⁻¹	101
Ni(PPh ₂ (n-Pr)) ₂ Br ₂	178, 162	101
Ni(PF ₃) ₄	219, 195(R)	87
Ni(P(OCH ₂) ₃ CCH ₃) ₄	157	81
Ni(P(OCH ₃) ₃) ₄	178	102
Ni(P(OEt) ₃) ₄	210, 305, 335	86
Ni(P(OEt) ₃) ₄	299	81
Pd(P(OEt) ₃) ₄	200, 290, 335	86
Pd(P(OCH ₂) ₃ CCH ₃) ₄	192, 142	81
Pt(P(OEt) ₃) ₄	215, 290, 332	86
Pt(P(OCH ₂) ₃ CCH ₃) ₄	191, 160	81
Pt(P(CHO) ₃ (CH ₂) ₃) ₄	194, 170	81
(Cu(P(OCH ₂) ₃ CCH ₃) ₄)ClO ₄	132	81
(Ag(P(OCH ₂) ₃ CCH ₃) ₄)ClO ₄	112	81

complexes have ν (M-P) absorptions at the lower energies, usually below 300 cm^{-1} .

In an attempt to locate the metal-phosphorus stretching bands for the present complexes, infrared and Raman spectra were obtained in the low energy regions. Unfortunately, infrared data could not be obtained below 200 cm^{-1} , so only Raman data are available in this region. The samples in all cases were Nujol mulls between CsI plates for the infrared determinations, and powders or single crystals for the Raman determinations. Neat samples of the free ligand were used in the infrared and Raman studies. The iron and cobalt complexes were included in this study. The infrared and Raman spectra are displayed in Figures 15 and 16. The palladium complex decomposed rapidly upon exposure to the exciting radiation of the Raman spectrophotometer, but a rapid scan over the lower energy region indicated the presence of a band between 160 and 190 cm^{-1} . The infrared spectrum of the palladium compound is nearly identical to that of the platinum complex. The frequencies which are believed to represent the metal-phosphorus stretching modes for the present complexes are given in Table 17.

As has been the case in previous studies of this type, there is some ambiguity in these assignments because of the relatively close ligand mode at 199 cm^{-1} . By comparison

Figure 15.

Low Energy Infrared and Raman
Spectra for PhP(OEt)_2 ,
 $\text{HCo(PhP(OEt)}_2)_4$, and
 $\text{H}_2\text{Fe(PhP(OEt)}_2)_4$

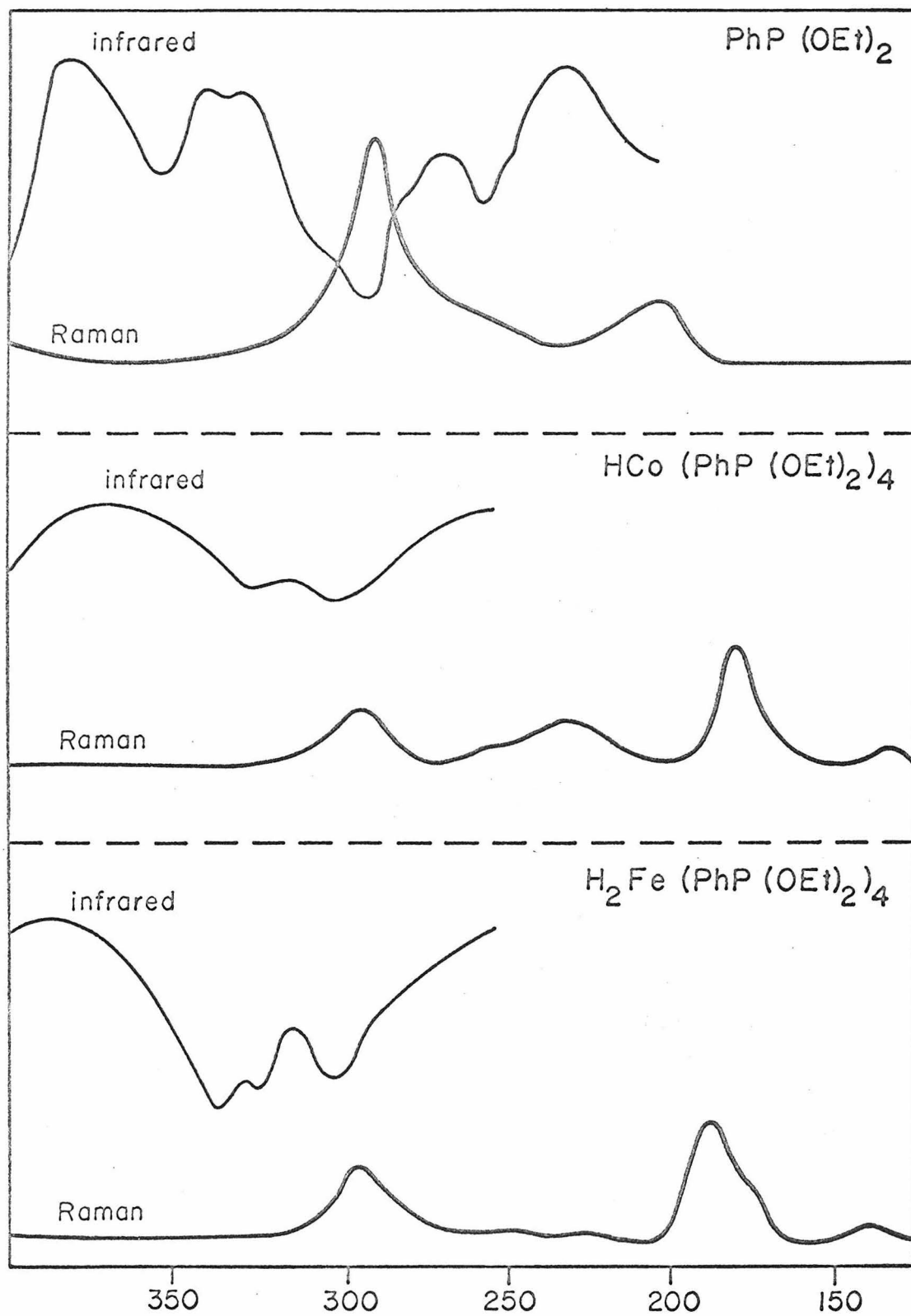


Figure 15.

 cm^{-1}

Figure 16.

Low Energy Infrared and Raman
Spectra of $\text{Ni}(\text{PhP}(\text{OEt})_2)_4$,
 $(\text{Cu}(\text{PhP}(\text{OEt})_2)_4)\text{Cl}$, and
 $\text{Pt}(\text{PhP}(\text{OEt})_2)_4$

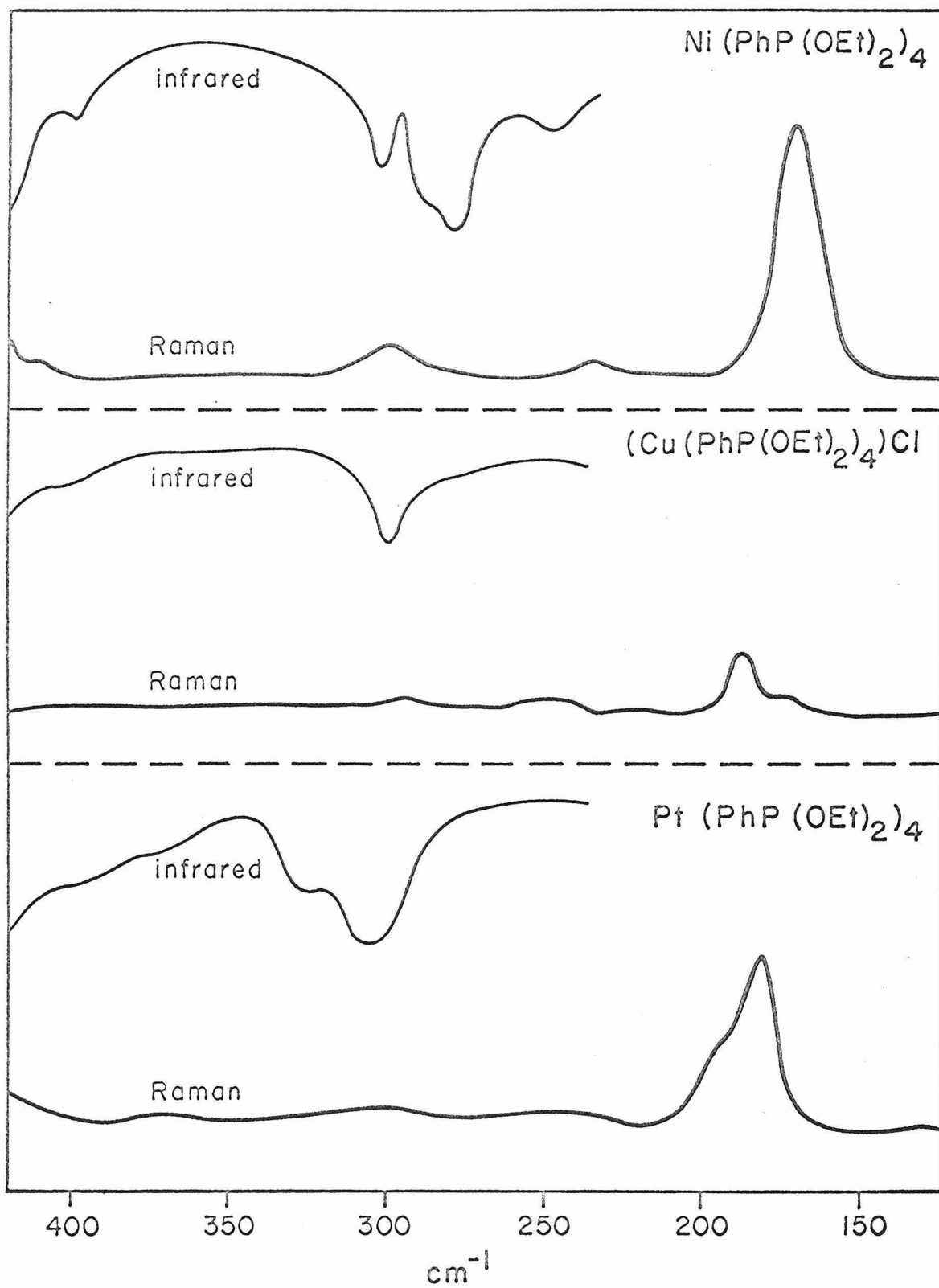


Figure 16.

Table 17. Metal-Phosphorus Stretching Frequencies for
Tetrakisdiethylphenylphosphonite Complexes

<u>Compound</u>	<u>ν (M-P)</u>
$\text{H}_2\text{Fe}(\text{PhP}(\text{OEt})_2)_4$	183, 174 _{sh} cm^{-1}
$\text{HCo}(\text{PhP}(\text{OEt})_2)_4$	181
$\text{Ni}(\text{PhP}(\text{OEt})_2)_4$	172
$(\text{Cu}(\text{PhP}(\text{OEt})_2)_4)\text{Cl}$	189
$\text{Pt}(\text{PhP}(\text{OEt})_2)_4$	184, 193 _{sh}

with the reported values for $\text{Ni}(\text{PF}_3)_4$, which were based on polarization studies, and those of the $\text{Ni}(\text{PPh}_3)_2\text{Br}_2$ complex, which were based on isotopic substitution experiments, it seems likely that the $\nu(\text{M-P})$ frequencies should be expected at or below 200 cm^{-1} . The relatively high intensities of the bands observed, and the lack of more intense bands at higher or lower energies, suggests (from a comparison with the spectrum of the free ligand) that they are at least partially the result of metal-phosphorus stretching. An examination of the values reported in Tables 16 and 17 does not reveal an obvious trend with a change in the metal atom, implying that at least in some cases the stretching modes are altered by mixing with other vibrational modes of the complexes.

Except for the palladium complex, all of the compounds in the present study can be exposed to air for brief periods (generally a few hours maximum) without noticeable deterioration. The order of stability to air is $\text{Ni} > \text{Co}$, $\text{Pt} > \text{Fe}$, $\text{Cu} \gg \text{Pd}$. The complexes are insoluble in and are apparently not affected by deoxygenated water. They do decompose rapidly, however, in any solvent which contains dissolved oxygen. They are soluble in most organic solvents, the solubility decreasing with increasing polarity of the solvents.

SUMMARY

The prevailing theme throughout the present work has been the tetrahedral arrangement of the phosphonite ligands about the metal atom. Such an arrangement is easy to accept in the case of the four-coordinate complexes, but is, of course, more difficult to rationalize for five- and six-coordinate species. In the discussion of rapid rearrangements of such molecules, it is common (and logical) to consider the ground state structure in solution to be an octahedron (six-coordinate species) or a trigonal bipyramid (five-coordinate species). In the present case, however, the four phosphonite ligands dominate the space about the metal atom, while the hydride ligands apparently squeeze in wherever possible. Thus, even though we are dealing with five- and six-coordinate complexes (the hydrides do take up specific sites), the dominance of the comparatively huge phosphonite ligands in effect gives the complexes decided four-coordinate character. Note that there is no implication of weak metal-hydrogen bonds in this discussion; on the contrary, the hydride hydrogens were found to be relatively inert, and could not be induced to exchange with D_2 or C_2H_5OD under a variety of conditions.

The question might well arise as to the necessity of speaking of the hydride complexes as basically distorted tetrahedra rather than distorted octahedra. We are, after

all, only discussing relative shapes, and since the established standards are based upon octahedra, it may seem superfluous to establish another base. For purposes of visualizing the spacial problems of these molecules, however, a tetrahedral foundation provides an easy rationalization for some of the problems encountered. Take, for example, the infrared spectra of the iron complex. Two isomers were found to exist in solution at low temperature, neither of which appeared to have a true trans dihydride configuration. The relative low energy of one of the ir. bands indicated that a species approaching a trans isomer ($\angle \text{H-Fe-H}$ somewhat less than 180°) was present. The application of a distorted octahedral model to this problem (29) presents no obvious reason why such an arrangement should exist. On the other hand, if a tetrahedral model is utilized (see Figure 8), an "almost trans" (E) isomer is a natural result of the geometry. The apparent predominance of cis (A) dihydride isomers in solution (48) can also be rationalized on the basis of a tetrahedral phosphorus ligand skeleton. The A arrangement is the only configuration which does not require that one of the hydrides occupy an energetically unfavorable edge position. On such a basis, $\text{H}_2\text{Fe}((\text{C}_6\text{H}_5)\text{P}(\text{OC}_2\text{H}_5)_2)_4$ occurs in two isomers, one with the two hydrides occupying faces of the phosphorus tetrahedron, (the cis or A isomer), and

the other with the hydrides occupying a face and a non-adjacent edge (the "trans" or E isomer). In the cobalt complex, $\text{HCo}((\text{C}_6\text{H}_5)\text{P}(\text{OC}_2\text{H}_5)_2)_4$, the hydride occupies a facial position.

The solid state structures of the two hydride complexes are quite similar, and it is possible that the single hydride of the cobalt complex can occupy either of the two facial positions which correspond to the hydride locations in the cis iron complex. As would be expected, the phosphorus atom skeleton is more tetrahedral in the cobalt complex.

As with other phosphine metal hydrides (excluding those of PF_3), the present complexes show no acidic character. They can be prepared in low yield without the addition of borohydride, presumably abstracting a hydride from the α -carbon of the solvent ethanol (22,64).

Diethylphenylphosphonite, $\text{C}_6\text{H}_5\text{P}(\text{OC}_2\text{H}_5)_2$, is the only monodentate phosphorus ligand known which forms a trans (C) dihydride isomer in the solid state. All other trans complexes of this type involve bidentate ligands. Although the reason for this is not well understood, it may result from the ability of the phosphonite ligands to distort from the ideal tetrahedral geometry, and thus reduce the steric hindrance of the edge positions (see Section II).

In light of these observations, it would be interesting to study the complexing properties of $o\text{-C}_6\text{H}_4\text{-(P(OC}_2\text{H}_5)_2)_2$. Unfortunately, the synthesis of this compound is a problem in itself. The major difficulty is in obtaining $o\text{-C}_6\text{H}_4\text{(PCl}_2)_2$, from which the ethyl ester could easily be prepared. A recent publication implies that preparation of this chloride might be achieved with reasonable results (103). If the bidentate ligand could be prepared, it might well be expected to produce trans (C) dihydride complexes.

REFERENCES

- 1) J. Chatt, Nature, 165, 637 (1950).
- 2) A. Pidcock, R. E. Richards, and L. M. Venanzi, J. Chem. Soc. (A), 1707 (1966);
L. M. Venanzi, Chem. Brit., 4, 162 (1968).
- 3) Th. Kruck, Angew. Chem. Int. Edit., 6, 53 (1967).
- 4) L. S. Meriwether and M. L. Fiene, J. Am. Chem. Soc., 81, 4200 (1959).
- 5) W. D. Horrocks, Jr., and R. C. Taylor, Inorg. Chem., 2, 723 (1963).
- 6) B. B. Chastain, E. A. Rick, R. L. Pruett, and H. B. Gray, J. Am. Chem. Soc., 90, 3994 (1968).
- 7) A. A. Orio, B. B. Chastain, and H. B. Gray, Inorg. Chim. Acta, 3, 8 (1969).
- 8) W. Hieber and F. Leutert, Naturwiss., 19, 360 (1931).
- 9) W. Hieber, K. Kramer, and H. Schuiter, Angew. Chem., 49, 463 (1936).
- 10) A. Sacco and M. Rossi, Inorg. Chim. Acta, 2, 127 (1968).
- 11) M. Rossi and A. Sacco, Chem. Comm., 471 (1969).
- 12) A. Misono, Y. Uchida, T. Saito, and K. M. Song, Chem. Comm., 419 (1967).
- 13) A. Sacco and M. Rossi, Chem. Comm., 316 (1967).
- 14) A. Sacco and M. Aresta, Chem. Comm., 1223 (1968).
- 15) J. Lorberth, H. Noth, P. V. Rinze, J. Organometal. Chem., 16, Pl (1969).
- 16) S. C. Srivastava and M. Bigorgne, J. Organometal. Chem., 19, 241 (1969).
- 17) J. R. Shapley and J. A. Osborn, J. Am. Chem. Soc., 92, 6976 (1970).

- 18) R. Rabinowitz and J. Pellon, J. Org. Chem., 26, 4623 (1961).
- 19) L. W. Daasch and D. C. Smith, Analytical Chemistry, 23, 853 (1951).
- 20) H. Schindlbauer, Monatshefte Chemie, 96, 1936 (1965).
- 21) J. Chatt and B. L. Shaw, Chem. Ind. London, 290 (1961);
J. Chatt, Proc. Chem. Soc., 318 (1962).
- 22) W. Hieber and H. Vetter, Z. Anorg. Allgem. Chem., 212, 145 (1933).
- 23) A. P. Ginsberg, R. L. Carlin, Ed., Transition Metal Chemistry, 1, Marcel Dekker, New York, 111 (1965).
- 24) R. V. G. Ewens and M. W. Lister, Trans. Faraday Soc., 35, 681 (1939).
- 25) E. O. Bishop, J. L. Down, P. R. Entage, R. E. Richards, and G. Wilkinson, J. Chem. Soc., 2484 (1959).
- 26) S. J. LaPlaca, W. C. Hamilton, J. A. Ibers, A. Davison, Inorg. Chem., 8, 1928 (1969).
- 27) K. Farmery, M. Kilner, J. Chem. Soc., (A) 634 (1970).
- 28) J. Chatt, F. A. Hart, and R. G. Hayter, Nature, 187, 55 (1960).
- 29) F. N. Tebbe, P. Meakin, J. P. Jesson, E. L. Muetterties, J. Am. Chem. Soc., 92, 1068 (1970).
- 30) J. Chatt, F. A. Hart, D. T. Rosevear, J. Chem. Soc., 5504 (1961).
- 31) J. Chatt and R. G. Hayter, J. Chem. Soc., 5507 (1961).
- 32) P. Krumholz and H. M. A. Stettiner, J. Am. Chem. Soc., 71, 3035 (1949).
- 33) F. A. Cotton, Inorg. Chem., 3, 702 (1964).
- 34) A. Loutellier and M. Birgorgne, Bull. Soc. Chim. France, 3186 (1965).
- 35) G. Wilkinson, J. Am. Chem. Soc., 73, 5501 (1951).

- 36) J. Chatt and A. A. Williams, J. Chem. Soc., 3061 (1951).
- 37) J. C. Green, D. I. King, J. H. D. Eland, Chem. Comm., 1121 (1970).
- 38) W. Kruse and R. H. Atalla, Chem. Comm., 921 (1968).
- 39) A. A. Orio, Private Communication.
- 40) A. E. Schweizer, Private Communication.
- 41) M. Gerloch, R. Mason, J. Chem. Soc., 296 (1965).
- 42) E. R. Howells, D. C. Phillips, and D. Rogers, Acta Cryst., 3, 210 (1950).
- 43) Dr. R. E. Marsh is noted for his ability to apply the visual test. When confronted with a Weissenberg photograph of $\text{H}_2\text{Fe}((\text{C}_6\text{H}_5)\text{P}(\text{OC}_2\text{H}_5)_2)_4$, Dr. Marsh exclaimed, "This just has to have a center of symmetry!" Q. E. D.
- 44) International Tables for X-Ray Crystallography, Vol. III, Kynoch Press, Birmingham, England (1962).
- 45) D. T. Cromer, Acta Cryst., 18, 17 (1965).
- 46) J. Karle and I. L. Karle, Acta Cryst., 21, 849 (1966).
- 47) S. J. LaPlaca, J. A. Ibers, J. Amer. Chem. Soc., 85, 3501 (1963);
S. J. LaPlaca and J. A. Ibers, Acta Cryst., 18, 511 (1965).
- 48) P. Meakin, L. J. Guggenberger, J. P. Jesson, D. H. Gerlach, F. N. Tebbe, W. G. Peet, E. L. Muetterties, J. Am. Chem. Soc., 92, 3482 (1970).
- 49) L. J. Guggenberger, Private Communication.
- 50) V. A. Semion, Yu Struchkov, Zh. Struk. Khim., 10, 88 (1969).
- 51) R. L. Avoyan, Yo. A. Chopovakii, Zh. Struck. Khim., 7, 900 (1966).

- 52) V. G. Andrianov and Yo. T. Struchkov, Zh. Struck. Khim., 9, 240 (1968);
V. G. Andrianov and Yo. T. Struchkov, Zh. Struck. Khim., 9, 503 (1968).
- 53) D. J. Dahm and R. A. Jacobson, Chem. Comm., 496 (1966).
- 54) B. R. Davis, N. C. Payne, J. A. Ibers, J. Amer. Chem. Soc., 91, 1240 (1969).
- 55) J. K. Stalick and J. A. Ibers, Inorg. Chem., 8, 1084 (1969).
- 56) P. W. R. Corfield, R. J. Doedens, and J. A. Ibers, Inorg. Chem., 6, 197 (1967).
- 57) K. C. Dewhirst, W. Keim, and C. A. Reilly, Inorg. Chem., 7, 546 (1968).
- 58) D. K. Ottesen, Private Communication.
- 59) J. Chatt and R. G. Hayter, J. Chem. Soc., 2605 (1961).
- 60) J. A. Chopoorian, J. Lewis, and R. S. Nyholm, Nature, 190, 528 (1961).
- 61) L. Malatesta and R. Ugo, J. Chem. Soc., 2080 (1963).
- 62) S. D. Ibekwe and U. A. Raeburn, J. Organometal. Chem., 19, 447 (1969).
- 63) L. Vaska, J. Chem. Soc., 83, 756 (1961).
- 64) M. Angoletta and A. Araneo, Gazz. Chim. Ital., 93, 1343 (1963).
- 65) J. Chatt and B. L. Shaw, J. Chem. Soc., 5075 (1962);
J. Chatt, L. A. Duncanson, and B. L. Shaw, Chem. Ind. London, 859 (1958).
- 66) A. D. Buckingham and P. J. Stephens, J. Chem. Soc., 2747 (1964).
- 67) G. W. Coleman and A. A. Blanchard, J. Am. Chem. Soc., 58, 2160 (1936).
- 68) W. Hieber and H. Schulten, Z. Anorg. Allgem. Chem., 232, 29 (1937).

- 69) W. Hieber and W. Hubel, Z. Elektrochem., 57, 235 (1953).
- 70) F. Zinglues, F. Canziani, and A. Chiesa, Inorg. Chem., 2, 1303 (1963).
- 71) A. Sacco, R. Ugo, J. Chem. Soc., 3274 (1964).
- 72) Th. Kruck and W. Lung, Angew. Chem. Int. Edit., 4, 870 (1965).
- 73) B. A. Frenz and J. A. Ibers, Inorg. Chem., 9, 2403 (1970).
- 74) J. J. Levison, and S. D. Robinson, J. Chem. Soc., (A), 96 (1970);
J. J. Levison and S. D. Robinson, Chem. Comm., 1405 (1967).
- 75) H. P. Hanson, R. Herman, J. D. Lea, and S. Skillman, Acta Cryst., 17, 1040 (1964).
- 76) R. F. Stewart, E. R. Davidson, and W. T. Simpson, J. Chem. Phys., 42, 3175 (1965).
- 77) S. Benazeth, A. Loutellier, and M. Bigorgne, J. Organometal. Chem., 24, 479 (1970).
- 78) W. F. Edgell and R. Summitt, J. Am. Chem. Soc., 83, 1772 (1961).
- 79) R. A. Schunn, Inorg. Chem., 9, 2567 (1970).
- 80) R. W. Baker and P. Pauling, Chem. Comm., 1495 (1969).
- 81) R. L. Keiter and J. G. Verkade, Inorg. Chem., 9, 404 (1970).
- 82) A. C. Vandenbroucke, D. G. Hendricker, R. E. McCarley, and J. G. Verkade, Inorg. Chem., 7, 1825 (1968).
- 83) J. G. Verkade and T. S. Piper, Inorg. Chem., 1, 453 (1962).
- 84) R. S. Vinal and L. T. Reynolds, Inorg. Chem., 3, 1062 (1964).

- 85) L. Malatesta and C. Cariello, J. Chem. Soc., 2323 (1958);
L. Malatesta and C. Cariello, J. Inorg. Nucl. Chem., 8, 561 (1958).
- 86) V. G. Myers, F. Basolo, and K. Nakamoto, Inorg. Chem., 8, 1204 (1969).
- 87) L. A. Woodward and J. R. Hall, Spectrochim. Acta, 16, 654 (1960).
- 88) L. Malatesta and M. Angoletta, J. Chem. Soc., 1186 (1957).
- 89) J. W. Irvine, Jr., and G. W. Wilkinson, Science, 113, 742 (1951).
- 90) J. R. Olechowski, C. G. McAlister, and R. F. Clark, Inorg. Chem., 4, 246 (1965).
- 91) J. Chatt and G. A. Rowe, Nature, 191, 1191 (1961).
- 92) J. Chatt, F.A. Hart, and H. R. Wattson, J. Chem. Soc., 2537 (1962).
- 93) J. Chatt and F. A. Hart, J. Chem. Soc., 1376 (1960).
- 94) G. Wilkinson, Z. Naturforsch., 96, 446 (1954).
- 95) L. Malatesta and F. Sacco, Ann. Chim. (Rome), 44, 134 (1954).
- 96) L. D. Quin, J. Am. Chem. Soc., 79, 3681 (1957).
- 97) J. R. Leto and M. F. Leto, J. Am. Chem. Soc., 83, 2944 (1961).
- 98) J. J. Huttermann, Jr., B. M. Foxman, C. R. Sperati, and J. G. Verkade, Inorg. Chem., 4, 950 (1965).
- 99) J. P. Birk, J. Halpern, and A. L. Pickard, J. Am. Chem. Soc., 90, 4491 (1968).
- 100) D. M. Adams, Metal-Ligand and Related Vibrations, St. Martin's Press, New York (1968) p. 321.
- 101) J. T. Wand, C. Udovich, K. Nakamoto, A. Quattrochi, and J. R. Ferraro, Inorg. Chem., 9, 2675 (1970).

- 102) M. Bigorne, Compt. rend., 250, 3484 (1960).
- 103) Yu. I. Baranov, O. F. Filippov, S. L. Varshavskii,
and M. I. Kabachnik, Dokl. Akad. Nauk SSSR, 182,
337 (1968).

APPENDIX I

ADDITIONAL STRUCTURAL DATA FOR

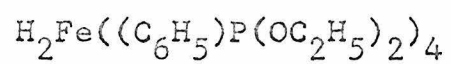


Table 18. Calculated and Observed Structure Factors for $\text{H}_2\text{Fe}((\text{C}_6\text{H}_5\text{P}(\text{OC}_2\text{H}_5)_2)_4$

The headings for each group give the k and l indices which apply to the group. The columns are in the order H , F_{obs} , F_{calc} .

To convert the present indices to those of the reduced cell (Table 1):

$$h_r = k + l$$

$$k_r = -l$$

$$l_r = h$$

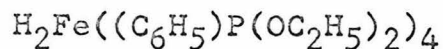
Table 18. Calculated and Observed Structure Factors

for $H_2Fe((C_6H_5)P(OC_2H_5)_2)_4$

H 4 -10	0 263 270	2 163 -163	0 318 313	5 357 361	4 184 182	5 529 -539	8 438 442	8 421 -426	7 400 398	13 95 -62
1 287 300	1 321 310	3 233 418	1 111 -49	6 324 366	5 207 -201	5 182 -180	9 528 -509	9 73 -11	8 91 91	8 55 -21
2 115 98	2 303 -189	4 78 -40	2 561 -579	7 213 -182	6 92 -76	6 365 368	10 256 -269	10 139 -124	H 5 -3	9 189 -171
3 141 -113	3 78 -40	H 1 -7	3 67 -19	8 80 26	7 232 226	7 335 -334	11 367 350	H 9 -3	10 133 -171	H -22
4 177 -142	4 282 -224	5 330 -351	5 110 -111	9 97 66	10 261 -270	9 194 191	13 81 -84	0 296 290	11 81 -15	H 7 -2
H 5 -10	1 101 -51	1 307 -308	6 255 -253	7 91 -76	H 8 -76	11 83 44	11 99 58	2 174 -184	3 116 97	0 88 61
0 123 -93	2 180 164	4 44 -34	H 10 -7	0 182 177	1 297 305	H 6 -5	H 4 -4	4 98 -34	4 105 -79	5 25 -7
1 287 300	3 101 -21	5 62 -13	0 142 140	1 497 17	2 247 17	3 217 -213	4 378 -331	5 102 -30	2 809 607	6 581 -603
2 76 -61	4 144 -106	6 227 -238	1 415 -426	2 347 -343	3 247 -415	4 343 -366	5 1241 1306	6 81 -50	7 137 32	7 150 120
3 86 35	5 119 -119	8 207 201	2 42 0	3 87 49	4 65 -96	5 232 -189	6 147 -180	7 137 -135	8 42 -64	9 55 37
4 143 118	6 110 -110	9 43 -37	3 238 231	4 194 -177	5 347 -421	6 217 172	7 160 -155	8 103 151	9 74 75	10 388 381
H 5 -10	8 82 42	10 154 153	4 68 -9	5 98 -92	6 80 -81	7 137 131	8 104 157	9 354 -370	10 166 -116	11 84 26
G 157 145	H 2 -8	H 2 -7	H 1 -76	8 60 7	9 85 -32	6 416 409	5 159 162	8 511 -532	2 196 195	10 155 140
1 496 313	0 324 -346	0 613 -605	0 168 178	1 415 -426	2 347 -343	3 247 -415	4 343 -366	5 1241 1306	6 81 -50	H 6 -2
2 115 98	1 304 -303	1 311 -11	3 37 -56	4 143 -143	5 207 -201	6 92 -76	7 232 226	8 438 442	9 528 -509	0 76 -84
3 141 -113	2 303 -189	3 233 418	2 59 -3	3 37 -56	4 143 -143	5 207 -201	6 92 -76	7 232 226	8 438 442	1 340 -345
4 177 -142	5 330 -351	5 110 -111	3 37 -56	4 143 -143	5 207 -201	6 92 -76	7 232 226	8 438 442	9 528 -509	2 143 -94
H 5 -10	1 101 -51	1 307 -308	4 44 -34	5 110 -111	6 255 -253	7 91 -76	8 80 26	9 97 66	10 261 -270	3 433 433
0 123 -93	2 180 164	4 44 -34	5 110 -111	6 255 -253	7 91 -76	8 80 26	9 97 66	10 261 -270	11 81 -15	4 231 249
1 287 300	3 101 -21	5 62 -13	0 142 140	1 497 17	2 347 -343	3 247 -415	4 343 -366	5 1241 1306	6 81 -50	5 115 -45
2 76 -61	4 144 -106	6 227 -238	1 415 -426	2 347 -343	3 247 -415	4 343 -366	5 1241 1306	6 81 -50	7 137 32	6 581 -603
3 86 35	5 119 -119	8 207 201	2 42 0	3 87 49	4 65 -96	5 232 -189	6 147 -180	7 137 -135	8 42 -64	9 55 37
4 143 118	6 110 -110	9 43 -37	3 238 231	4 194 -177	5 347 -421	6 217 172	7 160 -155	8 103 151	9 74 75	10 388 381
H 5 -10	8 82 42	10 154 153	4 68 -9	5 98 -92	6 80 -81	7 137 131	8 104 157	9 354 -370	10 166 -116	11 84 26
G 157 145	H 2 -8	H 2 -7	H 1 -76	8 60 7	9 85 -32	6 416 409	5 159 162	8 511 -532	2 196 195	10 155 140
1 496 313	0 324 -346	0 613 -605	0 168 178	1 415 -426	2 347 -343	3 247 -415	4 343 -366	5 1241 1306	6 81 -50	H 6 -2
2 115 98	1 304 -303	1 311 -11	3 37 -56	4 143 -143	5 207 -201	6 92 -76	7 232 226	8 438 442	9 528 -509	0 76 -84
3 141 -113	2 303 -189	3 233 418	2 59 -3	3 37 -56	4 143 -143	5 207 -201	6 92 -76	7 232 226	8 438 442	1 340 -345
4 177 -142	5 330 -351	5 110 -111	3 37 -56	4 143 -143	5 207 -201	6 92 -76	7 232 226	8 438 442	9 528 -509	2 143 -94
H 5 -10	1 101 -51	1 307 -308	4 44 -34	5 110 -111	6 255 -253	7 91 -76	8 80 26	9 97 66	10 261 -270	3 433 433
0 123 -93	2 180 164	4 44 -34	5 110 -111	6 255 -253	7 91 -76	8 80 26	9 97 66	10 261 -270	11 81 -15	4 231 249
1 287 300	3 101 -21	5 62 -13	0 142 140	1 497 17	2 347 -343	3 247 -415	4 343 -366	5 1241 1306	6 81 -50	5 115 -45
2 76 -61	4 144 -106	6 227 -238	1 415 -426	2 347 -343	3 247 -415	4 343 -366	5 1241 1306	6 81 -50	7 137 32	6 581 -603
3 86 35	5 119 -119	8 207 201	2 42 0	3 87 49	4 65 -96	5 232 -189	6 147 -180	7 137 -135	8 42 -64	9 55 37
4 143 118	6 110 -110	9 43 -37	3 238 231	4 194 -177	5 347 -421	6 217 172	7 160 -155	8 103 151	9 74 75	10 388 381
H 5 -10	8 82 42	10 154 153	4 68 -9	5 98 -92	6 80 -81	7 137 131	8 104 157	9 354 -370	10 166 -116	11 84 26
G 157 145	H 2 -8	H 2 -7	H 1 -76	8 60 7	9 85 -32	6 416 409	5 159 162	8 511 -532	2 196 195	10 155 140
1 496 313	0 324 -346	0 613 -605	0 168 178	1 415 -426	2 347 -343	3 247 -415	4 343 -366	5 1241 1306	6 81 -50	H 6 -2
2 115 98	1 304 -303	1 311 -11	3 37 -56	4 143 -143	5 207 -201	6 92 -76	7 232 226	8 438 442	9 528 -509	0 76 -84
3 141 -113	2 303 -189	3 233 418	2 59 -3	3 37 -56	4 143 -143	5 207 -201	6 92 -76	7 232 226	8 438 442	1 340 -345
4 177 -142	5 330 -351	5 110 -111	3 37 -56	4 143 -143	5 207 -201	6 92 -76	7 232 226	8 438 442	9 528 -509	2 143 -94
H 5 -10	1 101 -51	1 307 -308	4 44 -34	5 110 -111	6 255 -253	7 91 -76	8 80 26	9 97 66	10 261 -270	3 433 433
0 123 -93	2 180 164	4 44 -34	5 110 -111	6 255 -253	7 91 -76	8 80 26	9 97 66	10 261 -270	11 81 -15	4 231 249
1 287 300	3 101 -21	5 62 -13	0 142 140	1 497 17	2 347 -343	3 247 -415	4 343 -366	5 1241 1306	6 81 -50	5 115 -45
2 76 -61	4 144 -106	6 227 -238	1 415 -426	2 347 -343	3 247 -415	4 343 -366	5 1241 1306	6 81 -50	7 137 32	6 581 -603
3 86 35	5 119 -119	8 207 201	2 42 0	3 87 49	4 65 -96	5 232 -189	6 147 -180	7 137 -135	8 42 -64	9 55 37
4 143 118	6 110 -110	9 43 -37	3 238 231	4 194 -177	5 347 -421	6 217 172	7 160 -155	8 103 151	9 74 75	10 388 381
H 5 -10	8 82 42	10 154 153	4 68 -9	5 98 -92	6 80 -81	7 137 131	8 104 157	9 354 -370	10 166 -116	11 84 26
G 157 145	H 2 -8	H 2 -7	H 1 -76	8 60 7	9 85 -32	6 416 409	5 159 162	8 511 -532	2 196 195	10 155 140
1 496 313	0 324 -346	0 613 -605	0 168 178	1 415 -426	2 347 -343	3 247 -415	4 343 -366	5 1241 1306	6 81 -50	H 6 -2
2 115 98	1 304 -303	1 311 -11	3 37 -56	4 143 -143	5 207 -201	6 92 -76	7 232 226	8 438 442	9 528 -509	0 76 -84
3 141 -113	2 303 -189	3 233 418	2 59 -3	3 37 -56	4 143 -143	5 207 -201	6 92 -76	7 232 226	8 438 442	1 340 -345
4 177 -142	5 330 -351	5 110 -111	3 37 -56	4 143 -143	5 207 -201	6 92 -76	7 232 226	8 438 442	9 528 -509	2 143 -94
H 5 -10	1 101 -51	1 307 -308	4 44 -34	5 110 -111	6 255 -253	7 91 -76	8 80 26	9 97 66	10 261 -270	3 433 433
0 123 -93	2 180 164	4 44 -34	5 110 -111	6 255 -253	7 91 -76	8 80 26	9 97 66	10 261 -270	11 81 -15	4 231 249
1 287 300	3 101 -21	5 62 -13	0 142 140	1 497 17	2 347 -343	3 247 -415	4 343 -366	5 1241 1306	6 81 -50	5 115 -45
2 76 -61	4 144 -106	6 227 -238	1 415 -426	2 347 -343	3 247 -415	4 343 -366	5 1241 1306	6 81 -50	7 137 32	6 581 -603
3 86 35	5 119 -119	8 207 201	2 42 0	3 87 49	4 65 -96	5 232 -189	6 147 -180	7 137 -135	8 42 -64	9 55 37
4 143 118	6 110 -110	9 43 -37	3 238 231	4 194 -177	5 347 -421	6 217 172	7 160 -155	8 103 151	9 74 75	10 388 381
H 5 -10	8 82 42	10 154 153	4 68 -9	5 98 -92	6 80 -81	7 137 131	8 104 157	9 354 -370	10 166 -116	11 84 26
G 157 145	H 2 -8	H 2 -7	H 1 -76	8 60 7	9 85 -32	6 416 409	5 159 162	8 511 -532	2 196 195	10 155 140
1 496 313	0 324 -346	0 613 -605	0 168 178	1 415 -426	2 347 -343	3 247 -415	4 343 -366	5 1241 1306	6 81 -50	H 6 -2
2 115 98	1 304 -303	1 311 -11	3 37 -56	4 143 -143	5 207 -201	6 92 -76	7 232 226	8 438 442	9 528 -509	0 76 -84
3 141 -113	2 303 -189	3 233 418	2 59 -3	3 37 -56	4 143 -143	5 207 -201	6 92 -76	7 232 226	8 438 442	1 340 -345
4 177 -142	5 330 -351	5 110 -111	3 37 -56	4 143 -143	5 207 -201	6 92 -76	7 232 226	8 438 442	9 528 -509	2 143 -94
H 5 -10	1 101 -51	1 307 -308	4 44 -34	5 110 -111	6 255 -253	7 91 -76	8 80 26	9 97 66	10 261 -270	3 433 433
0 123 -93	2 180 164	4 44 -34	5 110 -111	6 255 -253	7 91 -76	8 80 26	9 97 66	10 261 -270	11 81 -15	4 231 249
1 287 300	3 101 -21	5 62 -13	0 142 140	1 497 17	2 347 -343	3 247 -415	4 343 -366	5 1241 1306	6 81 -50	5 115 -45
2 76 -61	4 144 -106	6 227 -238	1 415 -426	2 347 -343	3 247 -415	4 343 -366	5 1241 1306	6 81 -50	7 137 32	6 581 -603
3 86 35	5 119 -119	8 207 201	2 42 0	3 87 49	4 65 -96	5 232 -189	6 147 -180	7 137 -135	8 42 -64	9 55 37
4 143 118	6 110 -110	9 43 -37	3 238 231	4 194 -177	5 347 -421	6 217 172	7 160 -155	8 103 151	9 74 75	10 388 381
H 5 -10	8 82 42	10 154 153	4 68 -9	5 98 -92	6 80 -81	7 137 131	8 104 157	9 354 -370	10 166 -116	11 84 26
G 157 145	H 2 -8	H 2 -7	H 1 -76	8 60 7	9 85 -32	6 416 409	5 159 162	8 511 -532	2 196 195	10 155 140
1 496 313	0 324 -346	0 613 -605	0 168 178	1 415 -426	2 347 -343	3 247 -415	4 343 -366	5 1241 1306	6 81 -50	H 6 -2
2 115 98	1 304 -303	1 311 -11	3 37 -56	4 143 -143	5 207 -201	6 92 -76	7 232 226	8 438 442	9	

Table 18. Continued

-15	115	-101	4	491	-494	10	107	-33	-4	1062	1143	-13	53	17	4	86	0	8	224	-236	13	77	105	3	221	190	13	154	-135	4	205	194									
-14	116	-102	11	485	-526	11	134	-104	-1	311	325	-12	174	162	5	119	-84	9	554	-577	4	165	-139	14	93	-17	5	181	185	5	181	185									
-13	148	132	12	211	214	H	-5	1	-1	590	-571	-10	135	102	H	-9	2	11	521	562	H	3	2	5	82	37	H	-2	3	7	146	132									
-12	46	-27								1561	1732	-9	75	-47				12	329	-307	-13	174	-166	H	-10	3				8	66	6									
-11	72	80	H	6	0					42	-45	-8	230	224	1	77	31	13	267	-245	-12	103	164				1	1269	1228	9	132	-136									
-10	182	133								676	-688	-7	83	82	2	493	502	14	156	-136	-11	147	131				1	108	102	2	138	1271	10	84	70						
-9	108	-110	-12	116	-108					1944	182	3	-3	8				-10	437	-436	2	86	-440	2	86	-440	3	487	-487	11	65	6									
-8	182	103	-11	188	-161					421	-237	4	180	-105	-5	128	107	4	204	-217	H	-1	2				1	91	102	4	551	-515	12	152	140						
-7	332	362	-10	158	-151					5	126	139	5	368	388	-4	370	-344	5	134	0						-8	414	-402	5	304	-300	5	494	494						
-6	45	-31	-9	153	186					6	179	197	6	57	88	3	486	400	6	78	0	1	389	-374				5	87	-7	6	479	486	H	3	3					
-5	232	-224	-8	184	-123					7	70	-82	7	584	-568	-2	851	-816	7	105	-74	2	654	-634	-6	76	18	6	412	440	7	233	-232								
-4	353	-335	-7	77	-31					8	74	-38	8	86	74	-1	280	-270	8	92	93	3	930	-910	-5	573	-553				8	89	56	-13	181	-154					
-3	347	409	-6	85	74					9	108	-81	9	133	-141	0	950	875	9	20	2	4	1785	1885	-4	168	88	H	-9	3	9	488	-477	-12	376	362					
-2	285	283	-5	315	486					10	83	-53	10	343	-380	1	224	-236	H	-2	2	5	680	709	-3	531	501				10	175	186	-11	363	295					
-1	831	-816	-4	109	-120					11	289	-243	11	29	-23												1	73	43	11	398	415	-10	531	-505						
0	377	-365	-3	64	-74					12	263	-277	12	331	315	3	115	114	1	430	225	7	481	-509	-1	334	-400	2	101	-91	12	261	-240	-9	510	-522					
1	572	-562	-2	490	479					13	109	62	13	177	177	4	228	240	2	331	-328	8	569	-596	0	334	-353	3	94	-61	13	270	268	-8	322	320					
2	754	-741	-1	326	-331					14	83	4	14	83	4	5	88	85	3	157	-139	9	746	727	1	47	-35	4	194	-44	14	165	-122	-7	515	517					
3	10	-19	0	60	-52					H	-5	1	H	1	1	7	54	77	5	78	-24	11	620	-591	3	83	64	6	143	-119	H	-1	3	5	585	-562					
4	373	305	1	254	-256					8	235	223	6	92	-32	12	251	-236	4	234	234	7	333	-364	4	234	234	7	333	-364	4	234	234	-4	49	-37					
5	523	-527	2	262	-268					11	931	882	-15	77	-26	9	71	-49	7	109	5	5	195	-178	5	195	-178	5	195	-178	5	195	-178	10	84	445	-2	273	284		
6	70	0	3	490	482					12	337	-369	10	243	-268	10	243	-268	10	243	-268	10	243	-268	10	243	-268	10	243	-268	10	243	-268	10	243	-268	10	243	-268		
7	573	594	4	128	132					13	789	-789	-11	89	-94	9	55	5	5	5	5	5	5	5	5	5	5	5	5	5	5	5	5	5	5	5	5	5	5		
8	152	55	5	456	-463					14	94	73	-12	119	110	11	80	-94	9	55	5	5	5	5	5	5	5	5	5	5	5	5	5	5	5	5	5	5	5		
9	430	-460	6	127	220					15	534	555	-12	119	25	12	198	216	10	111	145	H	0	2	8	56	3	H	-8	3	4	337	-333	0	130	-130	0	130	-130		
10	150	150	7	150	142					16	238	238	-11	101	-92																										
11	211	-211	8	189	-189					17	189	-189	-12	101	-92																										
12	45	-70	9	62	-76					18	290	-243	-13	257	-235																										
13	119	-119	10	75	80					19	256	257	-14	353	-340																										
14	237	-237	H	7	0					20	355	321	-7	79	-69																										
H	3	0								21	288	288	-8	329	-311																										
-14	51	17	-11	202	-206					22	732	769	-9	33	-14																										
-13	205	-206	-9	276	294					23	296	284	-10	102	-53																										
-12	85	-84	-8	140	-172					24	49	-75	-12	155	-147																										
-11	84	-74	-7	140	-91					25	105	-87	-13	254	218																										
-10	113	-92	-6	171	150					26	461	-412	-14	349	-335																										
-9	308	339	-5	73	-22					27	230	-239	-15	414	-409																										
-8	301	361	-4	236	-224					28	650	674	-16	557	548																										
-7	364	-380	-3	227	263					29	616	613	0	616	613																										
-6	601	-581	-2	216	214					30	82	92	1	54	18																										
-5	126	-126	-1	276	-276					31	960	-979	-2	960	-979																										
-4	433	424	0	149	-142					32	675	647	3	169	-164																										
-3	731	893	1	225	-210					33	590	577	4	579	563																										
-2	764	-742	2	231	238					34	398	-398	5	243	-237																										
-1	181	-173	3	321	330					35	216	-224	6	191	-177																										
0	676	636	4	171	163					36	108	106	7	261	261																										
1	69	41	5	64	-47					37	112	93	8	327	332																										
2	279	256	6	135	-130					38	225	-216	9	269	-290																										
3	48	-62	7	68	-66					39	391	-379	10	391	-379																										
4	153	-176	8	181	182					40	220	215	11	220	215																										
5	291	-270	H	2	1					41	1210	-1141	12	1210	-1141																										
6	76	60	H	8	0					42	179	180	13	179	180																										
7	252	261	-9	67	-38					43	296	284	-14	102	-53																										
8	134	-128	-9	85	-26					44	49	-75	-15	155	-147																										
9	7	-45	-7	92	33					45																															

Table 19. Positional Parameters for

<u>Atom</u>	<u>-- X --</u>	<u>-- Y --</u>	<u>-- Z --</u>
FE	0.23276(8)	0.22531(13)	-.00173(13)
P1	0.17602(12)	0.22071(20)	-.16287(21)
P2	0.21345(12)	0.29782(20)	0.20267(20)
P3	0.34375(12)	0.30307(19)	-.01217(20)
P4	0.25354(12)	0.03660(19)	-.06691(20)
O1	0.08432(28)	0.21592(50)	-.14844(51)
O2	0.18153(34)	0.11884(52)	-.32278(50)
O3	0.27810(29)	0.36994(47)	0.32482(47)
O4	0.17223(29)	0.19197(44)	0.22365(46)
O5	0.41716(27)	0.27721(45)	0.04976(46)
O6	0.35810(28)	0.45376(42)	0.05727(48)
O7	0.30101(28)	-.04113(44)	-.20200(46)
O8	0.18240(28)	-.06719(46)	-.10281(55)
C1	0.19228(46)	0.35564(77)	-.17560(78)
C2	0.21798(55)	0.35082(85)	-.28673(90)
C3	0.22996(62)	0.45790(113)	-.28959(105)
C4	0.21600(56)	0.57186(101)	-.18160(123)
C5	0.19039(55)	0.58001(89)	-.06985(102)
C6	0.17923(52)	0.47171(89)	-.06878(96)
C7	0.03115(54)	0.22023(94)	-.23548(98)
C8	-.03766(62)	0.26961(113)	-.16780(118)
C9	0.17064(65)	-.01177(99)	-.38222(97)
C10	0.19444(83)	-.08103(107)	-.51582(109)
C11	0.14702(45)	0.41989(74)	0.28303(79)
C12	0.08090(49)	0.40937(75)	0.21591(85)
C13	0.02629(51)	0.49315(98)	0.27396(108)
C14	0.03960(67)	0.59202(100)	0.40198(118)
C15	0.10478(74)	0.60785(98)	0.47220(102)
C16	0.15864(56)	0.52392(89)	0.41378(85)
C17	0.34433(47)	0.31384(81)	0.32384(79)
C18	0.40371(50)	0.41085(85)	0.42534(85)
C19	0.15240(60)	0.21904(85)	0.35331(88)
C20	0.10361(63)	0.12227(100)	0.34555(97)
C21	0.38099(43)	0.26552(70)	-.17278(71)
C22	0.39091(57)	0.14203(81)	-.26927(92)
C23	0.41862(63)	0.10924(87)	-.39083(92)

Table 19. Continued

C24	0.43539(59)	0.19497(101)	-.42009(94)
C25	0.42616(61)	0.31586(97)	-.32599(98)
C26	0.39868(54)	0.35119(79)	-.20460(82)
C27	0.49459(48)	0.32450(86)	0.04971(91)
C28	0.54644(48)	0.31667(80)	0.13954(90)
C29	0.33659(54)	0.54326(79)	0.18920(86)
C30	0.35500(58)	0.67046(78)	0.22047(86)
C31	0.30713(45)	0.00483(64)	0.04043(72)
C32	0.38672(50)	0.02930(73)	0.05832(79)
C33	0.42892(54)	0.00798(85)	0.14061(94)
C34	0.39209(72)	-.03789(85)	0.20718(90)
C35	0.31484(66)	-.06124(89)	0.19452(93)
C36	0.27293(51)	-.04395(79)	0.10942(87)
C37	0.30939(51)	-.17266(77)	-.26674(83)
C38	0.36014(64)	-.21289(86)	-.37804(95)
C39	0.10541(50)	-.05703(83)	-.10779(97)
C40	0.05683(55)	-.15160(102)	-.11110(116)
H1	0.15249(331)	0.20940(537)	0.01542(573)
H2	0.20965(319)	0.36112(533)	0.05586(571)
H1	0.150 (-)	0.226 (-)	0.110 (-) *
H2	0.207 (-)	0.359 (-)	0.650 (-) *

* Derived from difference Fourier map

Table 20. Thermal Parameters for $\text{H}_2\text{Fe}((\text{C}_6\text{H}_5)\text{P}(\text{OC}_2\text{H}_5)_2)_4$ ($\times 10^5$)

The form of the anisotropic thermal ellipsoid is

$$\exp(-(\text{B11h}^2 + \text{B22k}^2 + \text{B33l}^2 + \text{B12hk} + \text{B13hl} + \text{B23kl}))$$

<u>Atom</u>	<u>B11</u>	<u>B22</u>	<u>B33</u>	<u>B12</u>	<u>B13</u>	<u>B23</u>
FE	289(7)	666(18)	603(19)	183(17)	133(18)	746(31)
P1	326(10)	833(27)	804(29)	78(26)	31(27)	987(47)
P2	321(10)	731(26)	660(27)	113(25)	122(25)	744(44)
P3	309(10)	647(25)	681(27)	133(24)	131(25)	687(44)
P4	293(10)	723(26)	758(28)	68(25)	56(25)	803(45)
O1	276(27)	1428(81)	1240(84)	-32(71)	-271(73)	1905(141)
O2	698(34)	973(76)	691(84)	18(84)	-123(80)	734(139)
O3	353(27)	1054(72)	707(72)	53(72)	-214(74)	836(120)
O4	488(28)	763(66)	669(72)	74(68)	326(70)	899(115)
O5	270(26)	930(68)	917(73)	8(66)	-7(69)	1129(118)
O6	448(27)	416(65)	885(75)	59(64)	314(71)	520(116)
O7	443(27)	654(66)	689(72)	393(68)	355(70)	608(116)
O8	206(25)	816(70)	1862(96)	-136(72)	41(78)	1316(136)
C1	434(43)	990(110)	736(109)	216(108)	100(107)	1069(186)
C2	722(56)	1153(125)	1198(133)	5(133)	23(134)	1510(225)
C3	825(66)	1948(175)	1598(172)	-101(179)	14(167)	2673(298)
C4	587(56)	1694(160)	2662(218)	-174(153)	-126(180)	3677(330)
C5	572(54)	1219(137)	1930(173)	299(134)	330(150)	1701(265)
C6	578(50)	1283(127)	1802(154)	189(128)	487(136)	2509(246)
C7	419(51)	1880(163)	1798(170)	201(142)	-133(147)	2338(281)
C8	555(59)	2704(205)	2520(210)	442(176)	-490(174)	3460(358)
C9	979(73)	1492(159)	1099(163)	552(177)	-276(171)	910(283)
C10	1599(110)	1601(178)	1177(168)	299(217)	-369(219)	728(286)
C11	317(40)	1020(111)	1070(122)	372(106)	347(109)	1382(199)

Table 20. Continued

<u>Atom</u>	<u>B11</u>	<u>B22</u>	<u>B33</u>	<u>B12</u>	<u>B13</u>	<u>B23</u>
C12	359(42)	834(108)	1447(138)	438(106)	494(119)	991(202)
C13	379(48)	1624(156)	1966(175)	470(140)	185(151)	1795(272)
C14	753(67)	1441(158)	1941(196)	1226(170)	1377(185)	1333(289)
C15	955(77)	1463(156)	1213(160)	900(180)	378(172)	208(250)
C16	693(56)	1381(133)	724(121)	755(137)	207(128)	529(209)
C17	349(45)	1312(129)	886(123)	-106(124)	-292(122)	1154(212)
C18	453(47)	1452(135)	1170(136)	128(129)	-188(130)	1441(229)
C19	947(69)	1219(134)	1120(146)	-409(150)	587(158)	1562(236)
C20	877(68)	1905(166)	1402(157)	-224(167)	753(163)	2241(279)
C21	341(38)	634(96)	644(104)	-137(94)	40(98)	638(167)
C22	818(59)	850(112)	1298(143)	189(127)	897(145)	1168(214)
C23	925(68)	1055(137)	1104(148)	138(147)	1130(159)	470(234)
C24	763(61)	1503(153)	1096(147)	-112(160)	667(146)	1130(245)
C25	910(64)	1581(146)	1213(153)	-206(159)	433(159)	2105(257)
C26	746(55)	964(114)	863(122)	44(121)	449(128)	1132(199)
C27	272(45)	1647(145)	1724(157)	-188(128)	-200(132)	2117(258)
C28	370(45)	1131(123)	1669(153)	-35(117)	-208(130)	1497(231)
C29	679(55)	764(120)	1105(136)	106(127)	391(136)	766(217)
C30	824(60)	690(116)	1084(134)	351(133)	299(139)	464(208)
C31	380(40)	447(92)	804(107)	226(94)	219(103)	656(168)
C32	458(43)	862(107)	973(122)	8(106)	-202(113)	974(191)
C33	560(52)	1137(127)	1325(152)	232(125)	-562(136)	1053(226)
C34	1027(77)	959(129)	986(141)	956(168)	20(173)	867(215)
C35	833(65)	1463(144)	1329(150)	922(165)	788(172)	2028(253)
C36	545(48)	1031(114)	1264(132)	329(116)	206(124)	1543(209)
C37	587(51)	732(114)	999(134)	308(121)	173(130)	484(207)
C38	967(72)	992(131)	1270(152)	725(155)	790(170)	476(230)
C39	317(45)	1188(130)	2219(175)	-478(128)	-306(142)	2041(255)
C40	392(51)	1917(172)	2934(224)	-159(147)	382(165)	2704(332)

Table 21. Derived Parameters for the Hydrogen Atoms of
 $\text{H}_2\text{Fe}((\text{C}_6\text{H}_5)\text{P}(\text{OC}_2\text{H}_5)_2)_4$

<u>Atom</u>	<u>X</u>	<u>Y</u>	<u>Z</u>	<u>B</u> (Å ²)
H21	0.2273	0.2761	-.3595	5.63
H31	0.2471	0.4510	-.3636	6.30
H41	0.2236	0.6414	-.1840	6.17
H51	0.1808	0.6548	0.0024	6.08
H61	0.1626	0.4781	0.0058	5.00
H71	0.0169	0.1256	-.3232	5.56
H72	0.0567	0.2806	-.2666	5.56
H81	-.0782	0.2726	-.2353	7.04
H82	-.0236	0.3643	-.0801	7.04
H83	-.0634	0.2094	-.1367	7.04
H91	0.1098	-.0384	-.3831	6.20
H92	0.2036	-.0356	-.3228	6.20
H101	0.1846	-.1814	-.5571	7.47
H102	0.2554	-.0562	-.5566	7.47
H103	0.1616	-.0588	-.5768	7.47
H121	0.0726	0.3449	0.1300	5.06
H131	-.0175	0.4824	0.2277	6.20
H141	0.0045	0.6480	0.4408	6.67
H151	0.1128	0.6737	0.5575	6.58
H161	0.2025	0.5361	0.4607	5.51
H171	0.3674	0.2689	0.2249	4.91
H172	0.3295	0.2434	0.3473	4.91
H181	0.4547	0.3661	0.4235	5.88
H182	0.3810	0.4559	0.5245	5.88
H183	0.4188	0.4814	0.4022	5.88
H191	0.1237	0.3053	0.4044	5.63
H192	0.2050	0.2324	0.4106	5.63
H201	0.0906	0.1477	0.4461	6.82
H202	0.1318	0.0355	0.2954	6.82
H203	0.0505	0.1083	0.2891	6.82
H221	0.3791	0.0820	-.2525	5.44
H231	0.4255	0.0282	-.4517	6.28
H241	0.4524	0.1729	-.5005	6.07
H251	0.4385	0.3752	-.3437	6.13

Table 21. Continued

<u>Atom</u>	<u>X</u>	<u>Y</u>	<u>Z</u>	<u>B</u> (\AA^2)
H261	0.3922	0.4326	-.1449	5.13
H271	0.4951	0.4226	0.0813	5.42
H272	0.5144	0.2694	-.0514	5.42
H281	0.6043	0.3533	0.1365	5.91
H282	0.5467	0.2188	0.1086	5.91
H283	0.5274	0.3720	0.2411	5.91
H291	0.3678	0.5321	0.2607	5.39
H292	0.2751	0.5276	0.1955	5.39
H301	0.3384	0.7383	0.3213	5.92
H302	0.3238	0.6819	0.1492	5.92
H303	0.4165	0.6864	0.2144	5.92
H321	0.4114	0.0601	0.0147	4.86
H331	0.4803	0.0243	0.1501	5.83
H341	0.4194	-.0529	0.2603	5.99
H351	0.2908	-.0883	0.2421	5.84
H361	0.2219	-.0648	0.0980	5.58
H371	0.2532	-.2258	-.3050	5.12
H372	0.3341	-.1900	-.1950	5.12
H381	0.3663	-.3130	-.4270	6.37
H382	0.4163	-.1599	-.3400	6.37
H383	0.3355	-.1957	-.4500	6.37
H391	0.0917	-.0580	-.1975	5.47
H392	0.0935	0.0328	-.0196	5.47
H401	-.0028	-.1340	-.1150	6.88
H402	0.0686	-.1519	-.0216	6.88
H403	0.0668	-.2427	-.1994	6.88

APPENDIX II

ADDITIONAL STRUCTURAL DATA FOR

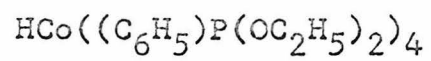


Table 22. Calculated and Observed Structure Factors for $\text{HCo}((\text{C}_6\text{H}_5)\text{P}(\text{OC}_2\text{H}_5)_2)_4$

The headings for each group give the h and k indices which are constant for that group. The columns are in the order l , F_{obs} , F_{calc} .

To convert the present indices to those of the reduced cell (Table 8):

$$h_r = h + k$$

$$k_r = -h$$

$$l_r = l$$

Reflections marked with an asterisk were observed ≤ 0 , and were set $= 0$ with a 0 weight.

Table 23. Positional Parameters for $\text{HCo}((\text{C}_6\text{H}_5)\text{P}(\text{OC}_2\text{H}_5)_2)_4$

<u>Atom</u>	<u>-- X --</u>	<u>-- Y --</u>	<u>-- Z --</u>
C0	-.00001(6)	0.22351(6)	0.23963(4)
P1	-.14186(11)	0.23894(10)	0.17903(6)
P2	0.20226(10)	0.31038(9)	0.21396(6)
P3	-.06159(10)	0.03837(9)	0.25720(6)
P4	-.00890(10)	0.30609(9)	0.34783(6)
O1	-.30309(28)	0.14680(27)	0.18634(19)
O2	-.13070(32)	0.22330(29)	0.08802(15)
O3	0.23017(26)	0.20962(24)	0.16968(16)
O4	0.32706(25)	0.38480(24)	0.27764(16)
O5	-.19783(25)	-.04097(23)	0.30261(15)
O6	-.09267(30)	-.06370(25)	0.18531(15)
O7	0.05397(26)	0.28139(23)	0.41992(14)
O8	0.05783(25)	0.45568(22)	0.36240(16)
C1	-.37021(52)	0.01850(56)	0.18576(38)
C2	-.50514(61)	-.04417(62)	0.20341(47)
C3	-.21431(69)	0.23387(67)	0.03575(31)
C4	-.19259(111)	0.22787(116)	-.03241(46)
C5	-.14167(44)	0.38219(41)	0.19127(23)
C6	-.25015(51)	0.38618(48)	0.21255(30)
C7	-.24302(65)	0.49956(62)	0.22105(35)
C8	-.12832(76)	0.60657(56)	0.20913(33)
C9	0.01965(60)	0.60570(48)	0.18928(33)
C10	0.02634(52)	0.49401(46)	0.17989(28)
C11	0.36116(50)	0.24635(50)	0.14609(35)
C12	0.36173(59)	0.14530(60)	0.10890(40)
C13	0.32773(41)	0.32361(40)	0.34096(25)
C14	0.42878(48)	0.41786(46)	0.40033(30)
C15	0.27724(41)	0.43266(38)	0.14971(24)
C16	0.21057(48)	0.41053(42)	0.08105(27)
C17	0.26521(63)	0.49576(58)	0.02807(30)
C18	0.38481(70)	0.60280(63)	0.04373(40)
C19	0.45193(63)	0.62931(56)	0.11202(44)
C20	0.39831(50)	0.54437(47)	0.16466(31)
C21	-.26166(45)	-.17238(40)	0.31045(28)
C22	-.37749(53)	-.21386(47)	0.35683(36)
C23	-.11242(59)	-.05522(50)	0.10962(29)

Table 23. Continued

<u>Atom</u>	<u>-- X --</u>	<u>-- Y --</u>	<u>-- Z --</u>
C24	-.11584(82)	-.14721(67)	0.05891(34)
C25	0.04775(37)	0.00866(33)	0.31017(23)
C26	0.06241(43)	0.03263(38)	0.38831(26)
C27	0.14509(51)	0.01252(43)	0.43040(29)
C28	0.21307(48)	-.03231(48)	0.39461(39)
C29	0.20369(51)	-.05378(47)	0.31841(38)
C30	0.12030(45)	-.03479(40)	0.27534(27)
C31	0.05413(52)	0.33195(48)	0.49607(26)
C32	0.13975(52)	0.31930(45)	0.54777(26)
C33	0.18959(44)	0.54430(38)	0.34142(29)
C34	0.21897(49)	0.67149(40)	0.36252(31)
C35	-.17101(38)	0.26556(35)	0.38208(22)
C36	-.20913(44)	0.34834(40)	0.39273(29)
C37	-.33296(52)	0.31196(51)	0.41847(36)
C38	-.42154(48)	0.19349(53)	0.43373(33)
C39	-.38686(48)	0.10936(45)	0.42321(31)
C40	-.26191(46)	0.14494(41)	0.39789(30)
H	0.01570(414)	0.18913(385)	0.16623(250)
H	0.012 (-)	0.174 (-)	0.162 (-) *

* Derived from difference Fourier map

Table 24. Thermal Parameters for $\text{HCo}((\text{C}_6\text{H}_5)\text{P}(\text{OC}_2\text{H}_5)_2)_4$ ($\times 10^5$)

The form of the anisotropic thermal ellipsoid is

$$\exp(-(\text{B11h}^2 + \text{B22k}^2 + \text{B33l}^2 + \text{B12hk} + \text{B13hl} + \text{B23kl}))$$

<u>Atom</u>	<u>B11</u>	<u>B22</u>	<u>B33</u>	<u>B12</u>	<u>B13</u>	<u>B23</u>
CO	1004(9)	982(7)	341(3)	1218(13)	214(7)	298(7)
P1	1289(16)	1163(13)	358(5)	1535(24)	-72(14)	73(12)
P2	997(14)	870(11)	377(5)	969(20)	221(12)	145(11)
P3	1051(14)	909(11)	334(4)	1091(21)	89(12)	117(11)
P4	966(13)	807(11)	374(5)	1025(20)	152(12)	182(11)
O1	1202(40)	1281(36)	764(18)	1298(66)	-345(41)	108(40)
O2	2251(51)	1989(43)	316(12)	3004(82)	-238(39)	37(36)
O3	1111(37)	1187(32)	591(15)	1441(58)	464(36)	109(34)
O4	1013(34)	1096(29)	467(13)	882(53)	0(32)	234(31)
O5	1048(34)	1000(30)	509(13)	1042(54)	272(33)	391(31)
O6	2174(50)	1170(32)	338(12)	1721(68)	-46(39)	-104(33)
O7	1389(37)	1209(31)	349(11)	1724(58)	-43(32)	55(30)
O8	1187(37)	798(27)	545(13)	1012(54)	393(35)	190(30)
C1	1339(78)	2075(82)	1136(40)	1836(138)	169(88)	1097(94)
C2	1710(91)	2325(95)	1529(55)	1780(156)	-6(110)	883(116)
C3	3710(133)	3747(127)	374(24)	5489(231)	-464(95)	75(91)
C4	7114(257)	8364(285)	677(38)	13327(501)	-594(153)	268(164)
C5	1524(65)	1416(55)	384(19)	2102(105)	-124(55)	130(52)
C6	1881(78)	1856(70)	697(28)	2630(129)	-6(72)	79(70)
C7	2856(117)	2465(96)	896(36)	4450(190)	36(102)	-84(98)
C8	3722(123)	1903(75)	723(30)	4259(172)	-347(94)	-11(74)
C9	2735(106)	1394(63)	764(31)	2445(142)	155(89)	445(69)
C10	2205(84)	1459(61)	576(25)	2462(125)	289(72)	428(62)
C11	1433(74)	1867(74)	1019(36)	2071(125)	675(81)	-31(82)

Table 24. Continued

<u>Atom</u>	<u>B11</u>	<u>B22</u>	<u>B33</u>	<u>B12</u>	<u>B13</u>	<u>B23</u>
C12	2188(96)	2551(95)	1158(42)	3424(169)	1351(102)	698(102)
C13	1219(60)	1245(51)	495(21)	1283(95)	-17(57)	316(54)
C14	1554(72)	1607(63)	665(27)	1586(114)	-381(69)	248(66)
C15	1256(57)	1103(46)	418(19)	1206(87)	335(52)	264(47)
C16	1814(74)	1352(56)	456(22)	1448(108)	446(64)	382(57)
C17	2699(108)	2293(87)	512(26)	2687(163)	814(88)	1031(83)
C18	2651(114)	2279(91)	917(38)	2239(172)	1562(104)	1903(101)
C19	2215(104)	1733(78)	1108(45)	425(146)	382(107)	1376(102)
C20	1587(76)	1495(63)	691(28)	514(115)	149(72)	855(70)
C21	1401(67)	1082(53)	672(26)	1015(100)	219(65)	505(58)
C22	1715(80)	1421(63)	962(35)	899(118)	778(86)	806(76)
C23	2998(107)	1939(74)	439(24)	3027(153)	-209(79)	-409(67)
C24	5131(177)	2996(114)	476(28)	5166(249)	-84(110)	-184(89)
C25	1007(52)	759(41)	437(19)	957(78)	105(51)	155(45)
C26	1400(62)	1112(49)	528(22)	1503(94)	-104(59)	181(53)
C27	1848(81)	1314(58)	586(25)	1416(114)	-559(71)	260(60)
C28	1275(72)	1542(68)	1038(39)	1414(115)	-130(87)	1030(87)
C29	1680(76)	1552(65)	1033(36)	2333(123)	688(88)	876(83)
C30	1555(67)	1242(53)	617(24)	1747(103)	417(63)	489(57)
C31	2344(86)	2083(73)	386(21)	3095(139)	-273(66)	-219(61)
C32	2220(82)	1592(61)	408(21)	2069(121)	-264(65)	1(57)
C33	1406(67)	940(48)	765(27)	1145(96)	489(67)	251(57)
C34	1743(75)	987(51)	842(30)	1193(103)	617(75)	412(62)
C35	1116(54)	961(46)	357(18)	1212(88)	90(48)	104(44)
C36	1260(64)	1192(53)	733(27)	1505(101)	362(64)	120(58)
C37	1480(79)	1775(75)	1136(39)	2249(133)	457(88)	-132(87)
C38	1166(70)	1888(79)	888(33)	1444(124)	566(75)	-238(82)
C39	1368(72)	1324(62)	780(30)	665(109)	886(74)	224(67)
C40	1474(70)	1187(56)	774(28)	1497(106)	819(71)	388(63)

Table 25. Derived Parameters for the Hydrogen Atoms of
 $\text{HCo}((\text{C}_6\text{H}_5)\text{P}(\text{OC}_2\text{H}_5)_2)_4$

<u>Atom</u>	<u>X</u>	<u>Y</u>	<u>Z</u>	<u>B</u> (\AA^2)
H11	-.3176	-.0003	0.2271	7.23
H12	-.3660	-.0201	0.1290	7.23
H21	-.5469	-.1441	0.2011	11.92
H22	-.5610	-.0285	0.1624	11.92
H23	-.5127	-.0088	0.2604	11.92
H31	-.2022	0.3238	0.0514	6.95
H32	-.3177	0.1586	0.0425	6.95
H41	-.2626	0.2371	-.0659	9.12
H42	-.2057	0.1380	-.0502	9.12
H43	-.0903	0.3031	-.0413	9.12
H61	-.3343	0.3282	0.2235	7.27
H71	-.3153	0.5005	0.2345	6.52
H81	-.1241	0.6791	0.2144	6.38
H91	0.0574	0.6778	0.1821	6.04
H101	0.0467	0.4947	0.1660	6.24
H111	0.4305	0.2847	0.1962	6.62
H112	0.3938	0.3178	0.1074	6.62
H121	0.4626	0.1772	0.0920	8.28
H122	0.2932	0.1065	0.0585	8.28
H123	0.3298	0.0735	0.1472	8.28
H131	0.3528	0.2557	0.3223	5.35
H132	0.2290	0.2758	0.3642	5.35
H141	0.4296	0.3715	0.4487	6.66
H142	0.4038	0.4858	0.4190	6.66
H143	0.5275	0.4657	0.3771	6.66
H161	0.1297	0.3392	0.0703	5.12
H171	0.2204	0.4793	-.0169	5.98
H181	0.4210	0.6575	0.0088	6.91
H191	0.5313	0.7023	0.1228	6.83
H201	0.4434	0.5624	0.2097	5.38
H211	-.1906	-.1872	0.3379	5.53
H212	-.2945	-.2258	0.2543	5.53
H221	-.4256	-.3130	0.3627	7.22
H222	-.4486	-.1991	0.3295	7.22
H223	-.3448	-.1605	0.4129	7.22
H231	-.0310	0.0359	0.0955	6.92

Table 25. Continued

<u>Atom</u>	<u>X</u>	<u>Y</u>	<u>Z</u>	<u>B</u> (\AA^2)
H232	-.2075	-.0629	0.1026	6.92
H241	-.1317	-.1339	0.0009	8.84
H242	-.1974	-.2392	0.0716	8.84
H243	-.0211	-.1405	0.0645	8.84
H261	0.0171	0.0621	0.4126	5.00
H271	0.1536	0.0292	0.4814	5.57
H281	0.2648	-.0478	0.4220	5.93
H291	0.2518	-.0808	0.2949	5.88
H301	0.1137	-.0510	0.2243	5.14
H311	-.0478	0.2817	0.5149	10.80
H312	0.0913	0.4307	0.4965	10.80
H321	0.1386	0.3581	0.6052	6.92
H322	0.2419	0.3696	0.5292	6.92
H323	0.1029	0.2207	0.5476	6.92
H331	0.1958	0.5295	0.2802	5.70
H332	0.2617	0.5335	0.3714	5.70
H341	0.3197	0.7406	0.3468	6.56
H342	0.2124	0.6859	0.4237	6.56
H343	0.1465	0.6819	0.3326	6.56
H361	-.1525	0.4278	0.3828	5.36
H371	-.3556	0.3684	0.4253	6.00
H381	-.5022	0.1711	0.4506	6.33
H391	-.4451	0.0299	0.4327	5.27
H401	-.2397	0.0881	0.3916	5.00

PROPOSITIONS

PROPOSITION 1

In recent years, photoelectron spectroscopy has risen from an experimental curiosity to an apparently useful laboratory tool. Much of this progress has been due to the efforts of Siegbahn and coworkers (1) who pioneered in this field and established the popular method now in use, commonly referred to as ESCA (Electron Spectroscopy for Chemical Analysis).

The method is somewhat similar to x-ray absorption spectroscopy, except that instead of measuring the energy of the transmitted photons, the kinetic energies of the expelled core electrons are measured in an electron spectrometer. If the incident x-radiation is monochromatic, the binding energy of the expelled electron can be calculated from the expression:

$$E_b = E_{x\text{-ray}} - E_{\text{kin}}$$

where $E_{x\text{-ray}}$ is the energy of the incident radiation and E_{kin} is the kinetic energy of the expelled electrons.

Properly, a work function for the spectrometer should also be subtracted from the x-ray energy, but it is more common merely to calibrate the instrument to known energy bands (1).

If the process were this simple, of course, ESCA would have little value except in elemental analysis. Fortunately, however, changes in the electron density about an atom induce small changes in the binding energies of the core electrons. An increase in binding energy implies a reduction in electron density (1,2). If this effect can be observed, or, to be more specific, if the chemical shift is greater than the line width of the exciting radiation, some very interesting studies are possible. It has been shown (1,3,4) that in most cases the shift is observable, although at times the resolution appears marginal.

It is general practice in studies of this chemical shift to measure the binding energies of electrons in a particular shell of an atom in a series of chemical situations. Because the subject of interest in many cases is a comparison of calculated and derived atomic charges, this information is probably sufficient. However, for studies of bonding, it would be of interest to measure in addition the binding energies of electrons in the atoms associated with the atom under investigation. This would give an indication of the electron "flow" which takes place in going from one system to the next. In systems

which display significant chemical shifts, it should be possible to tell just where the electrons go (relative to some standard) upon bond formation.

One problem to which this method might well be applied is the flow of electrons in transition metal phosphine complexes. It has been generally accepted that phosphorus ligands can act as σ -donors, π -acceptors, or a combination of both, depending upon the electronegativity of the phosphorus substituents (5). On the basis of n.m.r. studies, however, it has been postulated that very little π bonding does, indeed, occur (6). Since phosphines and phosphites are formally donor molecules, it is expected that with coordination, the electron density at the phosphorus atom will be reduced. If, however, there is significant π back-bonding in the complex, the reduction will not be as large or may not appear at all.

Considering the current interest in ESCA, it is surprising that still only very few data are available for phosphine complexes (7,8). From phosphorus 2p binding energies of three triphenylphosphine complexes it has been concluded that triphenylphosphine is as good a π -acceptor as it is a σ -donor (8). It is doubtful that such a conclusion can safely be drawn from the limited data available. It should also be noted that merely because the electron density does not change appreciably upon

coordination, there is no requirement that σ -donation and π -acceptance are evenly balanced. Also, since π -acceptance (or whatever unknown mechanism which gives the appearance of π -acceptance) increases with the electronegativity of the phosphorus substituents, it seems necessary that a wider range of phosphines and phosphites be investigated. It will be necessary also to look at more than the effect of coordination upon the phosphorus atom alone. The metal atom, as well as the phosphorus substituent atoms, should be investigated.

It is proposed that an investigation of several metal-phosphine and phosphite complexes be undertaken using the ESCA method. Table I lists some molecules and atoms which, if the specified binding energies can be obtained, should produce a healthy cross section of results. An investigation of all of the complexes mentioned would be a large undertaking; it is probable that experimental difficulties will make the investigation of some of the compounds impossible. The palladium complexes, for example, are notoriously unstable.

Hopefully, when the data are collected, changes in the electron "flow" will be observed with each group of metal complexes. The electron density of the metal can be expected to decrease in going from the triphenylphosphine complex. It should be possible to see whether the electrons

Table 1. Ligands and Complexes to be Studied by ESCA

<u>Ligands</u>	<u>Binding Energies Sought</u>
PPh_3	P(2p), C(1s)
PhP(OEt)_2	P(2p), C(1s), O(1s)
P(OEt)_3	P(2p), O(1s)
$\text{P(OCH}_2)_3\text{CCH}_3$	P(2p), O(1s)
PF_3	P(2p), F(1s)
<u>Complexes</u>	
$\text{Pt(PPh}_3)_4$	Pt(4p), P(2p), C(1s)
$\text{Pt(PhP(OEt)}_2)_4$	Pt(4p), P(2p), C(1s), O(1s)
$\text{Pt(P(OEt)}_3)_4$	Pt(4p), P(2p), O(1s)
$\text{Pt(P(OCH}_2)_3\text{CCH}_3)_4$	Pt(4p), P(2p), O(1s)
$\text{Pt(PF}_3)_4$	Pt(4p), P(2p), F(1s)
$\text{Pd(PhP(OEt)}_2)_4$	Pd(3p), P(2p), C(1s), O(1s)
$\text{Pd(P(OEt)}_3)_4$	Pd(3p), P(2p), O(1s)
$\text{Pd(P(OCH}_2)_3\text{CCH}_3)_4$	Pd(3p), P(2p), O(1s)
$\text{Pd(PF}_3)_4$	Pd(3p), P(2p), F(1s)
$\text{Ni(PhP(OEt)}_2)_4$	Ni(2p), P(2p), C(1s), O(1s)
$\text{Ni(P(OEt)}_3)_4$	Ni(2p), P(2p), O(1s)
$\text{Ni(P(OCH}_2)_3\text{CCH}_3)_4$	Ni(2p), P(2p), O(1s)
$\text{Ni(PF}_3)_4$	Ni(2p), P(2p), F(1s)

of the donor phosphorus ligands move to the metal, or remain essentially unchanged. The binding energies for the phosphine substituents should indicate if the metal-donated electrons stop at the phosphorus, or move on to the substituents.

Unfortunately, even if relative changes in electron density are observed, the questions of σ and π bonding will remain unresolved. However, if the changes in electron density tend to agree with those predicted from a σ and π scheme, we can feel easier about applying this concept to discussion of bonding.

If successful, this investigation should lead to further studies which compare the electron flows in phosphine complexes with those in arsine, ammine, carbonyl, and other complexes. Phosphorus compounds were chosen in the present case because of the large variety of known complexes suitable for this type of study. However, the suggested method could be applied to any series which undergoes significant changes in electron density in moving from one member of the series to the next. In any case, little information about bonding can be expected if the electron binding energies of only one of the bonded atoms are investigated.

It is possible that there will be no observable trends in the data. If this is the case, then the work

will serve as a test of the limits of the ESCA method. Certainly the chemical shifts are not large (8), and it may be that such a determination is, indeed, beyond the capabilities of the ESCA system. Although the data presently available are not promising, the problems encountered appear to lie in a poor choice of models to study rather than an inherent weakness of the system.

References

- 1) K. Siegbahn, C. Nordling, A. Fahlman, R. Nordberg, K. Hamrin, J. Hedman, E. Johanson, T. Bergman, S. E. Karlsson, I. Lindgren, and B. Lindberg, Nova Acta Regiae Soc. Sci. Upsal, 20, 1 (1967).
- 2) R. S. Berry, Ann. Rev. Phys. Chem., 20, 357 (1969).
- 3) J. M. Hollander, D. N. Hendrickson, and W. L. Jolly, J. Chem. Phys., 49, 3315 (1968).
- 4) A. Fahlman, K. Hamrin, J. Hedman, R. Nordberg, C. Nordling, and K. Siegbahn, Nature, 210, 4 (1966).
- 5) W. D. Horrocks, Jr., and R. C. Taylor, Inorg. Chem., 2, 723 (1963).
- 6) L. M. Venanzi, Chemistry in Britain, 4, 162-167 (1968).
- 7) M. Pelavin, D. N. Hendrickson, J. M. Hollander, and W. L. Jolly, J. Phys. Chem., 74, 1116 (1970).
- 8) J. R. Blackburn, R. Nordberg, F. Stevie, R. G. Albridge, and M. M. Jones, Inorg. Chem., 9, 2374 (1970).

PROPOSITION 2

Mixed valence platinum complexes containing infinite chains of Pt(II) and Pt(IV) have been known for several years. Perhaps the best known example of this type of compound is Wolfram's red salt (1), $(\text{Pt}(\text{C}_2\text{H}_5\text{NH}_2)_4\text{Cl}_2)^{2+} - (\text{Pt}(\text{C}_2\text{H}_5\text{NH}_2)_4)^{2+}\text{Cl}_4^-$. This complex was postulated to contain two oxidation states of platinum in 1934 (2) and later to contain only Pt(III) (3). It was not until 1961 that the former formulation was confirmed by x-ray crystallography (4).

The crystal structures of several related complexes have been determined (5-8) but in all cases disordering in the crystals reduced the accuracy of the results. The nature of this disorder is interesting since it is largely one dimensional. The chains mentioned above follow the general pattern $-\text{Pt}(\text{II})-\text{X}-\text{Pt}(\text{IV})-\text{X}-\text{Pt}(\text{II})-\text{X}-\text{Pt}(\text{IV})-$, where X is either Cl^- or Br^- . While it is virtually certain that there is no interchange of atoms within each of these chains, in the crystals there is very little

correlation of the chains with one another. Thus, in the refinement of data from such crystals only average positions of the various atoms are obtained.

The disorder of the chains with respect to one another is observed in oscillation photographs (camera axis parallel to the chains) as diffuse bands in place of the odd-numbered layer lines. These diffuse layer bands have been observed in all of the Pt compounds thus far investigated, and possibly in a related Pd compound (9). The absence of such bands would be a hopeful sign as far as disorder among the chains is concerned.

One possible solution to the disorder problem would be to find some way of relating one chain to another. This could logically be achieved by replacing the non-bridging halides by large anions which could exert steric limitations upon the chains. One of the obvious choices for consideration is the perchlorate anion, and a perchlorate complex, $(Pt\ en_2)(PtCl_2en_2)(ClO_4)_4$, en = ethylenediamine has been reported (10). The complex is easily prepared and is stable to the atmosphere.

An examination of oscillation photographs of this complex reveals no sign of the layer line bands observed previously. Instead, definite reflections are observed in the odd-numbered, as well as the even-numbered, layer lines. Zero- and first-layer Weissenberg photographs

indicate that the unit cell is orthorhombic. It is apparent that this compound suffers much less from disorder than the previously investigated compounds.

As with many other mixed valence complexes, this compound shows some unusual spectral properties. With incident light polarized parallel to the chain axis, the transmitted light is red; with the light polarized perpendicular to the chain axis, the transmitted light is yellow (10). Although several studies have been carried out on complexes which lack a bridging halide atom (which show similar behavior) (11-16), very little information is available on the single crystal spectra of complexes with bridging halides (17). It now appears likely that in the cases of the non-bridged species (such as Magnus' green salt, $(\text{Pt}(\text{NH}_3)_4)(\text{PtCl}_4)$), that the unusual spectral features are not due to any metal-metal bonding, but to the perturbations of energy states by the close presence of the cation and anion (12). It seems probable at this point that the situation is similar in the bridged species and that there is no formal Pt(II)-X bond.

It is proposed that single crystal polarized absorption spectra be obtained for the complex $(\text{Pt en}_2)(\text{PtCl}_2\text{en}_2)(\text{ClO}_4)_4$ and that a comparison be made between these spectra and those of the non-bridged species; hopefully, it can be determined from these data if the unusual spectral features

result from charge transfer transitions or if they result from perturbations of the Pt(II) energy states by the nearby chloride ligands along the z axis. In addition, it is proposed that the structure of the complex be investigated by x-ray crystallography, in view of its apparent lack of disorder.

References

- 1) H. Wolffram, Dissertation, Königsberg (1900).
- 2) H. Reihlen and E. Flohr, Ber. dtsh chem. Ges, 67, 2010 (1934).
- 3) H. D. Drew and H. J. Tress, J. Chem. Soc., 1244 (1935).
- 4) B. M. Craven and D. Hall, Acta Cryst., 14, 475 (1961).
- 5) C. Brosset, Archiv Kemi. Min. Geol., 26A, No. 19 (1948); D. Hall and P. P. Williams, Acta Cryst., 11, 624 (1958).
- 6) T. D. Ryan and R. E. Rundle, J. Am. Chem. Soc., 83, 2814 (1961).
- 7) J. Wallen, C. Brosset, and N. G. Vannerberg, Arkiv Kemi, 18, 541 (1962).
- 8) B. M. Craven and D. Hall, Acta Cryst., 21, 177 (1966).
- 9) E. W. Hughes, Private Communication. Prof. Hughes now feels that the bands observed in oscillation photographs of $(\text{Pd}(\text{NH}_3)_2\text{Cl}_2)(\text{Pd}(\text{NH}_3)_2\text{Cl}_4)$ may also have been the result of iron contamination of the x-ray tube.
- 10) S. Kida, Bull. Chem. Soc. Japan, 38, 1804 (1965).
- 11) M. Atoji, J. W. Richardson, and R. E. Rundle, J. Am. Chem. Soc., 79, 3017 (1957).
- 12) P. Day, A. F. Orchard, A. J. Thompson, and R. J. P. Williams, J. Chem. Phys., 42, 1973 (1965).
- 13) P. Day, A. F. Orchard, A. J. Thompson, and R. J. P. Williams, J. Chem. Soc., (A), 668 (1968).
- 14) B. G. Anex, M. E. Ross, and M. W. Hedgcock, J. Chem. Phys., 46, 1090 (1967).

- 15) J. R. Miller, J. Chem. Soc., 713 (1965).
- 16) D. S. Martin, Jr., R. A. Jacobson, L. D. Hunter,
and J. E. Benson, Inorg. Chem., 9, 1276 (1970).
- 17) S. Yamada and R. Tsuchida, Bull. Chem. Soc. Japan,
29, 894 (1956).

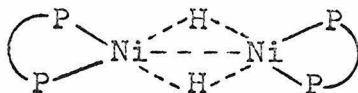
PROPOSITION 3

Although hydrido complexes of many transition metals are now known and in many cases are under extensive study, hydrido complexes of nickel have in the past received little attention. Although there are probably several reasons for this apparent neglect, the most obvious is the very small number of known stable nickel hydride complexes. Like the corresponding iron and cobalt carbonyl hydrides, the nickel carbonyl hydrides are extremely unstable (1).

As is the case with the other transition metals, phosphine ligands tend to stabilize hydride complexes to a greater extent, and some phosphine nickel hydrides of reasonable stability have been reported. A compound corresponding to the already well-characterized Pt(II) complexes, trans-hydrido-chlorobis(tricyclohexylphosphine)-nickel(II), has been prepared, and is reported to be stable to air for several hours in the solid state (2). The reaction of strong, nonaqueous acids with $((C_6H_5)_2PCH_2P(C_6H_5)_2)_2Ni$ has been shown to yield the cation

$((\text{C}_6\text{H}_5)_2\text{PCH}_2\text{CH}_2\text{P}(\text{C}_6\text{H}_5)_2)_2\text{NiH}^+$ (3). A hydrido nitrogen complex of nickel has also been reported. The compound is difficult to crystallize and decomposes even under an inert atmosphere after a few days (4). There is also some evidence for a borohydride nickel hydride complex, $(\text{R}_3\text{P})_2\text{NiH}(\text{BH}_4)$, for which it has been suggested that the nickel and boron are connected by two bridging hydrogens (5).

More recently two interesting dinuclear complexes have been reported (6). When complexes of the type $\text{R}_2\text{P}(\text{CH}_2)_n\text{PR}_2\text{NiCl}_2$ (R = cyclohexyl, n = 2 or 4) are treated with $\text{Na}(\text{HB}(\text{CH}_3)_3)$ in toluene, diamagnetic complexes are obtained which mass spectra and cryoscopic data indicate are dimeric. From the five line p.m.r. spectrum which was observed at high-field ($\tau = 21.4$), the authors suggested a structure of the type:



where the hydrogen atoms are bridging the two nickel atoms and lie above and below the molecular plane.

Since phosphine hydride complexes are notoriously non-rigid in solution, the n.m.r. data should not be taken

too seriously, although the dimeric nature of the complex seems to be well established. Bridging hydrogen atoms are not unknown in transition metal complexes, and some structural work has been carried out (7,8,9); the hydrogen atom position has been established in the structure determination of $((\text{CO})_4\text{Mn})_2(\text{H})(\text{P}(\text{C}_6\text{H}_5)_2)$ (8). No x-ray structural information is available for nickel hydride complexes.

It is proposed that low temperature n.m.r. spectra be obtained for the dimeric complexes in order to determine if the spectra are temperature independent. In view of the similar borohydride complex which has been reported (5), it seems very possible that the low temperature n.m.r. spectrum will continue to be consistent with the hydrogen-bridged structure. In addition, it is proposed that the unit cells and space groups of the complexes be determined in order to estimate the chances of locating the hydrogen atoms in complete x-ray structure determinations. If the cells are reasonably large ($\geq 10 \text{ \AA}$ each edge) and of reasonably low symmetry (preferably triclinic or monoclinic), the chances of finding the hydrogen atoms are good. It may be of advantage to utilize a more asymmetric form of the phosphorus ligand if the symmetry of the cell is too high. If a promising complex of this type can be obtained, an x-ray crystal determination should be carried out, since

structural data on double hydrogen bridges between transition metals are not available.

References

- 1) A. P. Ginsberg, Transition Metal Chemistry, 1, 111 (1965).
- 2) M. L. H. Green and T. Saito, Chem. Comm., 208 (1969).
- 3) R. A. Schunn, Inorg. Chem., 9, 394 (1970).
- 4) S. C. Srivastava and M. Bigorgne, J. Organometal. Chem., 18, P30 (1969).
- 5) M. L. H. Green, H. Manakata, and T. Saito, Chem. Comm., 128 (1969).
- 6) K. Jonas and G. Wilke, Angew. Chem. Int. Edit., 9, 312 (1970).
- 7) R. J. Doedens and L. F. Dahl, J. Am. Chem. Soc., 87, 2576 (1965).
- 8) R. J. Doedens, W. T. Robinson, J. A. Ibers, J. Am. Chem. Soc., 89, 4323 (1967).
- 9) M. R. Churchill and R. Bau, Inorg. Chem., 6, 2087 (1967).

PROPOSITION 4

Compounds of the fulminate anion (CNO^-) have been known for many years (1,2,3). Apparently, however, the well-known explosive nature of the early fulminate compounds has discouraged the study of the potentially interesting CNO^- ligand. Almost all of the studies of this ligand in transition metal complexes have been carried out by a single group headed by Wolfgang Beck at the University of Munich.

The simple fulminates, mercury, silver, and sodium, have been studied mainly for their explosive properties. The crystal structures of all three have been reported (4,5,6). The CNO^- anion is, as expected, linear, although in the silver compound, which appears to be essentially covalent, it was not possible to establish the identity of the atom bonded to the silver atom (4). It seems likely, however, that bonding occurs through the carbon atom.

It is somewhat surprising that stable fulminate

complexes can be prepared at all, in view of the explosive instability of the ionic compounds. In its complexes, the fulminate anion behaves much like a cyanide ion, except that it is not as stable to reducing agents. None of the fulminate complexes yet prepared is exceedingly stable, although most may be handled quite easily. Most do not explode unless placed in a flame, and many only decompose slowly without an explosion, even if exposed to a flame (7).

The infrared spectra of potassium and sodium fulminate have been reported (8). It is notable that Nujol mulls and KBr pellets were used in this determination, in spite of the explosive nature of these compounds. The KBr pellets showed no sign of decomposition in spite of the pressures required to prepare the pellets.

Several square planar complexes of the fulminate anion with Ni(II), Pd(II), and Pt(II) have been prepared (7). The complexes of the type $(R_3P)_2M(CNO)_2$ ($M = Ni, Pd, Pt$; $R = C_6H_5, C_2H_5$) are especially stable, and do not explode even when placed in a flame. The hydrido complex trans- $PtH(CNO)(P(C_2H_5)_3)_2$ has also been prepared; a comparison of its platinum-hydrogen stretching frequency in the infrared spectrum with those of the corresponding cyanide, thiocyanate, and cyanate complexes showed that the fulminate anion lies between cyanide and thiocyanate in the trans influence series (9). No kinetic studies have been carried

out, but it has been demonstrated (10) that, at least for Pt(II) complexes, the trans influence (structural) series parallels the trans effect (kinetic) series. As may be expected, the ligand field strength of the fulminate ion is high, although not as high as that of the cyanide ion(11).

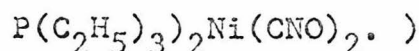
Although the fulminate ion appears to have the capabilities required to form complexes with metals in low oxidation states, it has proven to be very difficult to obtain such complexes. Reduction of the metal ion after substitution by fulminate appears to be impractical, since generally all that is reduced is the fulminate ion, producing the corresponding cyanide complex (12). Recently, the preparation of cis- $(M(CO)_4(CNO)_2)^{2-}$ (M = Cr, Mo, W) has been reported; the complexes result from the ultraviolet irradiation of a mixture of $M(CO)_6$ and sodium fulminate and subsequent precipitation by tetraphenylarsonium chloride (13).

Ruff (14) has reported the preparation of the anions $Fe(CO)_4CN^-$ and $Fe_2(CO)_8CN^-$ by the ultraviolet irradiation of a mixture of iron pentacarbonyl and bis(triphenylphosphine)iminium cyanide. Although the mononuclear complex probably has a structure similar to iron pentacarbonyl, the structure of the dinuclear species is unknown. Since the $\nu(C-N)$ is observed at a higher energy than in the mononuclear complex, it was suggested that the cyanide served

as a bridging ligand.

It is proposed that the preparation of similar zero-valent metal fulminate complexes be attempted, using iron and nickel carbonyls as starting materials. The complexes of these metals should prove to be interesting, especially if a species containing a bridging fulminate ion can be isolated. Infrared spectra will prove to be useful in this respect, since a bridging fulminate ion should be apparent from a decrease in the $\nu(\text{C-N})$ and $\nu(\text{N-O})$ frequencies.

(Although it would be desirable to have some x-ray data available for fulminate complexes, the zero-valent systems would be poor choices for study. The large tetraphenylarsonium cations necessary to stabilize the complexes would make the solution of a structure extremely unwieldy. At present the best candidate for x-ray work would be



In addition, it is proposed that the tris(acetonitrile)-tricarbonyl complexes of the chromium group (15) be treated with sodium fulminate and tetraphenylarsonium chloride in the solution in an attempt to prepare trisubstituted fulminate complexes of the type $(\text{M}(\text{CO})_3(\text{CNO})_3)^{3-}$ ($\text{M} = \text{Cr}, \text{Mo}, \text{W}$). The acetonitrile ligands are quite labile and should be easily replaced by the stronger bonding CNO^- ligands.

It is hoped that from these reactions will come a complex which is suitable for an extensive vibrational

analysis. Such an analysis, similar to that carried out for cyanide complexes (16) would give a better idea of the nature of bonding in the fulminate ligand. Although a vibrational study of one of the hexafulminate complexes might be a simpler undertaking, it would be interesting to see if π back-bonding is, as might well be expected, important in the zero-valent complexes.

References

- 1) J. V. Liebig, Liebigs Ann. Chem., 24, 315 (1823).
- 2) I. U. Nef, Liebigs Ann. Chem., 280, 303 (1894).
- 3) L. Wohler, A. Weber, and A. Berthmann, Ber. dtsh. Chem. Ges., 62, 2742, 2748 (1929).
- 4) D. Britton and J. D. Dunitz, Acta Cryst., 19, 662 (1965).
- 5) A. Suzuki, J. Industr. Explosives Soc. Japan, 14, 142 (1953).
- 6) Z. Iqbal and A. D. Yoffee, Proc. Roy. Soc., A302, 35 (1967).
- 7) W. Beck and E. Schuierer, Chem. Ber., 98, 298 (1965).
- 8) W. Beck, Chem. Ber., 95, 341 (1962).
- 9) W. Beck and K. Feldl, A. Naturforsch., 21b, 588 (1966).
- 10) J. Chatt and B. L. Shaw, J. Chem. Soc., 5075 (1962).
- 11) W. Beck, E. Schuierer and K. Feldl, Proceedings 8th International Conference on Coordination Chemistry, Springer, Vienna, p. 236 (1964).
- 12) W. Beck and F. Lux, Chem. Ber., 95, 1683 (1962).
- 13) W. Beck, P. Swoboda, K. Feldl, and E. Schuierer, Chem. Ber., 103, 3591 (1970).
- 14) J. K. Ruff, Inorg. Chem., 8, 86 (1969).
- 15) D. P. Tate, W. R. Knipple, and J. M. Augh, Inorg. Chem., 1, 433 (1962).
- 16) L. M. Jones, Inorg. Chem., 3, 1581 (1964);
L. M. Jones, Inorg. Chem., 4, 1472 (1965).

PROPOSITION 5

It is now well known that hydride, alkyl, and aryl (σ -bonded) ligands have a labilizing effect upon the ligands trans to them in transition metal complexes. This is generally thought to be a σ -bonding effect, and indeed, ligands which are thought to form π bonds with transition metals are usually not trans labilized significantly (1). In addition to the kinetic effects noted, it is now recognized that there is a structural influence of hydride and alkyl ligands which tends to lengthen metal-ligand bonds trans to them. In order to distinguish these structural effects from the kinetic trans effects, it has been proposed that the latter be referred to as trans "influence" (2). Although a great deal of work has been done in the study of the trans effects of several ligands (mostly in connection with platinum(II)), very little structural information is available concerning the trans influence of the ligands.

The structural data that are available for hydride

and alkyl transition metal complexes indicate that the trans bonds are lengthened up to 0.3 Å if the trans ligand is σ -bonded (Cl^- , NH_3 , etc.), but much less if the trans ligand is capable of forming π bonds with the metal. Apparently no unusually long trans carbonyl-metal bonds have been observed, although trans phosphite-metal (3) and cyanide-metal bonds (4) have been observed to be slightly longer than corresponding cis ligand-metal bonds. Unfortunately, the data are scattered throughout several different systems and several different transition metals. Any reliable correlation of bond lengths with trans influence is, therefore, difficult.

There is a need for a systematic study, similar to the kinetic studies which have been carried out, of the trans influence of hydride and σ -bonded carbon ligands. What is required, of course, is a system which forms stable compounds upon substitution by hydride and various alkyl, aryl, and other σ -bonded carbon ligands. Such systems are unfortunately not common, a fact which has probably helped to limit the amount of structural data available.

Since the problem can be attacked from several angles, a statement of scope seems to be in order. For the proposed work, we would like to examine the trans influence of several different ligands upon a single trans ligand. Since our variable species are to be ligands of high

σ -trans influence, the trans ligand should also be σ -bonding. There are several features which would be desirable in the chosen system: 1) The complexes should be as simple as possible, minimizing the number of atoms in each determination. 2) Since the accuracy of metal-ligand bond lengths tends to decrease with the increasing atomic weight of the metal, a lighter transition metal is preferred. 3) In order to have an internal check on the trans influence, the system should be structured such that there are identical ligands cis and trans to the trans influencing ligand. 4) And most important, the system chosen must form a large variety of σ -bonded carbon complexes.

Platinum probably forms more stable σ -bonded carbon complexes than any other metal, which, in part, accounts for its common usage in trans effect studies. However, since the bond lengths may not change a great deal from one trans influencing ligand to the next, accurate bond distances will be required. Platinum is one of the heaviest transition metals, and thus it would be better to choose a lighter metal in hopes of obtaining better bond length accuracy. In addition, platinum complexes, by comparison with those of the other transition metals, suffer from over-investigation, much to the disadvantage of the other transition metals.

Although a first row transition metal would be

desirable from a weight aspect, the alkyl substituted complexes of this series tend to have limited stability. The second row transition elements seem to show more promise. As a matter of fact, in consideration of the four stipulations made above, there is only one system presently known which would be suitable for the proposed study. Successful preparations have been reported for $(\text{Rh}(\text{NH}_3)_5\text{R})\text{SO}_4$ where $\text{R} = \text{H}, \text{Et}, \text{Pr}, \text{Bu}, \text{C}_3\text{F}_6\text{H},$ and $\text{C}_4\text{F}_8\text{H}$ (5). This system seems well suited for the suggested study since the ammine ligands are relatively simple and σ -bonding. Condition 3 is satisfied, giving an extra internal check on the trans bond lengthening. Also the simplicity of the preparations and stabilities of the products imply that additional complexes with different σ -bonding carbon ligands can be prepared.

Rhodium is not as light a metal as we might have hoped for, but the recent determination of the crystal structure of $(\text{Rh}(\text{NH}_3)_5\text{Et})\text{Br}_2$ indicates that bond length accuracy will not be a problem (6). In this case the difference in the cis and trans Rh-N bond distances was found to be 0.18 \AA .

It is proposed that the x-ray crystal structures be determined for several members of the system $(\text{Rh}(\text{NH}_3)_5\text{R})^{2+}$. Logical members for the initial study would be the hydride ($\text{R} = \text{H}$) and one of the fluorocarbon derivatives ($\text{R} = \text{C}_n\text{F}_{2n}\text{H}$). Depending upon the success of further preparations,

systems in which R = phenyl, fluorophenyl, and perhaps even acyl could be added to the series. A sterically hindered system, such as R = tertiary butyl, would also be of interest. With the information already available from the ethyl derivative, it thus will be possible to establish the relative strengths of σ -trans influencing ligands.

References

- 1) C. H. Langford and H. B. Gray, Ligand Substitution Processes, W. A. Benjamin, New York (1965).
- 2) L. M. Venanzi, Chem. Brit., 4, 162 (1968).
- 3) D. D. Titus, Ph.D. Thesis.
- 4) R. Mason and D. R. Russell, Chem. Comm., 182 (1965).
- 5) K. Thomas, J. A. Osborn, A. R. Powell, and G. Wilkinson, J. Chem. Soc., (A), 1801 (1968).
- 6) A. C. Skapski and P. G. H. Troughton, Chem. Comm., 666 (1969).